Supplementary Information for:

Chemical Constituents from *Morus alba* with Proprotein Convertase Subtilisin/Kexin Type 9 Expression and Secretion Inhibitory Activity

Hongic Won,[a] Min-Gyung Son,[a] Pisey Pel,[a] Piseth Nhoek,[a] Chae-Yeong An,[a] Young-Mi Kim,[a] Hee-Sung Chae,[a] Young-Won Chin*[a]

[a]College of Pharmacy and Research Institute of Pharmaceutical Sciences, Seoul National University, Seoul 08826, Republic of Korea

*Corresponding author

Tel.: +82 2 880 4022. Email: ywchin@snu.ac.kr

List of Supporting Information

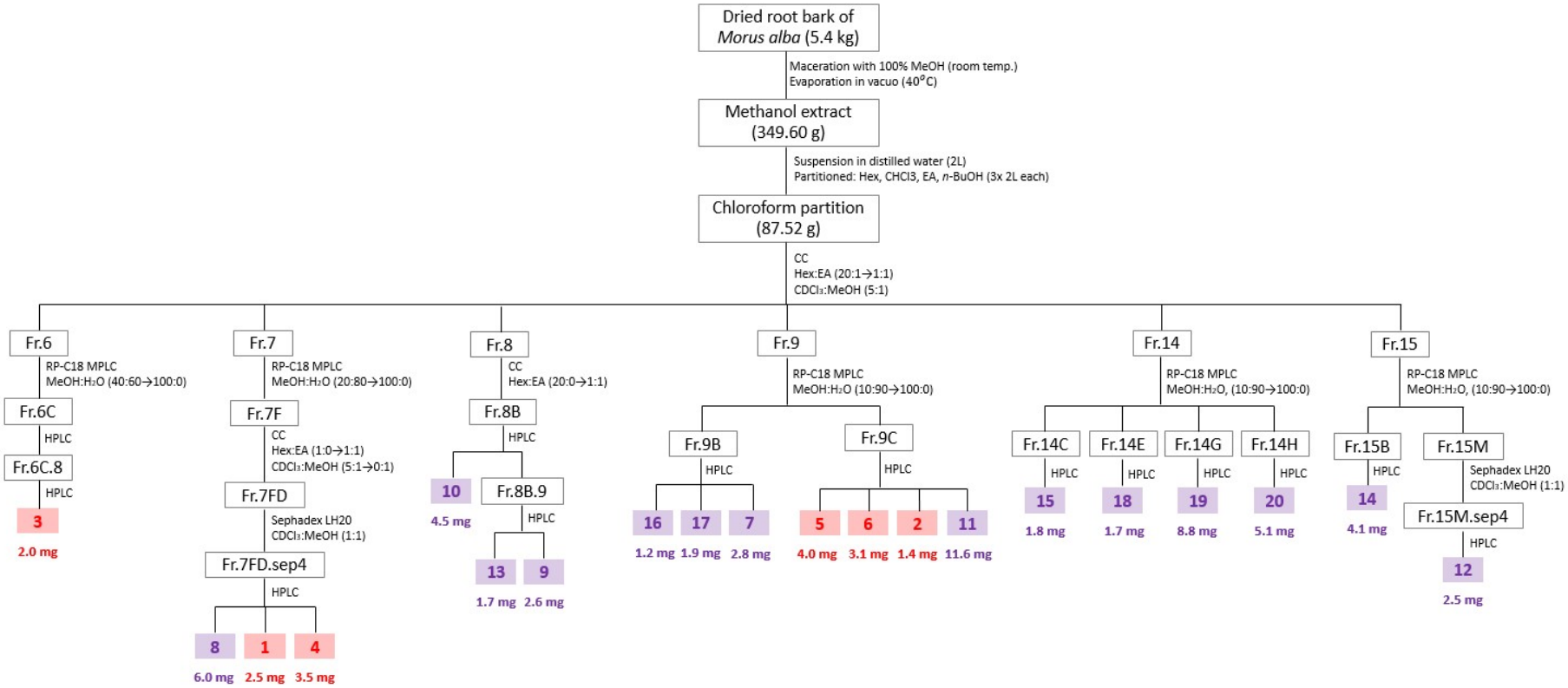

Scheme 1. Isolation scheme of compounds from *Morus alba*

Experimental

1. General experimental procedures

Column chromatography was conducted on silica gel (particle size: 40–60 μm, 230-400 mesh, Merck, Darmstadt, Germany). A Biotage Isolera One (Biotage, Uppsala, Sweden) with C18 RP silica gel (Cosmosil, Kyoto, Japan) was used for medium-pressure liquid chromatography (MPLC). High-performance liquid chromatography (HPLC) were performed with Gilson 321 pump and Gilson 172 diode array detector (Gilson, Madison, WI, USA), with aid of two columns; Luna, C18 (S-5 μm, 250 x 100 mm, Phenomenex, CA, USA), and J'sphere ODS-M80, HPLC column (S-4 μm, 250 x 4.6 mm, YMC Co., Ltd., Japan). Mass spectra data were measured using Waters Xevo G2 Q-TOF mass spectrometer, UHPLC-ESI-QTOF-MS (Waters, Medford, MA, USA) and TOF-MS (Agilent, Q-TOF 6530 MS / Agilent, 1290 Infinity) (No. 068) (USA). Nuclear magnetic resonance (NMR) spectra were recorded with JNM-ECA AVANCE 400 and 600 MHz spectrometer (JEOL Ltd., Japan) and Bruker AVANCE 500 MHz (Bruker, USA) and 800 MHz spectrometer (Bruker, Karlsruhe, Germany). Circular dichroism and ultraviolet-visible spectra were measured by Chirascan-Plus Electronic circular dichroism (Applied Photophysics Ltd, Japan). ASCO P-2000 digital polarimeter (JASCO, Tokyo, Japan/JASCO, Easton, MD, USA) was used to measure optical rotation. FT-IR (JASCO, FT/IR-4200) was used to measure infrared spectroscopy. Thin layer chromatography (TLC) analysis was performed on silica gel 60 F_{254} and silica gel RP-C_{18} plates (Merck, Darmstadt, Germany), and the spots were visualized by spraying anisaldehyde–H_2SO_4. Purified water was obtained using Milli-Q system (Waters Corporation, Milford, MA, USA).

2. Reagents

Solvents for extraction and isolation (methanol, hexane, chloroform, ethyl acetate, and *n*-butanol), and HPLC grade solvents for isolation [acetonitrile (CH_3CN), and methanol (MeOH)] were purchased from SK chemical (Seoul, Korea). Solvents for NMR spectroscopy ($CDCl_3$ and MeOH) were purchased from Cambridge Isotope Laboratories, Inc. (Andover, MA).

3. Plant material

The dried barks of root of *Morus alba*, originated from China, were purchased from a Korean market NAUM in March 2021 and were identified by Dr. H.-S. Chae. A voucher specimen (Voucher No. CYWSNU-KP0023) was deposited at the College of Pharmacy, Seoul National University, Republic of Korea.

4. Extraction and Isolation

The dried root barks (5.4 Kg) were extracted with 100% methanol (13 L) at room temperature for three times. The crude extract (349.60 g) was obtained after evaporation. The extract was

suspended in distilled water (2 L), then successively partitioned with hexane, chloroform, ethyl acetate, and *n*-butanol (3 x 2 L each). The chloroform-soluble extract (87.52 g, MAC) was fractionated using silica gel column chromatography (6 x 40 cm) starting with a gradient of hexane and ethyl acetate (20:1 to 1:1), followed by chloroform-methanol (5:1) to afford 22 fractions (MAC-1 to MAC-22). Next, several sub-fractions of chloroform fractions were found to actively inhibit PCSK9 (Figure **S3**) while up-regulating LDLR mRNA expression (Figure **S2**). These six sub-fractions, ranging from MAC-6 to MAC-9, MAC-14, and MAC-15, were chosen for further isolation work.

The fraction MAC-6 (3.2120 g) was separated by RP-MPLC with MeOH-H_2O (40:60 to 100:0) to obtain 4 fractions (MAC-6A to MAC-6D). The MAC-6C fraction (97.4 mg) was further separated by preparative HPLC (CH_3CN-H_2O (0.1% FA) 85% isocratic, 3 mL/min) to yield 8 sub-fractions (MAC-6C.1 to MAC-6C.8). The MAC-6C.8 (7.3 mg) fraction was purified using prep-HPLC (CH_3CN-H_2O (0.1% FA) 80% isocratic, 1 mL/min, 274 nm) to give **3** (2.0 mg, t_R = 31 min).

The MAC-7 fraction (1.3267 g) was separated by RP-MPLC and eluted with MeOH-H_2O (10:90 to 100:0) to afford 6 fractions (MAC-7A to MAC-7F). The MAC-7F fraction (973.6 mg) was separated using silica gel column chromatography (3 x 19 cm) starting from a gradient of hexane-ethyl acetate (1:0 to 1:1), then increased to chloroform-methanol (5:1), and finished by washing with 100% methanol to obtain 9 sub-fractions (MAC-7A to MAC-7I). The MAC-7FD fraction (528.9 mg) was separated by Sephadex LH-20 column (2 x 47 cm, $CHCl_3$:MeOH 1:1) to obtain 5 sub-fractions (MAC-7FD.sep1 to MAC-7FD.sep5). Finally, MAC-7FD.sep4 (40.8 mg) was purified with HPLC (MeOH-H_2O (0.1% FA) 85% isocratic, 3 mL/min) to obtain **8** (6.0 mg, t_R = 18 min), **1** (2.5 mg, t_R = 22 min) and **4** (3.5 mg, t_R = 36 min).

The MAC-8 fraction (3.0391 g) was chromatographed on a silica gel column (3 x 19 cm) starting with a gradient of hexane-ethyl acetate (20:1 to 1:1), then changed to CH_3Cl-MeOH (5:1) for wash to obtain 3 sub-fractions (MAC-8A to MAC-8C). MAC-8B (1.1388 g) was further separated using prep-HPLC (MeOH-H_2O (0.1% FA) 70 to 90%, gradient, 3 mL/min) to yield **10** (4.5 mg, t_R = 56 min) and MAC-8B.9 fraction (15.6 mg, t_R = 60 min), which was further purified using prep-HPLC (MeOH-H_2O (0.1% FA) 90% isocratic, 3 mL/min) to yield **13** (1.7 mg, t_R = 19 min) and **9** (2.6 mg, t_R = 20 min).

The MAC-9 fraction (4.3474 g) was separated by RP-MPLC eluting with MeOH-H_2O (10:90 to 100:0) to give 4 sub-fractions (MAC-9A to MAC-9D). The MAC-9B fraction (23.1 mg) was separated using prep-HPLC (CH_3CN-H_2O (0.1% FA) 65% isocratic (25 min) then 90% isocratic (13 min), 3 mL/min) to yield **16** (1.2 mg, t_R = 25 min), **17** (1.9 mg, tR = 34 min) and **7** (2.8 mg, t_R = 39 min). Small proportion (236.1 mg) of MAC-9C fraction (2.2522 g) was separated using prep-HPLC CH_3CN-H_2O (0.1% FA) 65% isocratic, 3 mL/min) to obtain **5** (4.0 mg, t_R = 37 min), **6** (3.1 mg, t_R = 39 min), **2** (1.4 mg, t_R = 50 min), and **11** (t_R = 53 min).

The MAC-14 fraction (5.3125 g) was separated by RP-MPLC using gradient MeOH-H_2O (1:99 to 100:0) to obtain 17 sub-fractions (MAC-14A to MAC-14P, and MAC-14R). All sub-fractions subjected to purification were separated by prep-HPLC (Luna 5 µm C18(2), 250

x 10 mm, 3 mL/min) at different concentration of acetonitrile. The MAC-14C fraction (7.6 mg) was purified with HPLC (CH_3CN-H_2O (0.1% FA) 15% isocratic) to obtain **15** (1.8 mg, t_R = 35 min). The MAC-14E fraction (11.0 mg) was purified with HPLC (CH_3CN-H_2O (0.1% FA) 25% isocratic) to isolate **18** (1.7 mg, t_R = 38 min). The MAC-14G fraction (40.4 mg) was purified with HPLC (CH_3CN-H_2O (0.1% FA) 35% isocratic) to gain **19** (8.8 mg, t_R = 39 min). Finally, the MAC-14H fraction (18.2 mg) was purified with HPLC (CH_3CN-H_2O (0.1% FA) 37% isocratic) to obtain **20** (5.1 mg, t_R = 46 min).

The MAC-15 fraction (2.2146 g) was separated by RP-MPLC eluting with MeOH-H_2O (10:90 to 100:0) to obtain 13 sub-fractions (MAC-15A to MAC-15O). The MAC-15B fraction (36.1 mg) was purified using prep-HPLC (MeOH-H_2O, 35% isocratic, 3 mL/min) to obtain **14** (4.1 mg, t_R = 20 min). The MAC-15M fraction (940.8 mg) was subjected to separation by Sephadex LH-20 column (2 x 47 cm, CH_3Cl-MeOH 1:1) to obtain 4 sub-fractions (MAC-15M.sep1 to MAC-15M.sep4). The MAC-15M.sep4 fraction (6.1 mg) was purified using prep-HPLC (MeOH-H_2O, 50% isocratic, 3 mL/min) to obtain **12** (2.5 mg, t_R = 28 min).

Sanggenol W (**1**): yellow oil; $[\alpha]^{20}_D$ –40.73 (*c* 0.12, MeOH); ECD (MeOH) λ_{max} ($\Delta\varepsilon$) 196 (–0.84), 217 (+0.78), 270 (–0.46) nm; UV (MeOH) λ_{max} (log ε) 228 (4.69), 271 (4.80) nm; IR (neat) ν_{max} 3300, 2973, 1754, 1639, 1453, 1350, 1298, 1158, 1119, 1044, 892, 817, 679 cm^{-1}; ^1H and ^{13}C NMR ($CDCl_3$), see Table 1; HRESIMS *m/z* 419.1476 $[M - H]^-$ (calcd for $C_{25}H_{23}O_6$, 419.1495)

Morusalnol D (**2**): colorless amorphous solid; $[\alpha]^{20}_D$ –20.01 (*c* 0.14, MeOH); ECD (MeOH) λ_{max} ($\Delta\varepsilon$) 196 (0.57), 222 (+0.98) nm; UV (MeOH) λ_{max} (log ε) 229 (4.43), 287 (4.46) nm; IR (neat) ν_{max} 3361, 2924, 1638, 1464, 1350, 1278, 1163, 1096, 834 cm^{-1}; ^1H and ^{13}C NMR ($CDCl_3$), see Table 1; HRESIMS *m/z* 489.2296 $[M - H]^-$ (calcd for $C_{30}H_{33}O_6$, 489.2283)

Morusalnol E (**3**): white amorphous solid; $[\alpha]^{20}_D$ +64.70 (*c* 0.10, MeOH); ECD (MeOH) λ_{max} ($\Delta\varepsilon$) 230 (+3.15), 295 (–2.32) nm; UV (MeOH) λ_{max} (log ε) 272 (4.63) nm; IR (neat) ν_{max} 3354, 2917, 1637, 1450, 1350, 1294, 1159, 1103, 825 cm^{-1}; ^1H and ^{13}C NMR (methanol-d_4), see Table 2; HRESIMS *m/z* 473.2351 $[M - H]^-$ (calcd for $C_{30}H_{33}O_5$, 473.2333)

Morusalnol F (**4**): yellow amorphous solid; $[\alpha]^{20}_D$ –3.84 (*c* 0.31, MeOH); ECD (MeOH) λ_{max} ($\Delta\varepsilon$) 195 (–0.76), 219 (+1.12) nm; UV (MeOH) λ_{max} (log ε) 207 (4.51), 227 (4.28), 272 (4.56) nm; IR (neat) ν_{max} 3411, 2973, 2925, 2279, 1753, 1638, 1456, 1380, 1301, 1162, 1102, 1037, 896, 817, 661 cm^{-1}; ^1H and ^{13}C NMR ($CDCl_3$), see Table 2; HRESIMS *m/z* 489.2304 $[M - H]^-$ (calcd for $C_{30}H_{33}O_6$, 489.2283)

Neovanone A (**5**): brown amorphous solid; $[\alpha]^{20}_D$ –32.15 (*c* 0.17, MeOH); ECD (MeOH) λ_{max} ($\Delta\varepsilon$) 232 (+7.88), 287 (–0.85), 312 (+1.80) nm; UV (MeOH) λ_{max} (log ε) 285 (4.47) nm; IR (neat) ν_{max} 3219, 2925, 1751, 1638, 1462, 1353, 1290, 1166, 1064, 828, 679 cm^{-1}; ^1H and ^{13}C NMR (methanol-d_4), see Table 3; HRESIMS *m/z* 437.1617 $[M - H]^-$ (calcd for $C_{25}H_{25}O_7$, 437.1606)

Neovanone B (**6**): brown amorphous solid; $[\alpha]^{20}_D$ +10.21 (*c* 0.31, MeOH); ECD (MeOH) λ_{max} ($\Delta\varepsilon$) 237 (+1.40), 290 (–1.75), 312 (+2.29), 354 (+1.61) nm; UV (MeOH) λ_{max} (log ε) 284

(4.47) nm; IR (neat) ν_{max} 2927, 1753, 1637, 1518, 1350, 1187, 679 cm^{-1}; ^{1}H and ^{13}C NMR (methanol-d_4), see Table 3; HRESIMS *m/z* 437.1616 $[M - H]^-$ (calcd for $C_{25}H_{25}O_7$, 437.1606)

5. Chemical and Spectral Data for compounds 7–20

Abyssinoflavanone V (**7**): colorless amorphous solid; ECD (MeOH) λ_{max} ($\Delta\varepsilon$) 286 (–15.4), 332 (+3.76) nm; HRESIMS *m/z* 337.1063 $[M - H]^-$ (calcd for $C_{20}H_{17}O_5$, 337.1076); $C_{20}H_{18}O_5$; ^{1}H NMR ($CDCl_3$, 400 MHz) δ 12.06 (1H, s), 7.17 (1H, dd, *J* = 2.2, 8.3 Hz), 7.06 (1H, d, *J* = 2.2 Hz), 6.81 (1H, d, *J* = 8.3 Hz), 6.33 (1H, d, *J* = 9.8 Hz), 5.99 (1H, s), 5.99 (1H, s), 5.66 (1H, d, *J* = 9.8 Hz), 5.31 (1H, dd, *J* = 3.0, 13.1 Hz), 3.09 (1H, dd, *J* = 13.1, 17.2 Hz), 2.77 (1H, dd, *J* = 3.0, 17.2 Hz) 1.45 (3H, s), 1.45 (3H, s); ^{13}C NMR ($CDCl_3$, 400 MHz) δ 28.1, 28.1, 43.2, 77.2, 79.1, 95.5, 96.7, 103.2, 116.6, 121.5, 121.9, 124.4, 127.2, 130.3, 131.5, 153.5, 163.3, 164.4, 164.5, 196.1.

Sanggenol O (**8**): yellow oil; ECD (MeOH) λ_{max} ($\Delta\varepsilon$) 215 (+18.6), 241 (–3.30), 257 (+3.44), 285 (–12.4) nm; HRESIMS *m/z* 419.1498 $[M - H]^-$ (calcd for $C_{25}H_{23}O_6$, 419.1495); $C_{25}H_{24}O_6$; ^{1}H NMR ($CDCl_3$, 400 MHz) δ 6.99 (s), 6.67 (1H, d, *J* = 10.0 Hz), 6.28 (1H, d, *J* = 9.8 Hz), 5.99 (1H, s, overlapped), 5.99 (1H, s, overlapped), 5.66 (1H, dd, *J* = 3.2, 13.3 Hz), 5.59 (1H, d, *J* = 10.0 Hz), 5.51 (1H, d, *J* = 9.8 Hz), 2.99 (1H, dd, *J* = 13.3, 17.3 Hz), 2.79 (1H, dd, *J* = 3.2, 17.3 Hz), 1.43 (3H, s), 1.43 (3H, s), 1.42 (3H, s), 1.39 (3H, s); ^{13}C NMR ($CDCl_3$, 400 MHz) δ 27.8, 28.0, 28.2, 28.2, 42.5, 74.1, 76.8, 77.2, 95.4, 96.5, 103.0, 110.0, 114.6, 116.6, 117.9, 122.1, 123.3, 128.3, 129.2, 148.9, 150.2, 163.9, 164.4, 164.5, 197.0.

Cyclomorusin (**9**): yellow amorphous solid; HRESIMS *m/z* 417.1328 $[M - H]^-$ (calcd for $C_{25}H_{21}O_6$, 417.1338); $C_{25}H_{22}O_6$; ^{1}H NMR (methanol-d_4, 400 MHz) δ 7.65 (1H, d, *J* = 8.4 Hz), 6.82 (1H, d, *J* = 9.9 Hz), 6.54 (1H, dd, *J* = 2.4, 8.4 Hz), 6.31 (1H, d, *J* = 2.4 Hz), 6.15 (1H, d, *J* = 9.3 Hz), 6.13 (1H, s), 5.72 (1H, d, *J* = 9.9 Hz), 5.41 (1H, d, *J* = 9.3 Hz), 1.94 (3H, s), 1.70 (3H, s), 1.46 (3H, s), 1.46 (3H, s) ; ^{13}C NMR (methanol-d_4, 400 MHz) δ 18.7, 26.0, 28.5, 28.5, 70.7, 79.3, 100.8, 102.8, 105.1, 106.4, 108.6, 110.4, 111.3, 115.6, 122.4, 126.4, 129.1, 140.0, 152.5, 157.3, 159.7, 160.5, 162.8, 165.1, 179.8.

Cycloaltilisin 7 (**10**): yellow amorphous solid; ECD (MeOH) λ_{max} ($\Delta\varepsilon$) 238 (+3.61), 293 (–3.55) nm; HRESIMS *m/z* 405.1708 $[M - H]^-$ (calcd for $C_{25}H_{25}O_5$, 405.1702); $C_{25}H_{26}O_5$; ^{1}H NMR ($CDCl_3$, 400 MHz) δ 12.29 (1H, br s), 7.32 (1H, d, *J* = 7.4 Hz), 7.32 (1H, d, *J* = 7.4 Hz), 6.88 (1H, d, *J* = 7.4 Hz), 6.88 (1H, d, *J* = 7.4 Hz), 6.66 (1H, d, *J* = 10.2 Hz), 5.94 (1H, s), 5.44 (1H, d, *J* = 10.2 Hz), 5.33 (1H, dd, *J* = 2.9, 13.0 Hz), 5.08 (1H, m), 3.07 (1H, dd, *J* = 13.0, 17.1 Hz), 2.77 (1H, dd, *J* = 2.9, 17.1 Hz), 2.06 (2H, m), 1.75–1.62 (2H, m, overlaid), 1.66 (3H, s), 1.57 (3H, s), 1.40 (3H, d, *J* = 2.2 Hz); ^{13}C NMR ($CDCl_3$, 400 MHz) δ 17.7, 22.6, 25.7, 41.7, 43.2, 78.9, 80.9, 96.0, 102.7, 102.8, 115.7, 115.7, 115.8, 123.8, 125.1, 127.0, 128.0, 130.6, 132.0, 156.1, 158.4, 162.5, 162.6, 196.0.

Sanggenol P (**11**): yellow amorphous solid; ECD (MeOH) λ_{max} ($\Delta\varepsilon$) 289 (–2.13) nm; HRESIMS *m/z* 491.2441 $[M - H]^-$ (calcd for $C_{30}H_{35}O_6$, 491.2439); $C_{30}H_{36}O_6$; ^{1}H NMR (methanol-d_4, 400 MHz) δ 6.96 (1H, s), 5.91 (1H, d, *J* = 2.1 Hz), 5.87 (1H, d, *J* = 2.1 Hz), 5.67

(1H, dd, J = 3.0, 12.4 Hz), 5.28 (1H, t, J = 7.1, 7.1 Hz), 5.19 (1H, t, J = 6.9, 6.9 Hz), 5.06 (1H, t, J = 7.1, 7.1 Hz), 3.41 (2H, d, J = 6.9 Hz), 3.25 (2H, d, J = 7.1 Hz), 3.06 (1H, dd, J = 12.4, 17.2 Hz), 2.73 (1H, dd, J = 3.0, 17.2 Hz), 2.07 (2H, m), 1.99 (2H, t, J = 7.4, 7.4 Hz), 1.79 (3H, s), 1.74 (3H, s), 1.69 (3H, s), 1.62 (3H, s), 1.57 (3H, s) ; ^{13}C NMR (methanol-d_4, 400 MHz) δ 16.4, 17.8, 17.9, 23.8, 25.9, 26.0, 27.7, 29.3, 40.9, 43.2, 76.7, 96.3, 97.0, 103.4, 118.7, 119.6, 122.1, 124.0, 124.0, 125.4, 125.5, 132.3, 133.5, 136.5, 151.8, 154.4, 165.2, 165.5, 168.3, 198.3.

Morachalcone A (**12**): golden powder; HRESIMS *m/z* 339.1237 $[M - H]^-$ (calcd for $C_{20}H_{19}O_5$, 339.1232); $C_{20}H_{20}O_5$; ^{1}H NMR (methanol-d_4, 400 MHz) δ 8.08 (1H, d, J = 15.5 Hz), 7.75 (1H, d, J = 8.8 Hz), 7.71 (1H, d, J = 15.5 Hz), 7.51 (1H, d, J = 8.3 Hz), 6.40 (1H, d, J = 8.8 Hz), 6.35 (1H, dd, J = 2.4, 8.3 Hz), 6.34 (1H, d, J = 2.4 Hz), 5.22 (1H, t, J = 7.3, 7.3 Hz), 1.78 (3H, s), 1.66 (3H, s); ^{13}C NMR (methanol-d_4, 400 MHz) δ 18.0, 22.6, 26.0, 103.6, 108.1, 109.1, 114.7, 115.7, 116.6, 117.8, 123.8, 130.2, 131.8, 132.3, 141.8, 160.8, 162.8, 163.4, 165.1, 194.4.

Betulinic acid (**13**): white amorphous powder; HRESIMS *m/z* 455.3542 $[M - H]^-$ (calcd for $C_{30}H_{47}O_3$, 455.3531); $C_{30}H_{48}O_3$; ^{1}H NMR ($CDCl_3$, 400 MHz) δ 4.76 (1H, s), 4.63 (1H, s), 3.19 (1H, dd, J = 5.0, 11.2 Hz), 3.01 (1H, m), 1.70 (3H, s), 0.99 (3H, s), 0.98 (3H, s), 0.95 (3H, s), 0.84 (3H, s), 0.77 (3H, s); ^{13}C NMR ($CDCl_3$, 400 MHz) δ 14.7, 15.3, 16.0, 16.1, 18.3, 19.4, 20.9, 25.7, 27.9, 29.7, 29.7, 30.6, 32.2, 34.3, 34.3, 37.2, 38.4, 38.7, 38.9, 40.7, 42.4, 45.9, 49.3, 50.5, 55.4, 56.3, .79.0, 109.7, 142.6, 178.6.

Scopoletin (**14**): yellow powder; HRESIMS *m/z* 191.0344 $[M - H]^-$ (calcd for $C_{10}H_7O_4$, 191.0344); $C_{10}H_8O_4$; ^{1}H NMR (methanol-d_4, 400 MHz) δ 7.86 (1H, d, J = 9.4 Hz), 7.10 (1H, s), 6.76 (1H, s), 6.20 (1H, d, J = 9.4 Hz), 3.90 (3H, s); ^{13}C NMR (methanol-d_4, 400 MHz) δ 164.2, 153.1, 151.6, 147.2, 146.2, 112.5, 112.5, 109.9, 104.0, 56.4.

Umbelliferone (**15**): white amorphous solid; HRESIMS *m/z* 161.0239 $[M - H]^-$ (calcd for $C_9H_5O_3$, 161.0244); $C_9H_6O_3$; ^{1}H NMR (methanol-d_4, 400 MHz) δ 7.85 (1H, d, J = 9.5 Hz), 7.45 (1H, d, J = 8.5 Hz), 6.79 (1H, dd, J = 2.3, 8.5 Hz), 6.70 (1H, d, J = 2.3 Hz), 6.18 (1H, d, J = 9.5 Hz); ^{13}C NMR (methanol-d_4, 600 MHz) δ 103.5, 112.2, 113.2, 114.6, 130.7, 146.1, 157.3, 163.3, 163.8.

Morusalfuran E (**16**): white amorphous solid; HRESIMS *m/z* 269.0808 $[M - H]^-$ (calcd for $C_{16}H_{13}O_4$, 269.0814); $C_{16}H_{14}O_4$; ^{1}H NMR ($CDCl_3$, 400 MHz) δ 7.44 (1H, d, J = 8.6 Hz), 7.06 (1H, d, J = 2.2 Hz), 6.96 (1H, t, J = 2.0, 2.0 Hz), 6.93 (1H, s), 6.90 (1H, t, J = 2.0, 2.0 Hz), 6.87 (1H, dd, J = 2.2, 8.6 Hz), 6.39 (1H, t, J = 2.0, 2.0 Hz), 3.88 (3H, s), 3.86 (3H, s); ^{13}C NMR ($CDCl_3$, 400 MHz) δ 55.5, 55.8, 95.9, 101.6, 101.9, 102.7, 104.1, 112.1, 121.1, 122.4, 132.8, 154.6 155.9, 156.9, 158.2, 161.3.

Sanggenofuran B (**17**): light brown amorphous solid; HRESIMS *m/z* 323.1280 $[M - H]^-$ (calcd for $C_{20}H_{19}O_4$, 323.1283); $C_{20}H_{20}O_4$; ^{1}H NMR ($CDCl_3$, 400 MHz) δ 7.42 (1H, d, J = 8.5 Hz), 7.04 (1H, d, J = 2.5 Hz), 6.88 (1H, s), 6.88 (1H, s), 6.87 (1H, dd, J = 2.5, 8.5 Hz), 6.86 (1H, s), 5.29 (1H, t, J = 7.1, 7.1 Hz), 3.87 (3H, s), 3.45 (2H, d, J = 7.1 Hz), 1.85 (3H, s), 1.78 (3H, s); ^{13}C NMR ($CDCl_3$, 400 MHz) δ 18.0, 22.6, 25.8, 55.8, 95.9, 101.2, 104.5, 104.5, 112.0, 113.7, 121.0, 121.2, 122.5, 129.9, 135.8, 154.6, 155.3, 155.3, 155.8, 158.1.

Moracin M (**18**): white amorphous solid; HRESIMS *m/z* 241.0513 $[M - H]^-$ (calcd for $C_{14}H_9O_4$, 241.0506); $C_{14}H_{10}O_4$; ^1H NMR (methanol-d_4, 400 MHz) δ 7.35 (1H, d, J = 8.4 Hz), 6.91 (1H, br s), 6.89 (1H, d, J = 2.1 Hz), 6.75 (1H, d, J = 2.2 Hz), 6.75 (1H, dd, J = 2.2 Hz), 6.73 (1H, dd, J = 2.1, 8.4 Hz) 6.24 (1H, t, J = 2.2, 2.2 Hz); ^{13}C NMR (methanol-d_4, 400 MHz) δ 98.5, 102.2, 103.6, 104.0, 104.0, 113.3, 122.1, 123.1, 133.9, 156.2, 156.9, 157.3, 160.0, 160.0.

Moracin B (**19**): light brown amorphous solid; HRESIMS *m/z* 285.0758 $[M - H]^-$ (calcd for $C_{16}H_{13}O_4$, 285.0768); $C_{16}H_{14}O_4$; ^1H NMR (methanol-d_4, 400 MHz) δ 7.14 (1H, s), 6.95 (1H, s), 6.92 (1H, s), 6.85 (1H, d, overlapped), 6.85 (1H, d, overlapped), 6.33 (1H, t, J = 2.2, 2.2 Hz), 3.92 (3H, s), 3.81 (3H, s); ^{13}C NMR (methanol-d_4, 400 MHz) δ 55.7, 56.7, 95.9, 102.1, 102.3, 102.5, 104.9, 106.2, 123.0, 133.9, 144.8, 148.3, 150.6, 156.3, 160.0, 162.7.

Moracin S (**20**): colorless amorphous solid; HRESIMS *m/z* 309.1123 $[M - H]^-$ (calcd for $C_{19}H_{17}O_4$, 309.1132); $C_{19}H_{18}O_4$; ^1H NMR (methanol-d_4, 400 MHz) δ 7.16 (1H, d, J = 8.3 Hz), 6.89 (1H, s), 6.78 (1H, d, J = 2.2 Hz), 6.78 (1H, d, J = 2.2 Hz), 6.72 (1H, d, J = 8.3 Hz), 6.24 (1H, t, J = 2.2, 2.2 Hz), 5.41 (1H, t, J = 7.3, 7.3 Hz), 3.59 (2H, d, J = 7.3 Hz), 1.89 (3H, s), 1.69 (3H, s); ^{13}C NMR (methanol-d_4, 400 MHz) δ 18.2, 23.7, 26.0, 102.6, 103.5, 104.0, 104.0, 112.7, 113.2, 119.0, 123.0, 123.6, 132.4, 134.1, 153.9, 155.9, 156.0, 160.0, 160.0.

6. Cell culture

The HepG2 human hepatocellular liver cell line was obtained from the Korea Research Institute of Bioscience and Biotechnology (South Korea) and grown in Dulbecco′s Modified Eagle′s Medium (DMEM) containing 10% fetal bovine serum (FBS) and 100 U/mL penicillin/streptomycin sulfate. Cells were incubated in a humidified 5% CO_2 atmosphere at 37 °C. DMEM, penicillin/streptomycin, and FBS were purchased from Hyclone (Logan, USA).

7. Cell viability test

Cell viability test was performed by WST plus-8 kit (GenDEPOT, USA) according to the manufacturer's instructions. Briefly, 5 x 10^3 human HepG2 cells were seeded in 96 well culture plate on the day before sample treatment. The compounds dissolved in DMSO were diluted to a concentration of 10 μM or 20 μM in DMEM without FBS for serum starvation. After treatment, cells were incubated for 24 hr for the WST-8 cell viability test.

8. Quantitative Real-time PCR

Total RNA was extracted from HepG2 treated with compounds using TRI Reagent® (Genbiotech, Argentina) in compliance to the manufacturer's instructions. The complementary DNA (cDNA) was synthesized from total RNA using Maxima First Strand cDNA Synthesis Kit (ThermoFisher Scientific, USA). Real time PCR for mRNA quantification was performed with TB Green® Premix Ex Taq™ Ⅱ (TaKaRa Biotechnology, China). The mRNA expression

was normalized to the GAPDH and calculated using the $2^{-\Delta\Delta Ct}$ method. The human primers were the following (5' to 3'): GAPDH: GTCTCCTCTGACTTCAACAGCG (forward), ACCACCCTGTTGCTGTAGCCAA (reverse); LDLR: GTGCTCCTCGTCTTCCTTTG (forward), TAGCTGTAGCCGTCCTGGTT (reverse), PCSK9: GACACCAGCATACAGAGTGAC (forward), GTGCCATGACTGTCACACTTGC (reverse); IDOL(MYLIP): ACGGTCACCAAGGAATCTGGGA (forward), CCTTCAAGTCACGGCTATACTGC. Gene-specific primers were custom-synthesized by Bioneer (Daejeon, Korea).

9. Western blot

HepG2 cells were lysed in RIPA buffer containing Pierce™ Protease and Phosphatase Inhibitor Mini Tablets (ThermoFisher Scientific, USA) on ice for 10 min. Cell lysates were centrifuged at 14,000 rpm for 15 min at 4 °C, and supernatants were quantified using the Protein assay reagent A, B (Bio-Rad, USA). Proteins were separated by electrophoresis on a 10% sodium dodecyl sulfate polyacrylamide gel (SDS-PAGE) and were transferred onto polyvinylidene difluoride (PVDF) membrane. The membrane was treated with 5% skimmed milk for 1 h and incubated overnight at 4 °C with primary antibodies in 3% bovine serum albumin (BSA). After washing with Tris-buffered saline with 0.1% Tween 20 (TBST), the membrane was incubated with the HRP-conjugated secondary antibody (1:5000) for 1 h at room temperature. The band images were acquired using a ChemiDoc Imaging system (Bio-Rad, USA) using SuperSignal™ West Pico PLUS Chemiluminescent Substrate (ThermoFisher Scientific, USA) or Immobilon® Western Chemiliminescent HRP Substrate (Millipore, USA).

10. ELISAs

Secreted PCSK9 level in culture medium of cells were measured using a Human Proprotein Convertase 9/PCSK9 ELISA kits (RayBiotech, USA) in accordance to the manufacturer's instructions. Color development at 450 nm was then measured using an automated microplate ELISA reader. In addition, a standard curve was generated for each assay plate by measuring the absorbance of serial dilutions of recombinant human PCSK9 at 450 nm.

11. Statistical Analysis

Data from the experiments are presented as the mean ± S.E.M. The level of statistical significance was determined by one-way analysis of variance (ANOVA) and Dunnett's t-test for multiple comparisons. P values less than 0.05 were considered significant.

Data from the experiments are presented as the mean ± S.E.M. The level of statistical significance was determined by one-way analysis of variance (ANOVA) and Dunnett's t-test for multiple comparisons. P values less than 0.05 were considered significant.

Figure S1. Effects of methanol extract (MAT), *n*-hexane fraction (MAH), chloroform fraction (MAC), ethyl acetate fraction (MAE), *n*-butanol fraction (MAB) and water fraction (MAW) of *Morus alba* on the LDLR and PCSK9 mRNA expressions in the HepG2 cells. **(A)** The expression of LDLR mRNA was assayed by qRT-PCR in cells treated with 40 μg/ml concentration of extract and fractions of *Morus alba*. **(B)** The expression of PCSK9 mRNA was assayed by qRT-PCR in cells treated with 40 μg/ml concentration of extract and fractions of *Morus alba*.

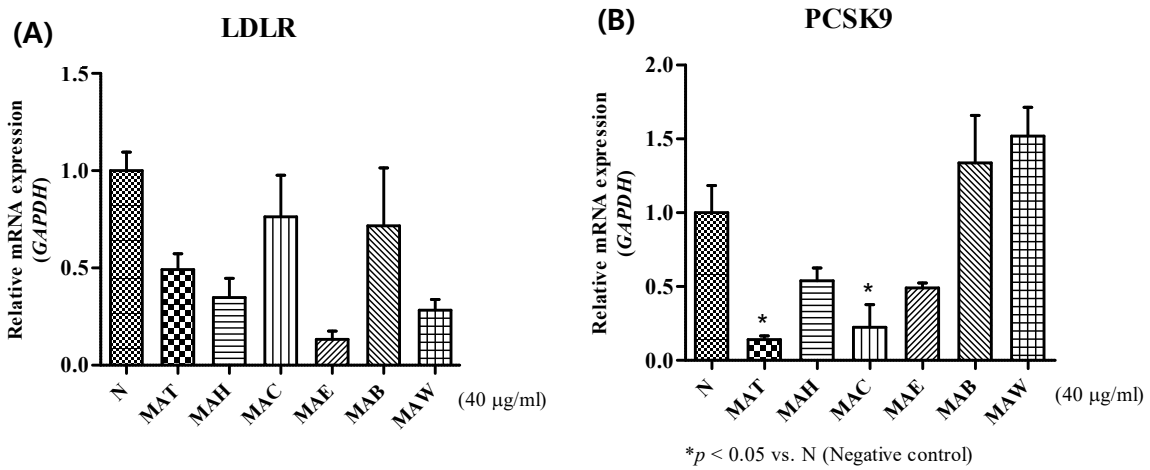

Figure S2. Effects of chloroform subfractions on LDLR mRNA expression in the HepG2 cells. Each subfraction was treated with 40 μg/ml concentration and MAC-10 to 13 were excluded due to their cytotoxicity.

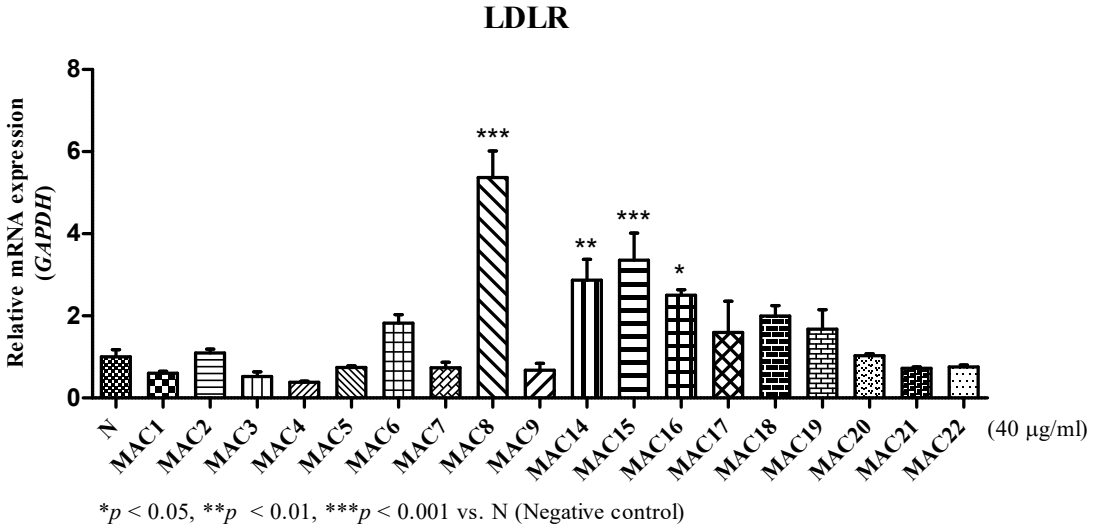

Figure S3. Effects of chloroform subfractions on PCSK9 mRNA expression in the HepG2 cells. Each subfraction was treated with 40 μg/ml concentration and MAC-10 to 13 were excluded due to their cytotoxicity.

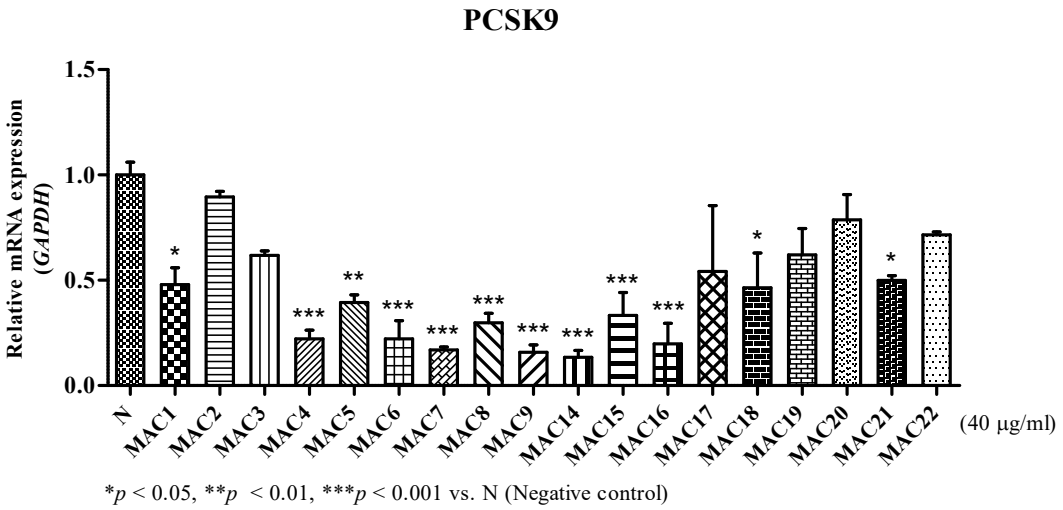

Figure S4. Cell viability test on the HepG2 cell by WST-8 assay of isolated compounds.

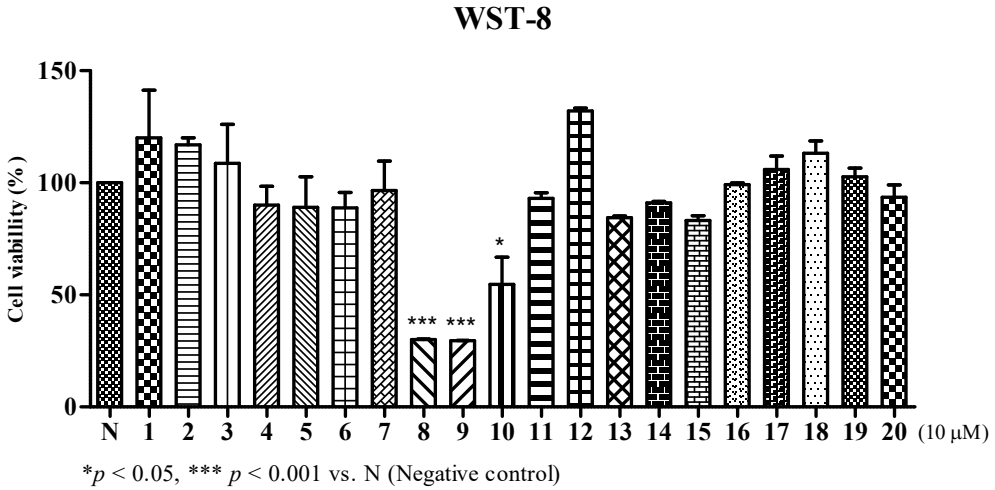

Figure S5. Effects of compounds **1-7**, **11-20** on the IDOL mRNA expressions in the HepG2 cells.

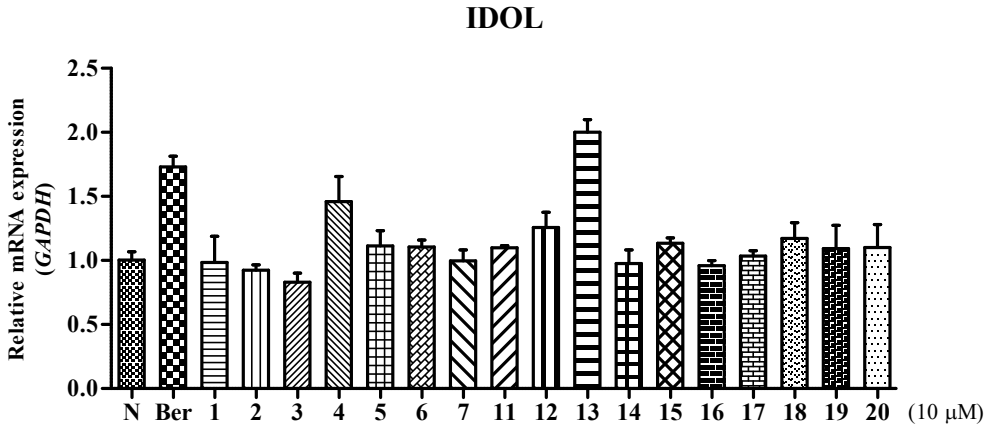

Figure S6. Effects of compound **13** and berberine chloride on the PCSK9 mRNA expressions at a range of concentrations in the HepG2 cells. **(A)** The expression of PCSK9 mRNA was assayed by qRT-PCR in cells treated with various range of compound **13**. **(B)** The expression of PCSK9 mRNA was assayed by qRT-PCR in cells treated with various range of berberine chloride.

Cell viability test on the HepG2 cell by WST-8 assay of compound **13** with 20 μM concentration.

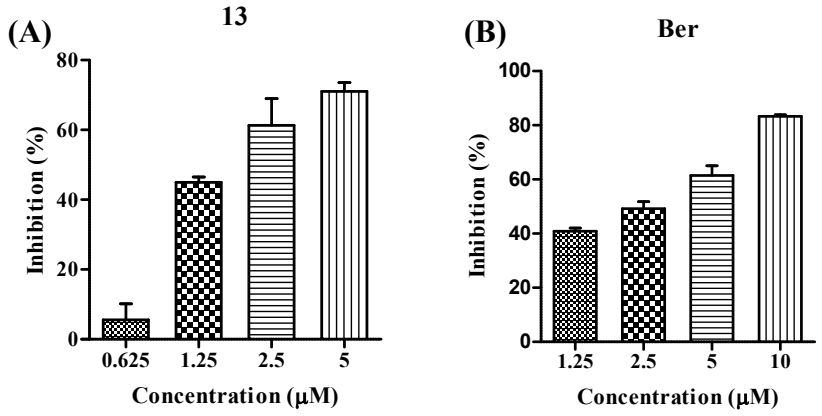

Figure S7. Cell viability test on the HepG2 cell by WST-8 assay of compound **13** with 20 μM concentration.

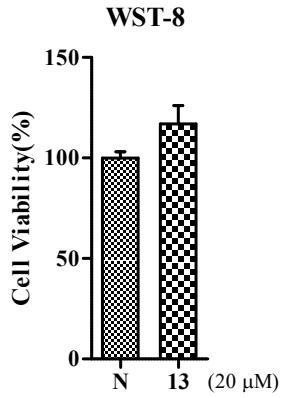

Figure S8. Effects of **13** on LDLR, PCSK9 and β−actin protein expression in HepG2 cells. The expressions of the proteins were examined by western blot analysis.

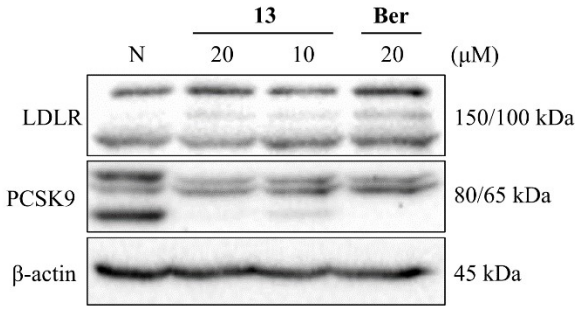

Figure S9. Raw data for the Western blots. **(A, C, E)** Raw data for Figure **4**. **(B, D, F)** Raw data for Figure **S8**.

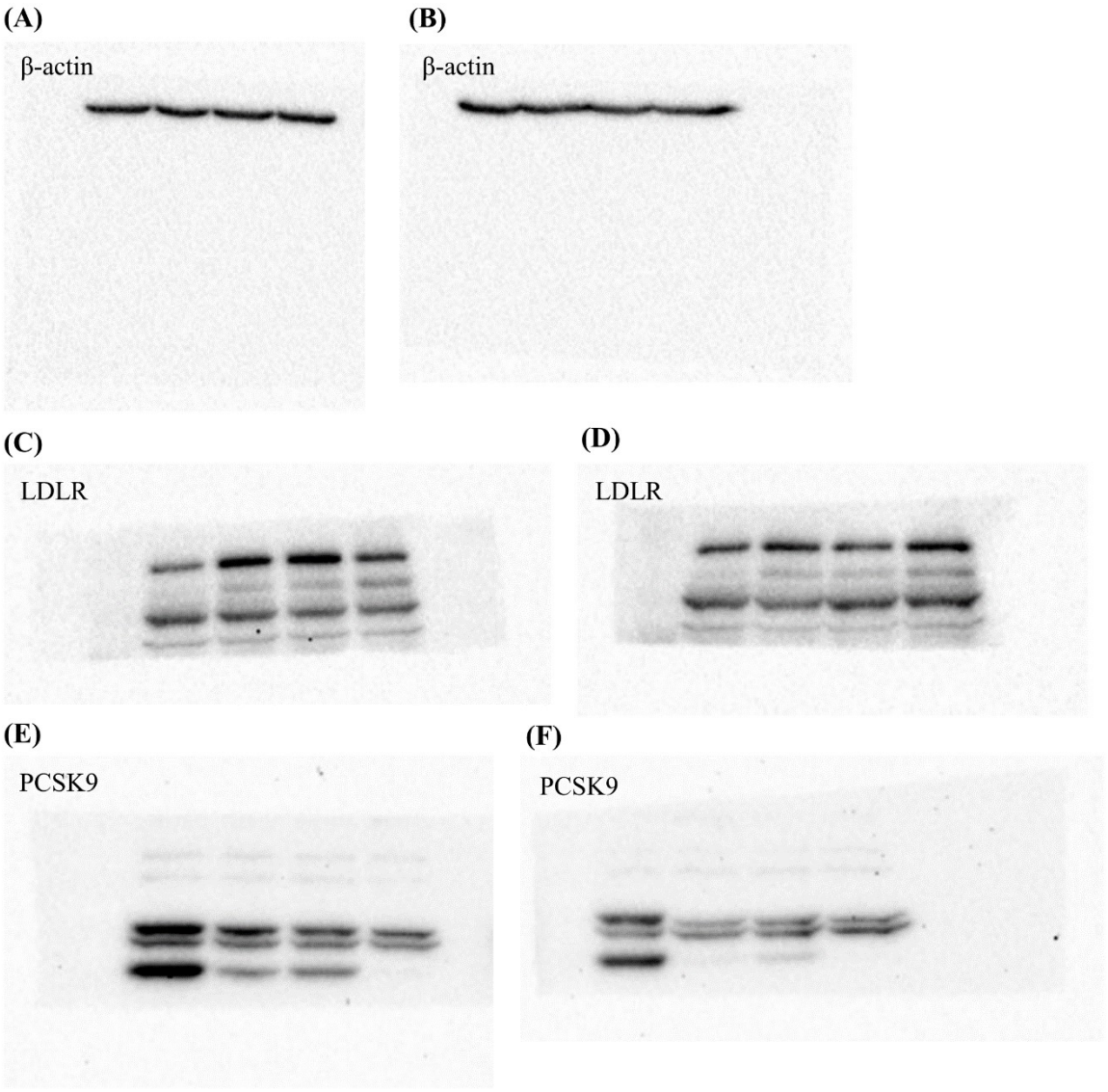

Figure S10–S17. 1D and 2D NMR, MS, and IR spectra of sanggenol W (**1**)

Figure S10. ^{1}H NMR spectrum of sanggenol W (**1**) in $CDCl_3$

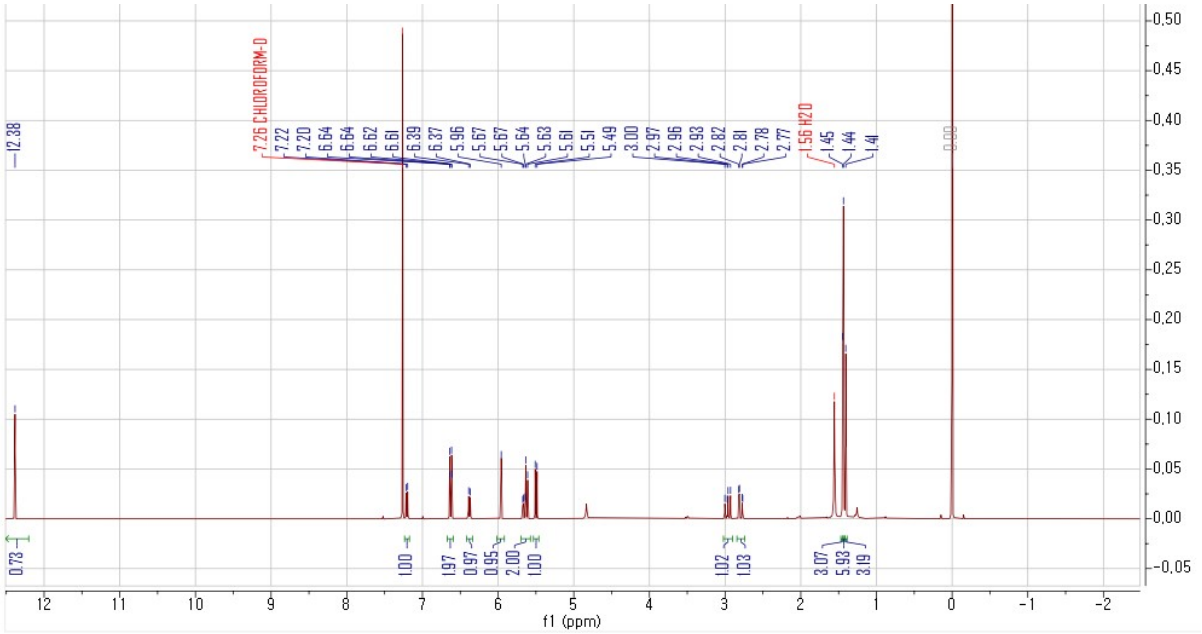

Figure S11. ^{13}C NMR spectrum of sanggenol W (**1**) in $CDCl_3$

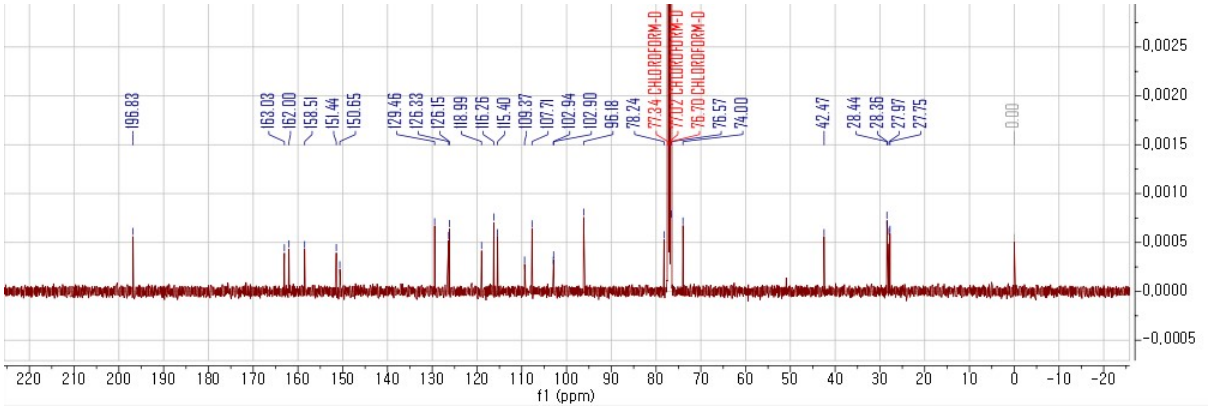

Figure S12. HSQC spectrum of sanggenol W (**1**) in $CDCl_3$

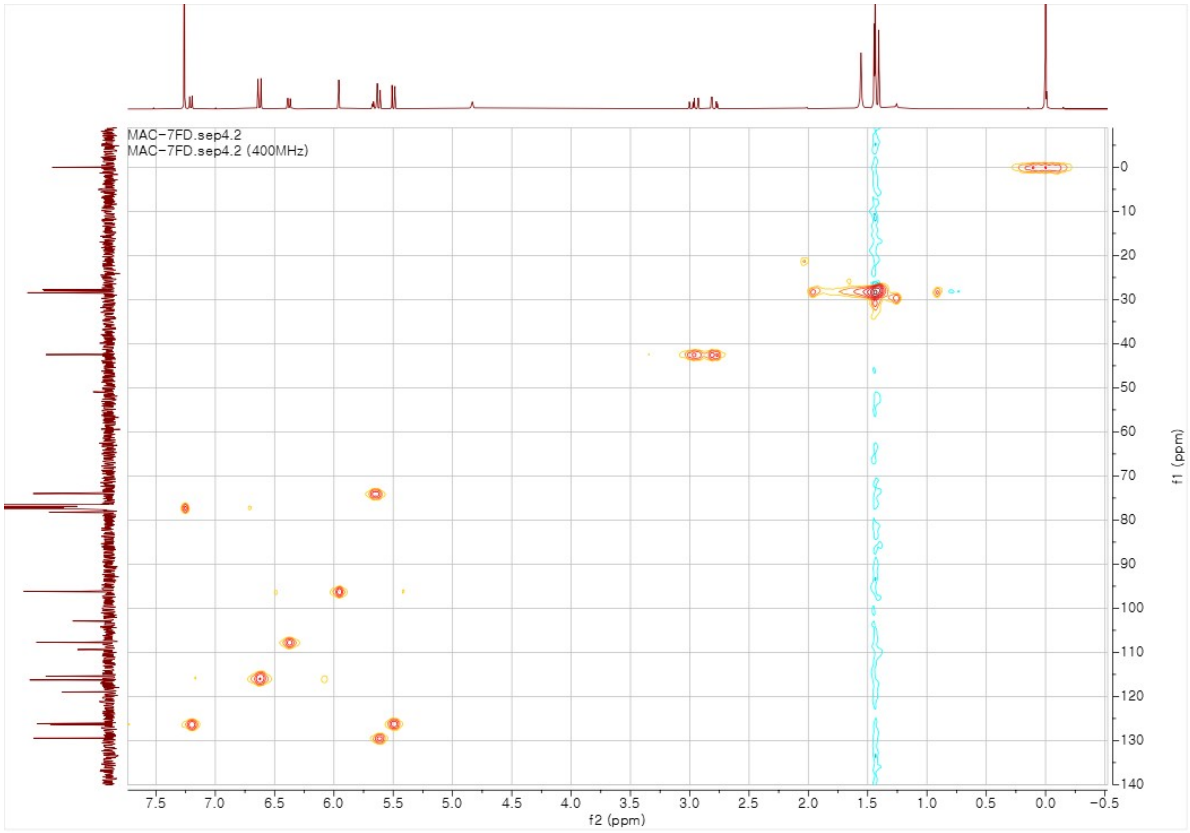

Figure S13. COSY spectrum of sanggenol W (**1**) in $CDCl_3$

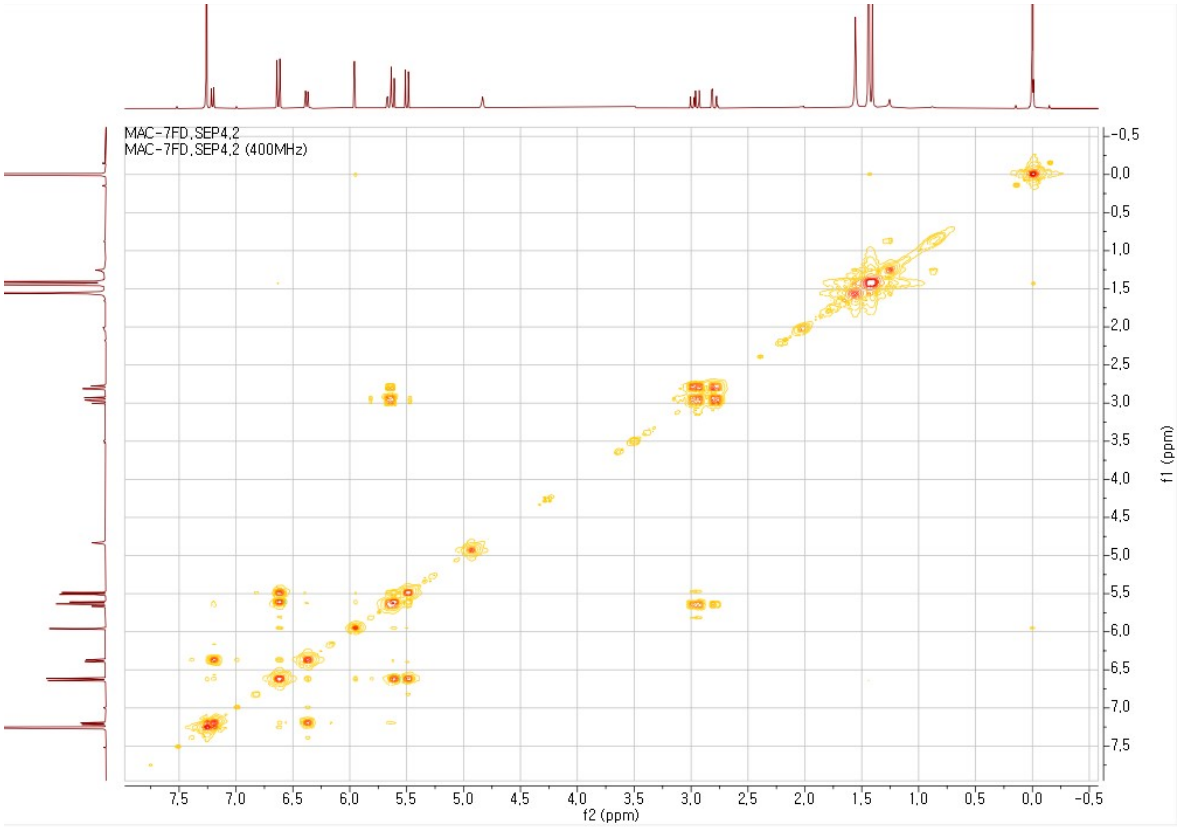

Figure S14. HMBC spectrum of sanggenol W (**1**) in $CDCl_3$

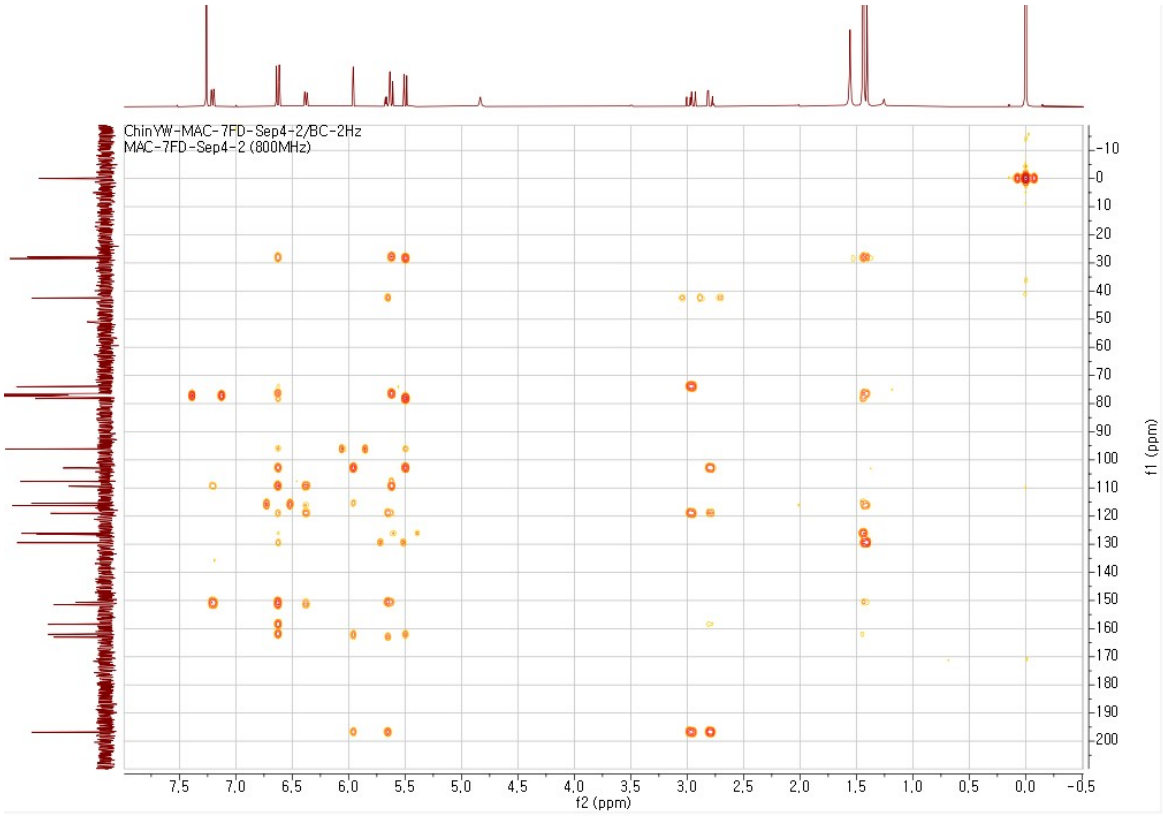

Figure S15. HRESIMS spectrum of sanggenol W (**1**)

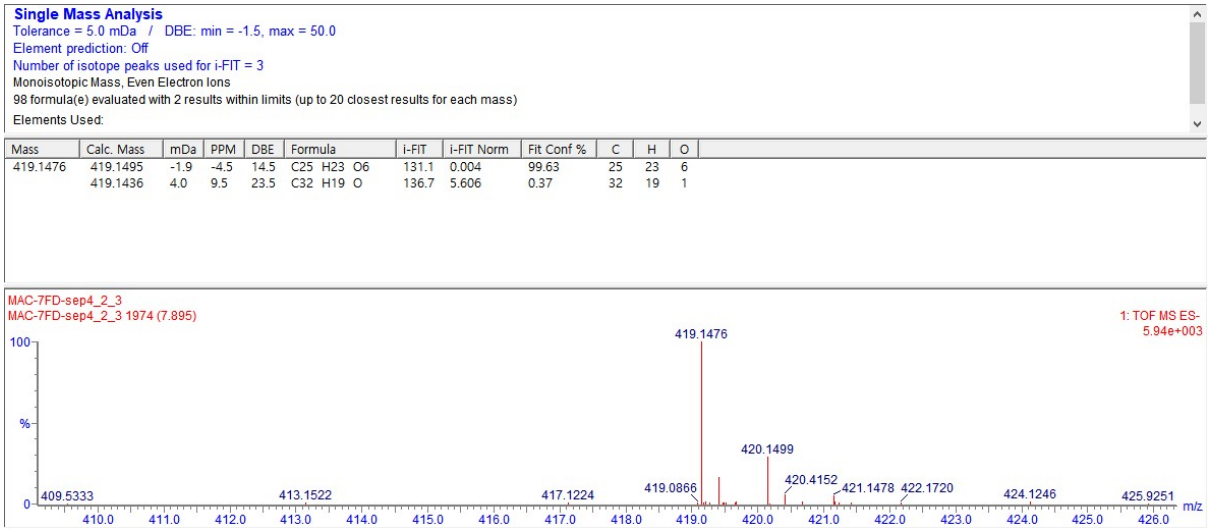

Figure S16. ECD spectrum of sanggenol W (**1**)

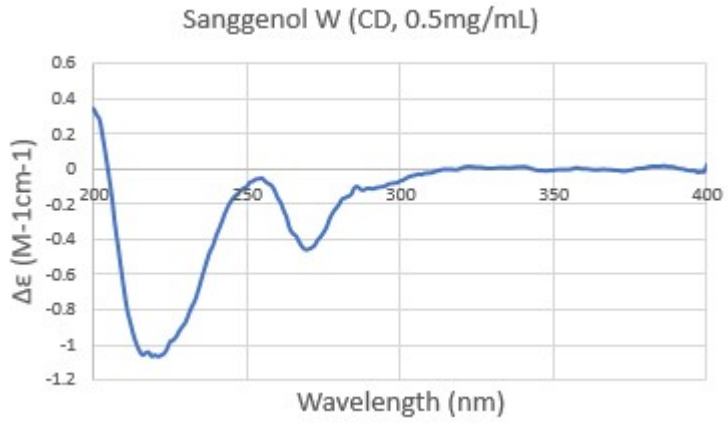

Figure S17. IR spectrum of sanggenol W (**1**)

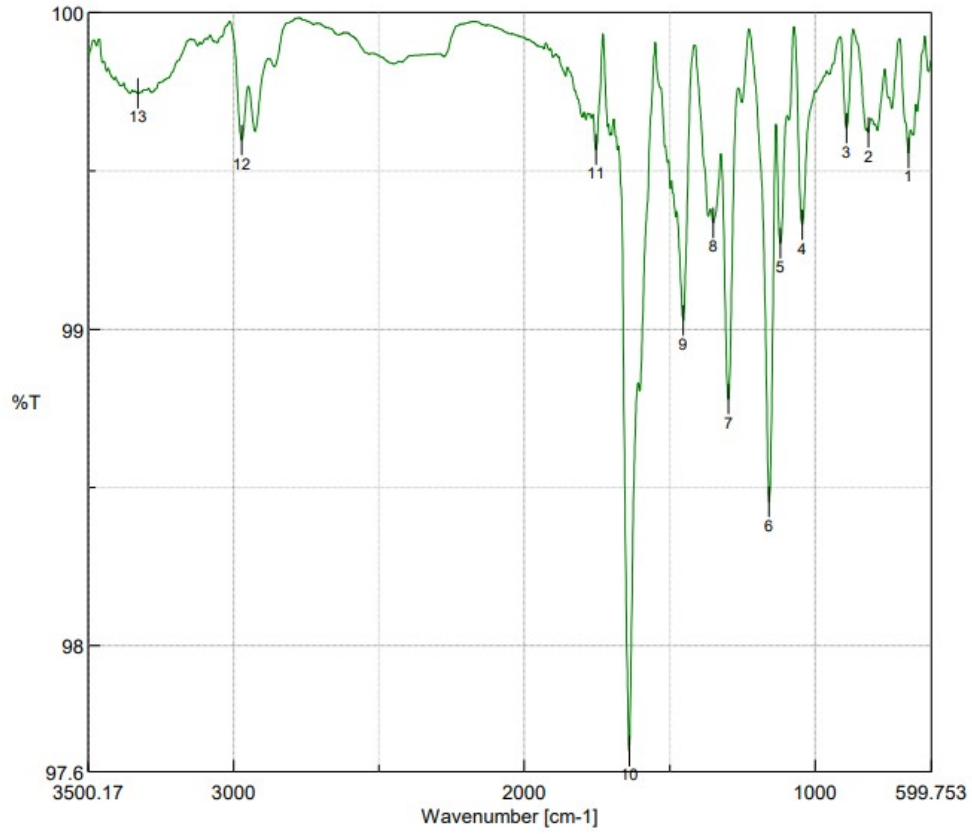

Result of Peak Picking

No.	Position	Intensity	No.	Position	Intensity
1	678.82	99.5559	2	816.706	99.6213
3	891.916	99.6336	4	1044.26	99.3296
5	1119.48	99.2707	6	1158.04	98.4535
7	1297.86	98.7775	8	1349.93	99.3345
9	1453.1	99.027	10	1639.2	97.6641
11	1753.94	99.5674	12	2972.73	99.5961
13	3329.5	99.7435			

Figure S18–S25. 1D and 2D NMR, MS, and IR spectra of morusalnol D (**2**)

Figure S18. ^{1}H NMR spectrum of morusalnol D (**2**) in $CDCl_3$

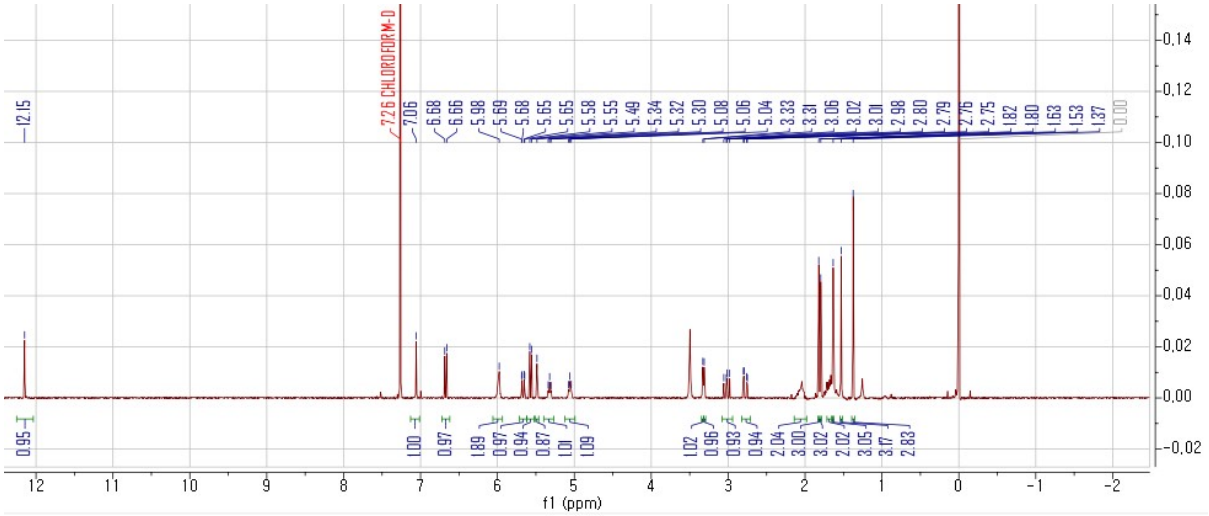

Figure S19. ^{13}C NMR spectrum of morusalnol D (**2**) in $CDCl_3$

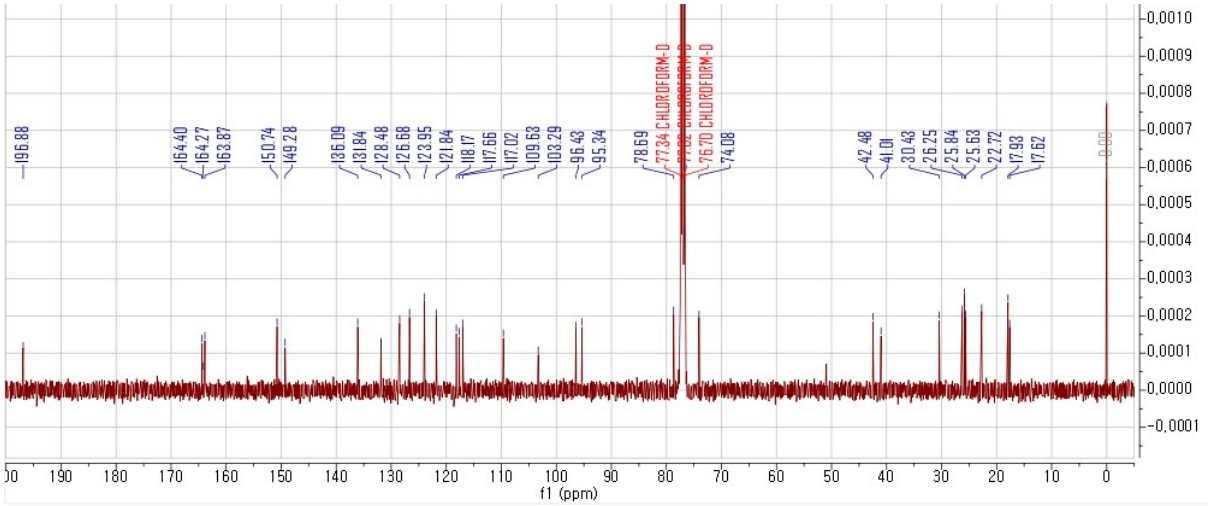

Figure S20. HSQC spectrum of morusalnol D (**2**) in $CDCl_3$

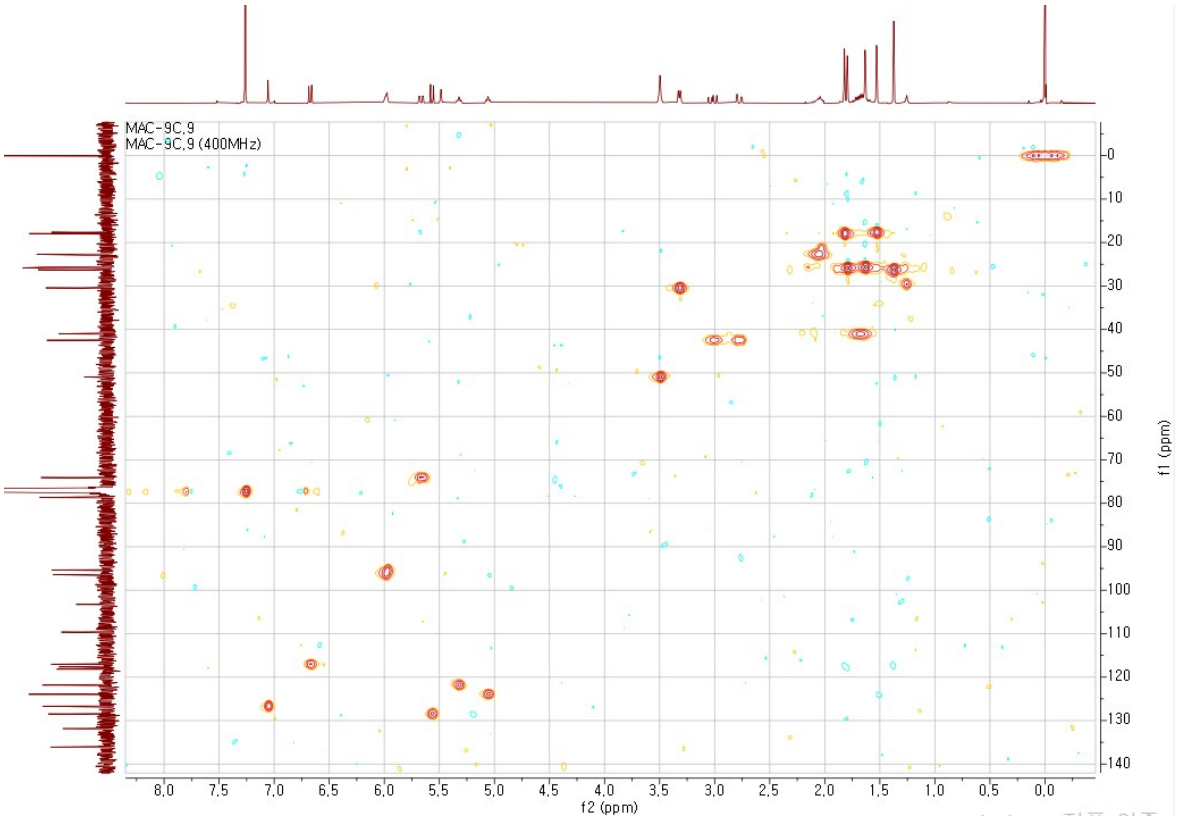

Figure S21. COSY spectrum of morusalnol D (**2**) in $CDCl_3$

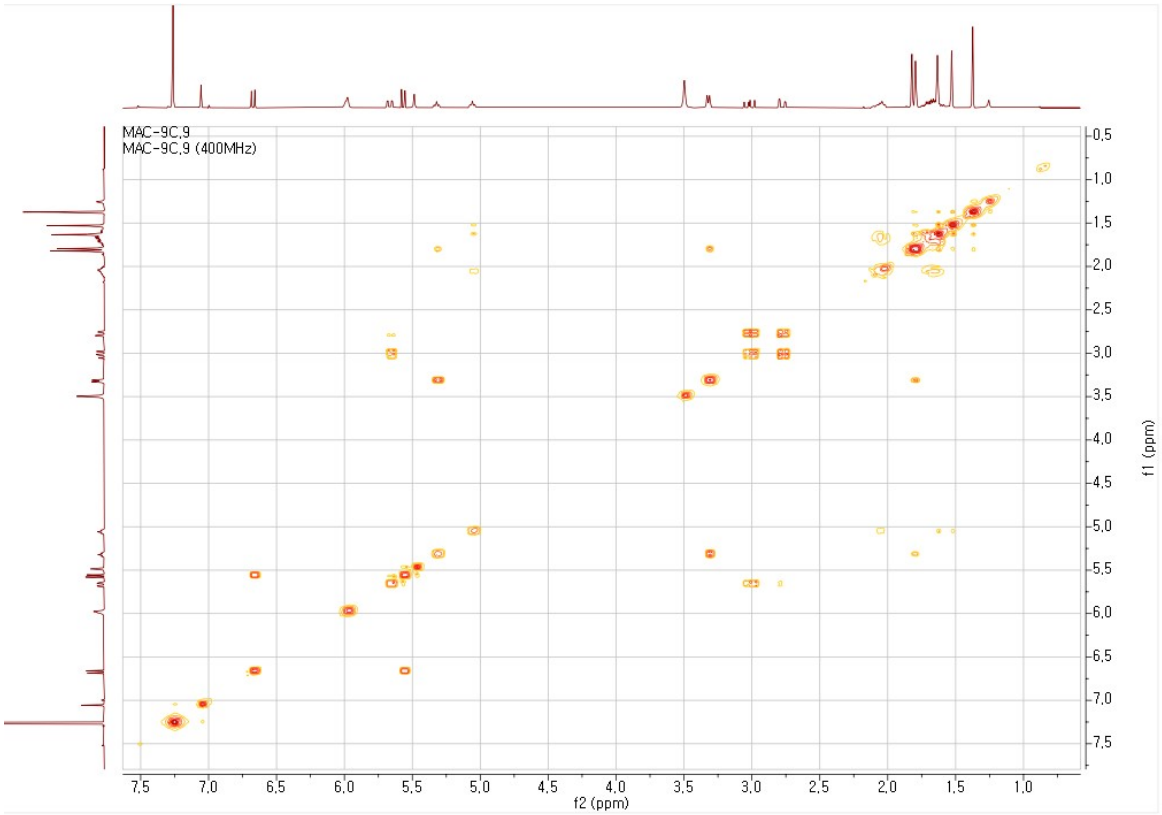

Figure S22. HMBC spectrum of morusalnol D (**2**) in $CDCl_3$

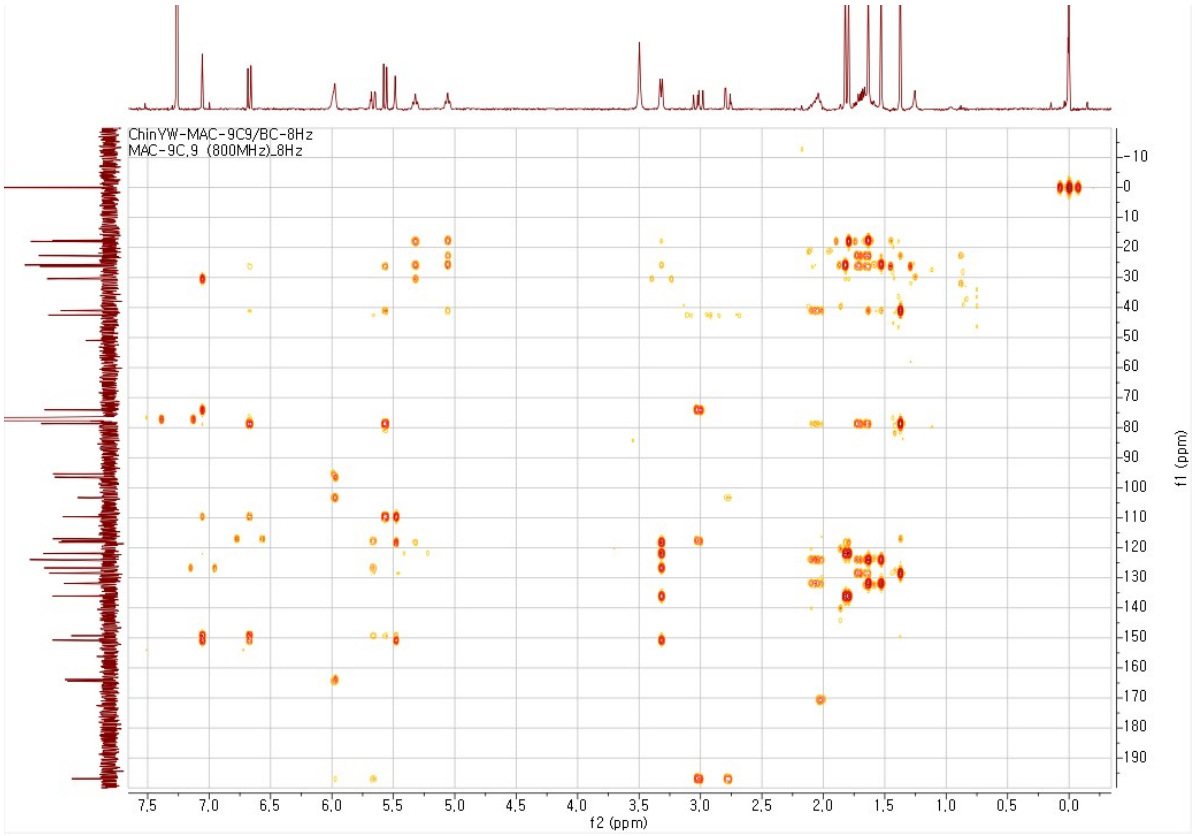

Figure S23. HRESIMS spectrum of morusalnol D (**2**)

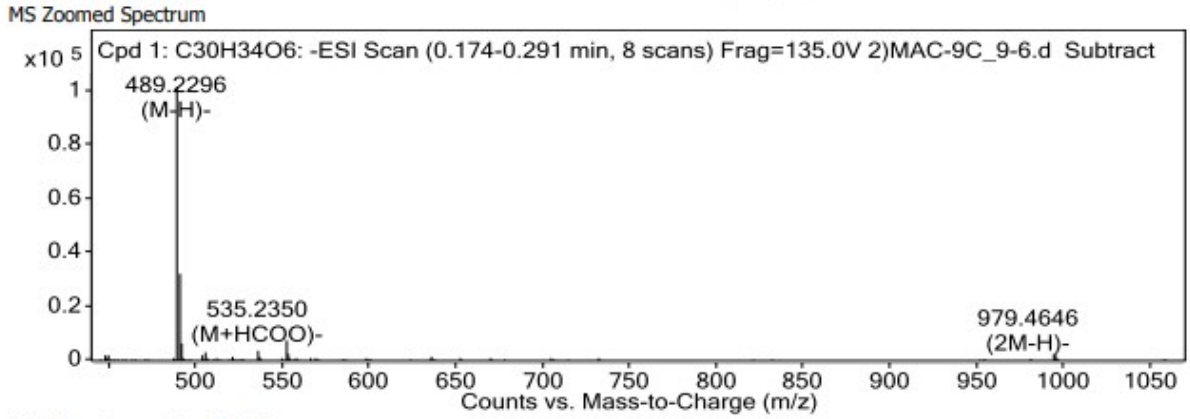

MS Spectrum Peak List

m/z	*Calc m/z*	Diff(ppm)	z	Abund	Formula	Ion
471.2094	471.2177	-17.64	-1	166	C30 H31 O5	(M-H)-[-H2O]
489.2296	489.2283	2.69		101413	C30 H33 O6	(M-H)-
525.2021	525.2049	-5.47	-1	625	C30 H34 Cl O6	(M+Cl)-
535.235	535.2337	2.4	-1	3946	C31 H35 O8	(M+HCOO)-
571.164	571.1529	19.4	-1	149	C30 H34 Br O6	(M+Br)-
585.2144	585.2106	6.5	-1	393	C32 H32 F3 O7	(M+CF3COO)-[-H2O]
603.2146	603.2211	-10.76	-1	166	C32 H34 F3 O8	(M+CF3COO)-
979.4646	979.4638	0.77	-1	571	C60 H67 O12	(2M-H)-
1025.4445	1025.4693	-24.2	-1	259	C61 H69 O14	(2M+HCOO)-
1039.4431	1039.4849	-40.26	-1	162	C62 H71 O14	(2M+CH3COO)-

Figure S24. ECD spectrum of morusalnol D (**2**)

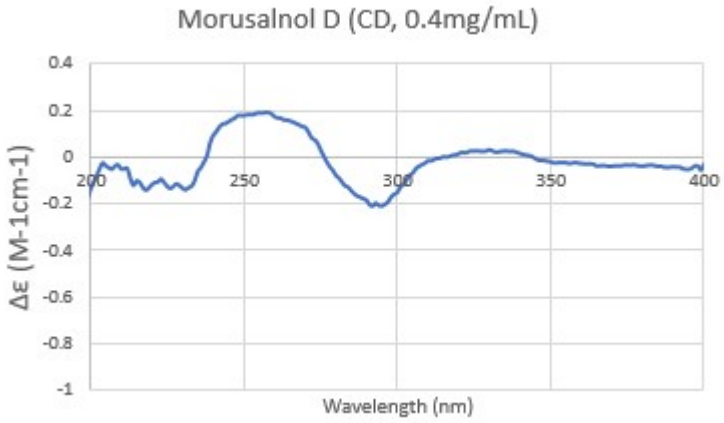

Figure S25. IR spectrum of morusalnol D (**2**)

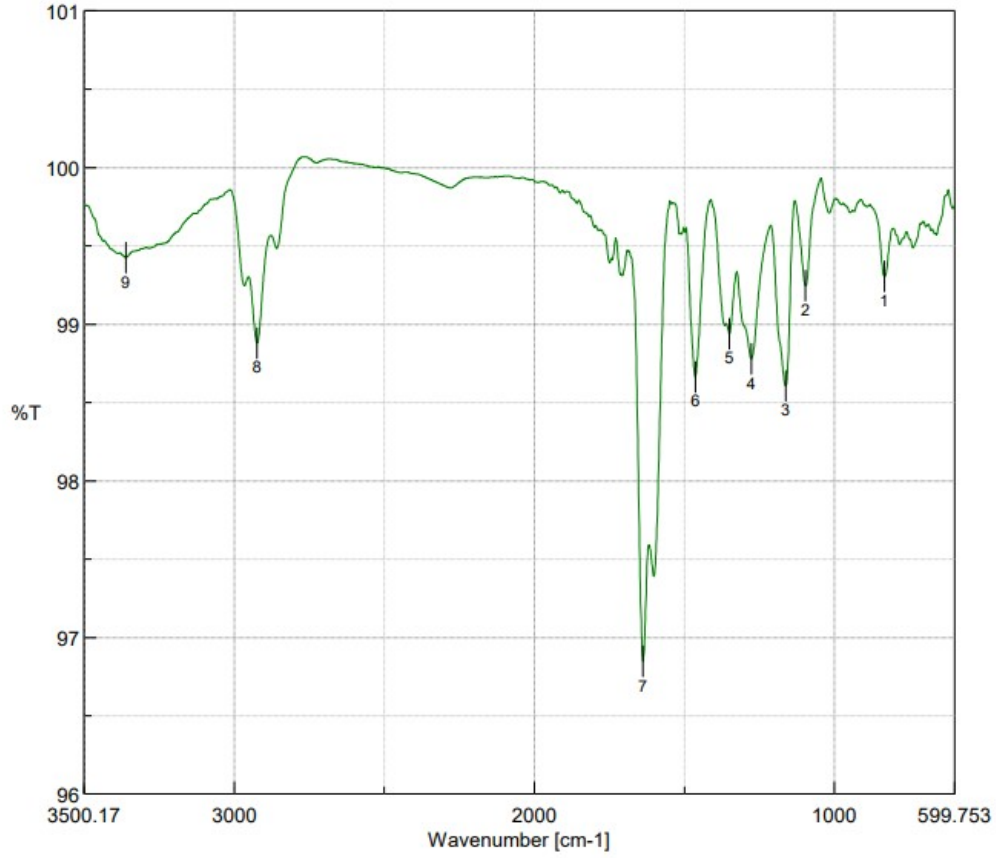

Result of Peak Picking

No.	Position	Intensity	No.	Position	Intensity
1	834.062	99.3027	2	1096.33	99.2437
3	1162.87	98.6058	4	1277.61	98.7784
5	1349.93	98.9367	6	1463.71	98.6628
7	1638.23	96.8474	8	2923.56	98.8782
9	3361.32	99.4242			

Figure S26–S33. 1D and 2D NMR, MS, and IR spectra of morusalnol E (**3**)

Figure S26. ^{1}H NMR spectrum of morusalnol E (**3**) in methanol-d_4

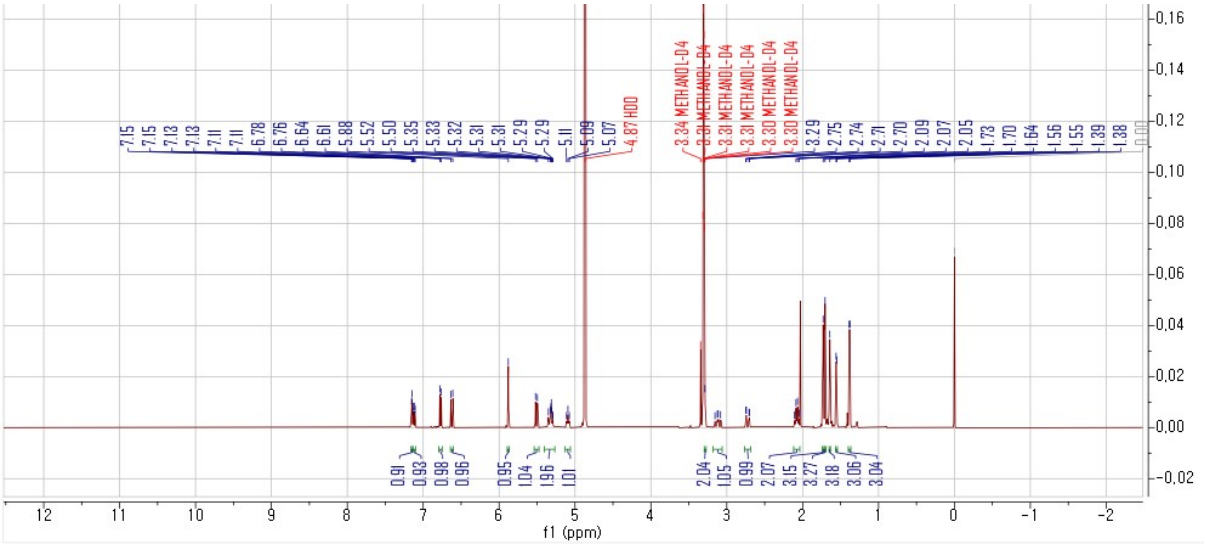

Figure S27. ^{13}C NMR spectrum of morusalnol E (**3**) in methanol-d_4

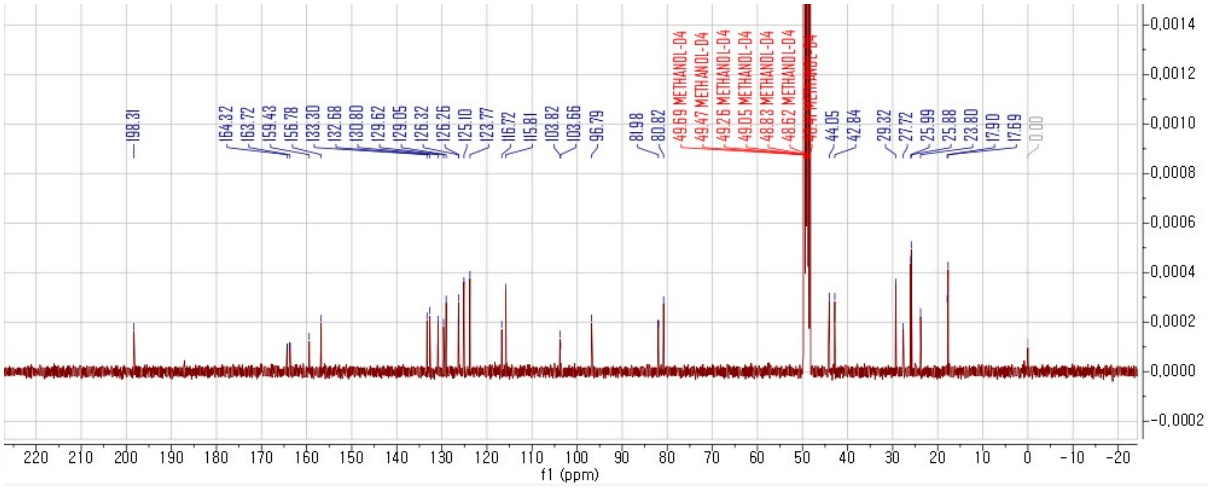

Figure S28. HSQC spectrum of morusalnol E (**3**) in methanol-d_4

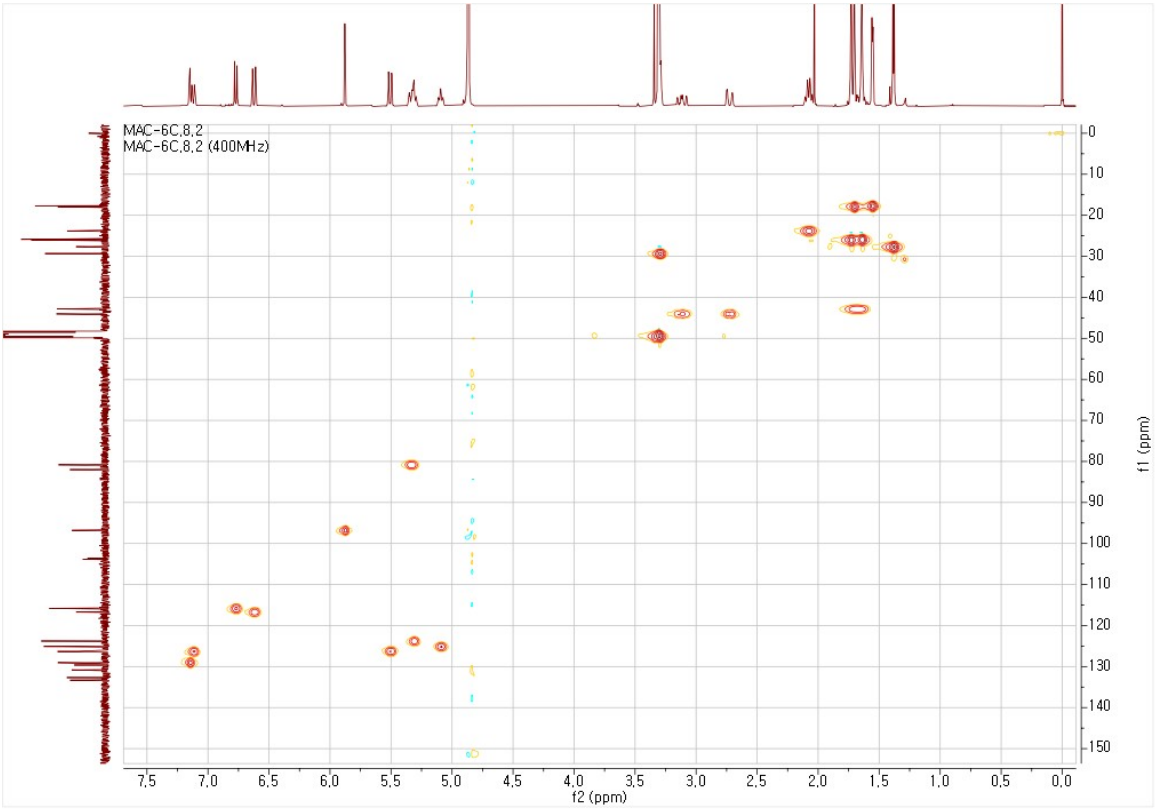

Figure S29. COSY spectrum of morusalnol E (**3**) in methanol-d_4

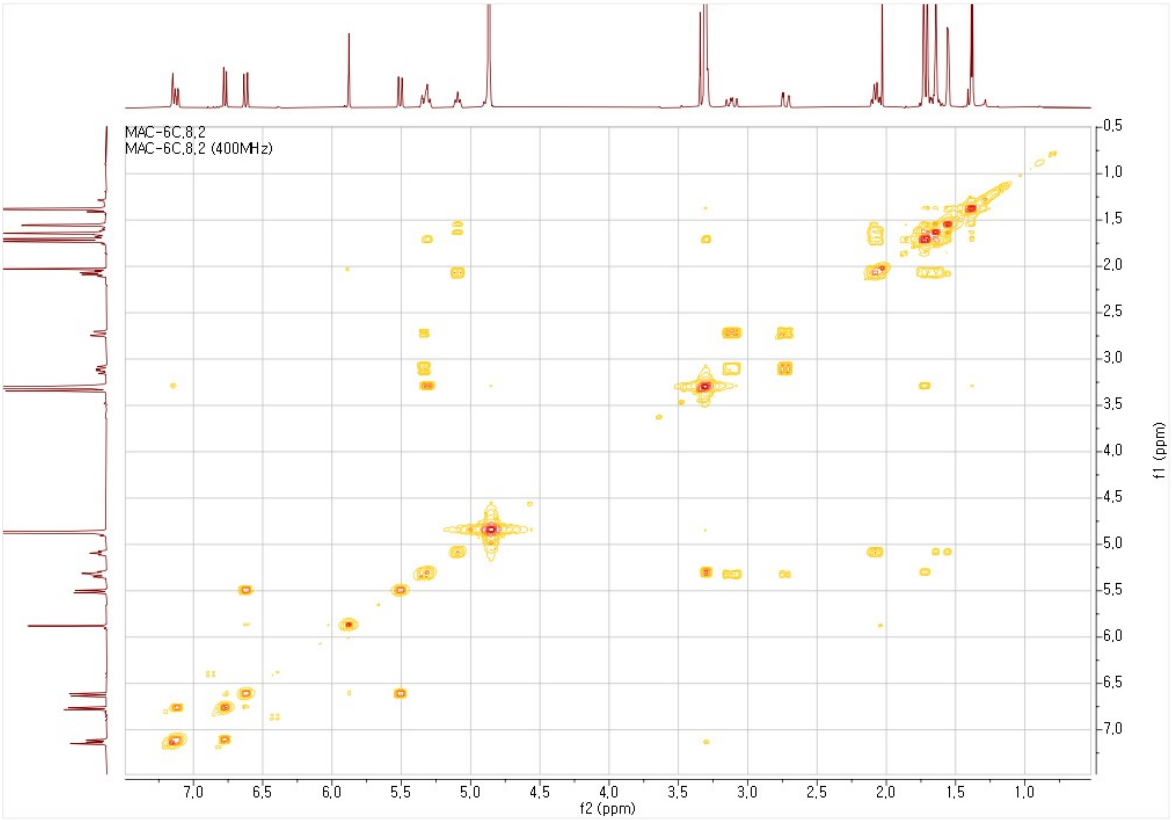

Figure S30. HMBC spectrum of morusalnol E (**3**) in methanol-d_4 (800 MHz)

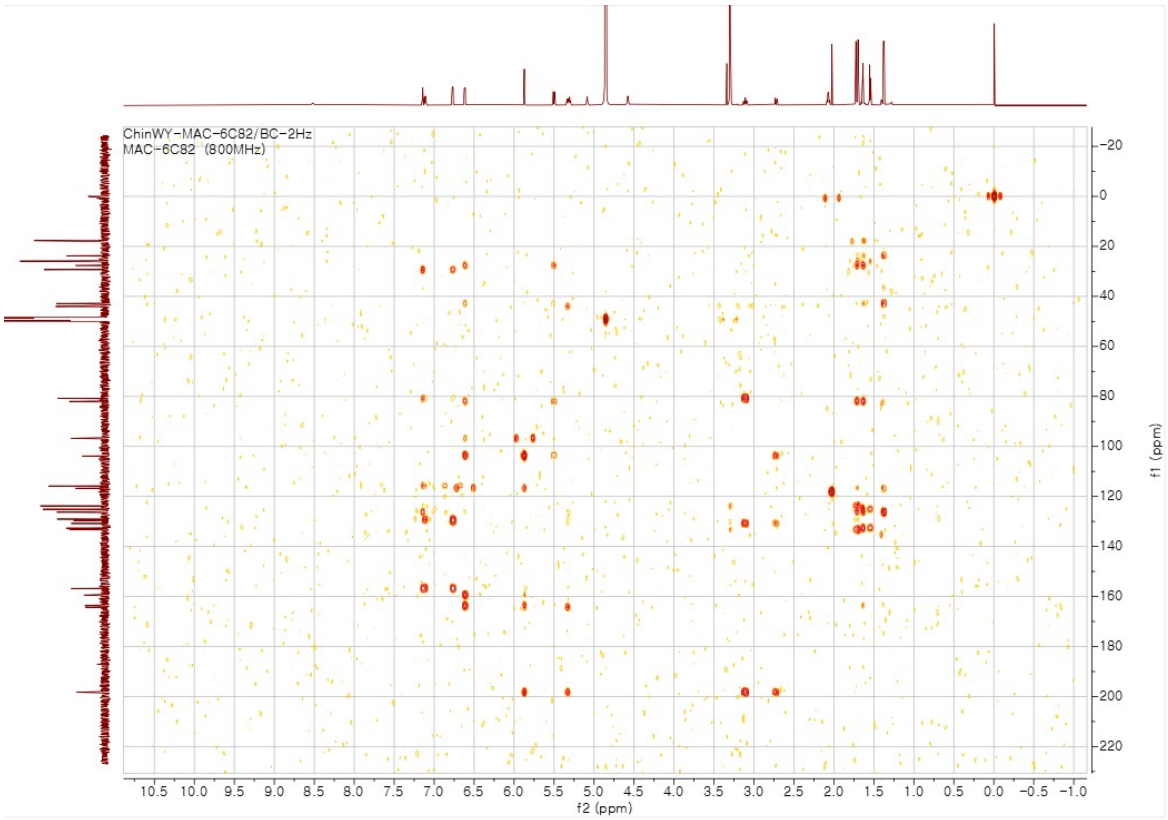

Figure S31. HRESIMS spectrum of morusalnol E (**3**)

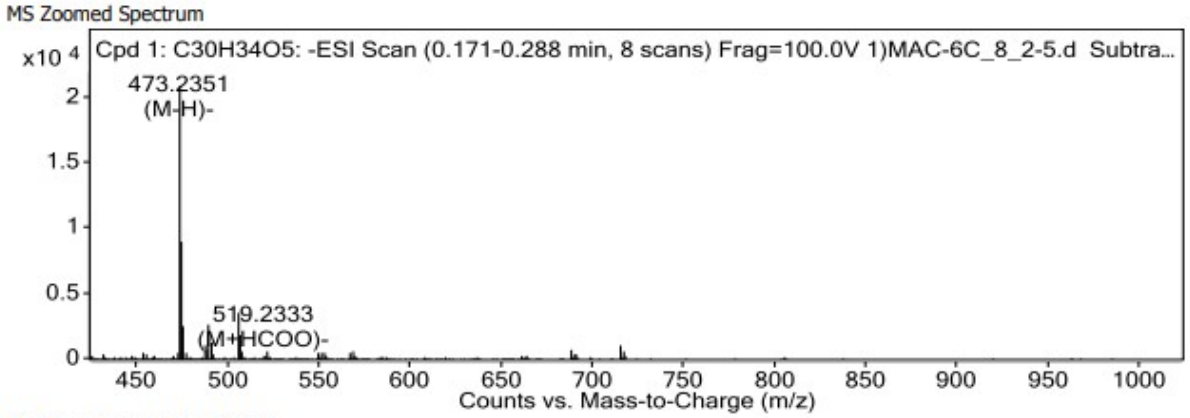

MS Spectrum Peak List

m/z	*Calc m/z*	Diff(ppm)	z	Abund	Formula	Ion
455.2268	455.2228	8.91	-1	64	C30 H31 O4	(M-H)-[-H2O]
473.2351	473.2333	3.72	-1	20859	C30 H33 O5	(M-H)-
491.1904	491.1995	-18.53	-1	82	C30 H32 Cl O4	(M+Cl)-[-H2O]
501.2209	501.2283	-14.77	-1	109	C31 H33 O6	(M+HCOO)-[-H2O]
509.2064	509.21	-7.2	-1	188	C30 H34 Cl O5	(M+Cl)-
519.2333	519.2388	-10.72	-1	376	C31 H35 O7	(M+HCOO)-
533.2375	533.2545	-31.86	-1	93	C32 H37 O7	(M+CH3COO)-
569.2223	569.2156	11.74	-1	372	C32 H32 F3 O6	(M+CF3COO)-[-H2O]
587.2204	587.2262	-9.96	-1	125	C32 H34 F3 O7	(M+CF3COO)-
993.4377	993.4795	-42.05	-1	55	C61 H69 O12	(2M+HCOO)-

Figure S32. ECD spectrum of morusalnol E (**3**)

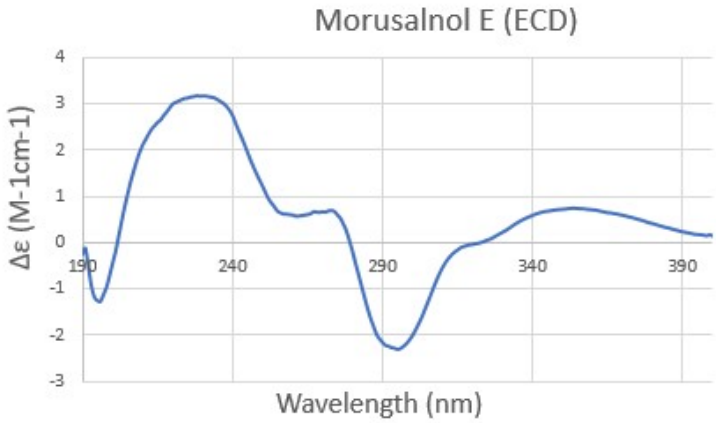

Figure S33. IR spectrum of morusalnol E (**3**)

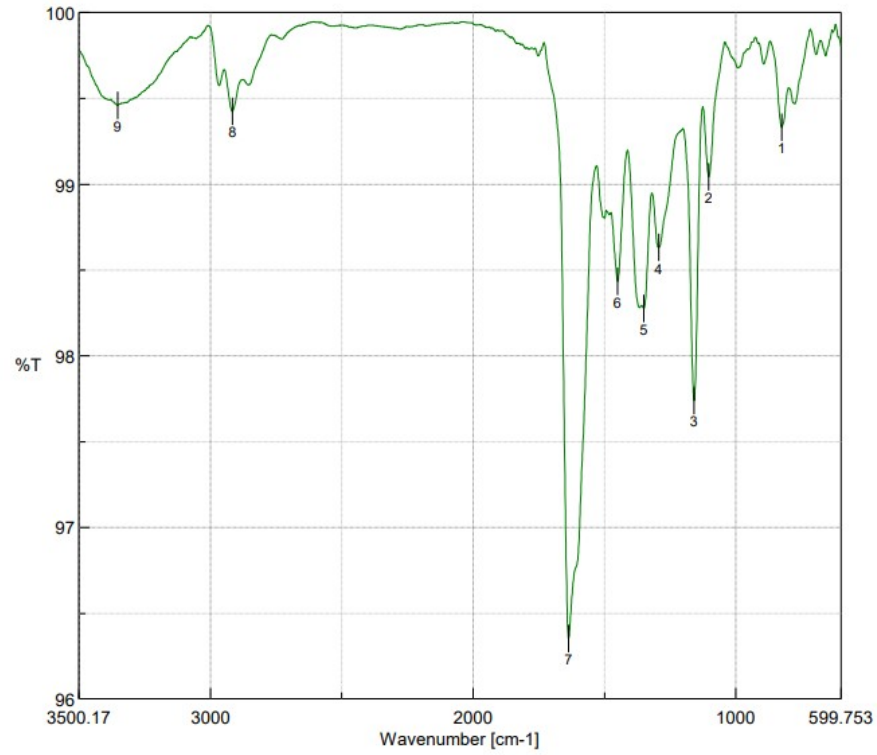

Result of Peak Picking

No.	Position	Intensity	No.	Position	Intensity
1	825.384	99.3305	2	1103.08	99.0419
3	1159.01	97.739	4	1294	98.63
5	1349.93	98.2747	6	1450.21	98.4334
7	1637.27	96.3512	8	2916.81	99.4227
9	3353.6	99.4588			

Figure S34–S41. 1D and 2D NMR, MS, and IR spectra of morusalnol F (**4**)

Figure S34. ^{1}H NMR spectrum of morusalnol F (**4**) in $CDCl_3$

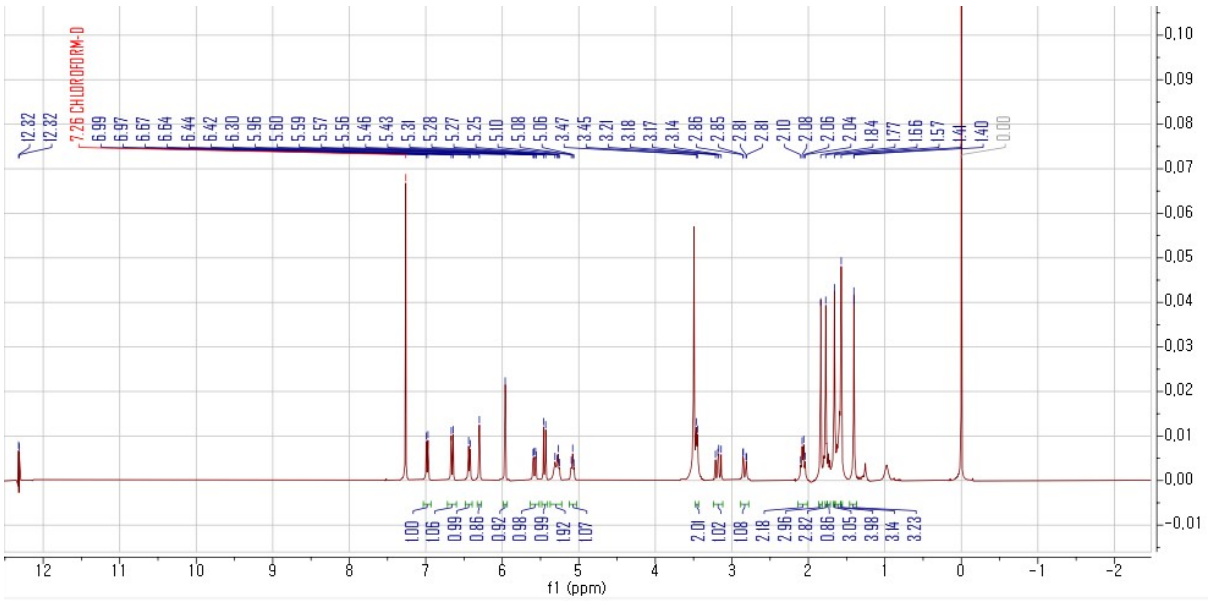

Figure S35. ^{13}C NMR spectrum of morusalnol F (**4**) in $CDCl_3$

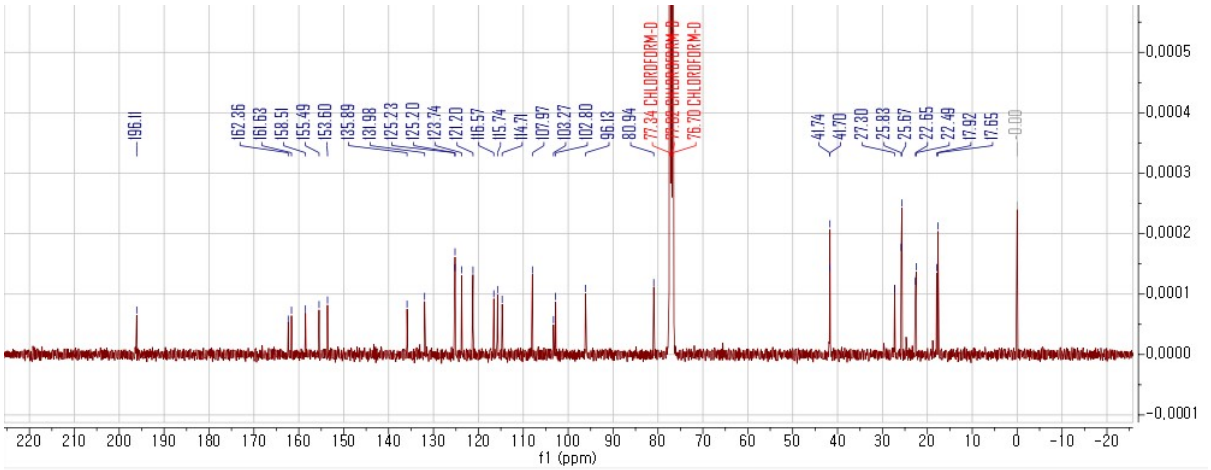

Figure S36. HSQC spectrum of morusalnol F (**4**) in $CDCl_3$

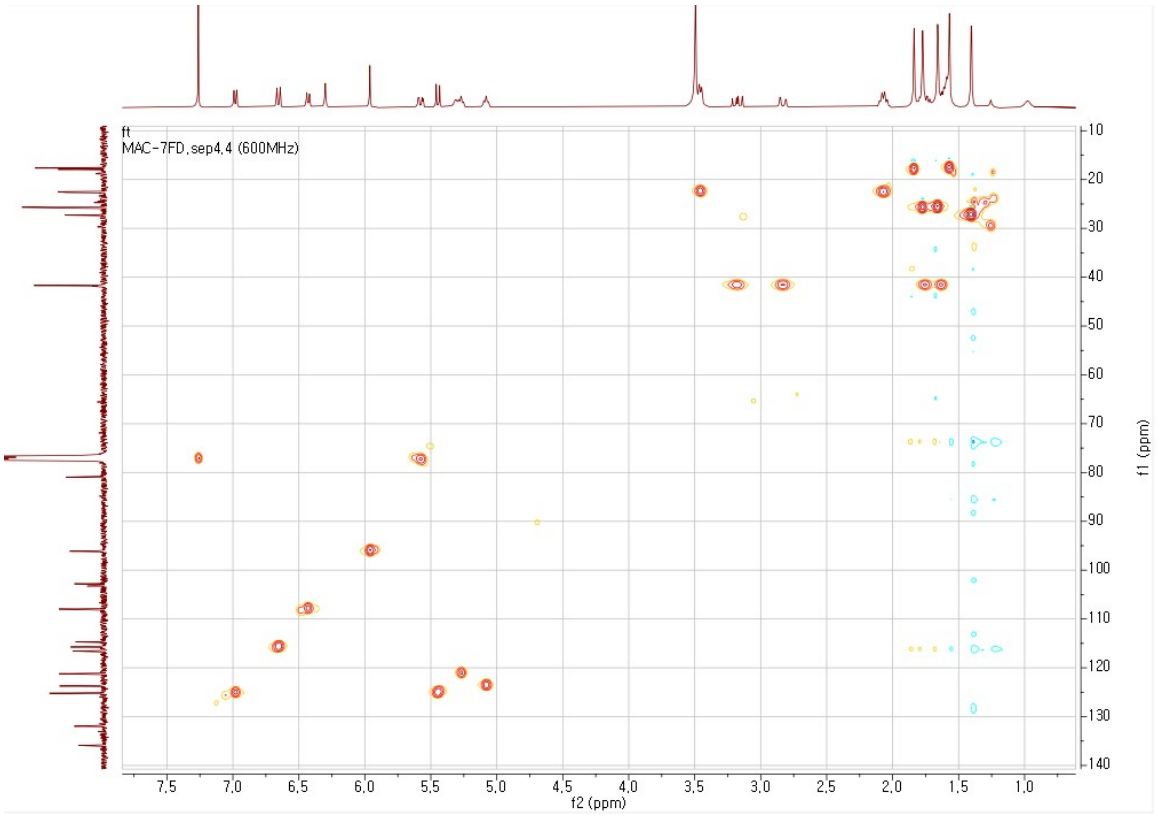

Figure S37. COSY spectrum of morusalnol F (**4**) in $CDCl_3$

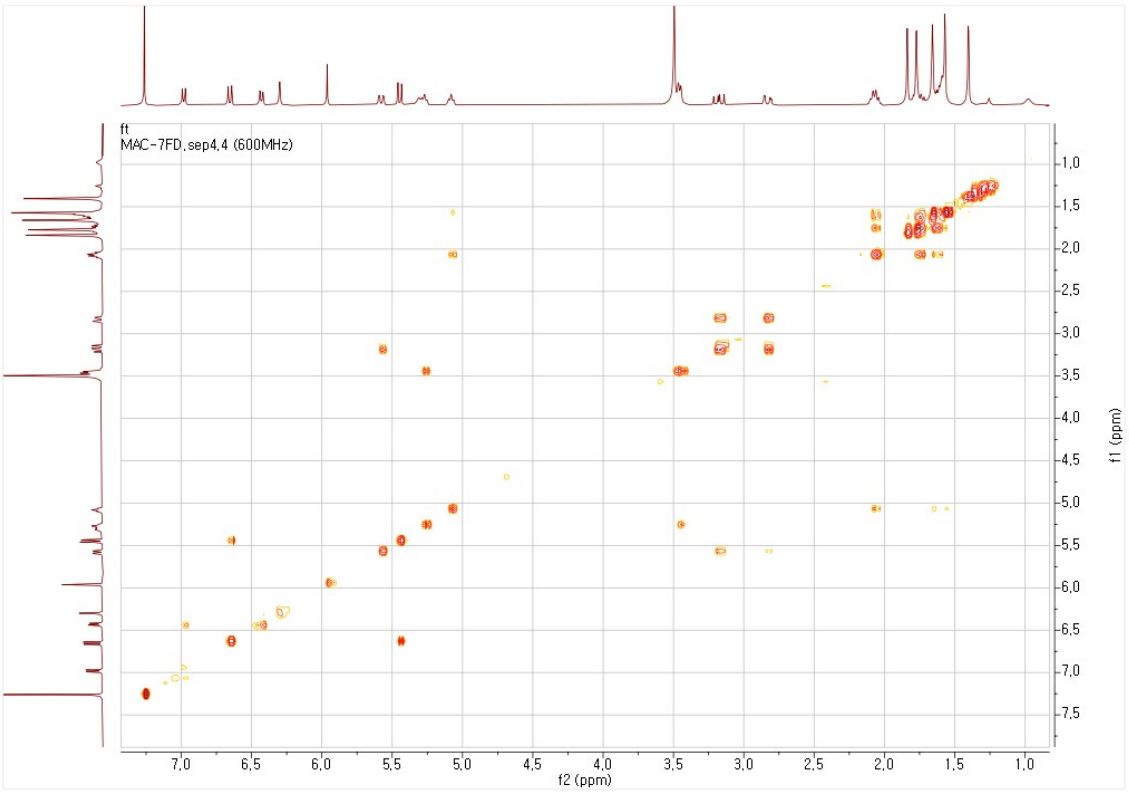

Figure S38. HMBC spectrum of morusalnol F (**4**) in $CDCl_3$

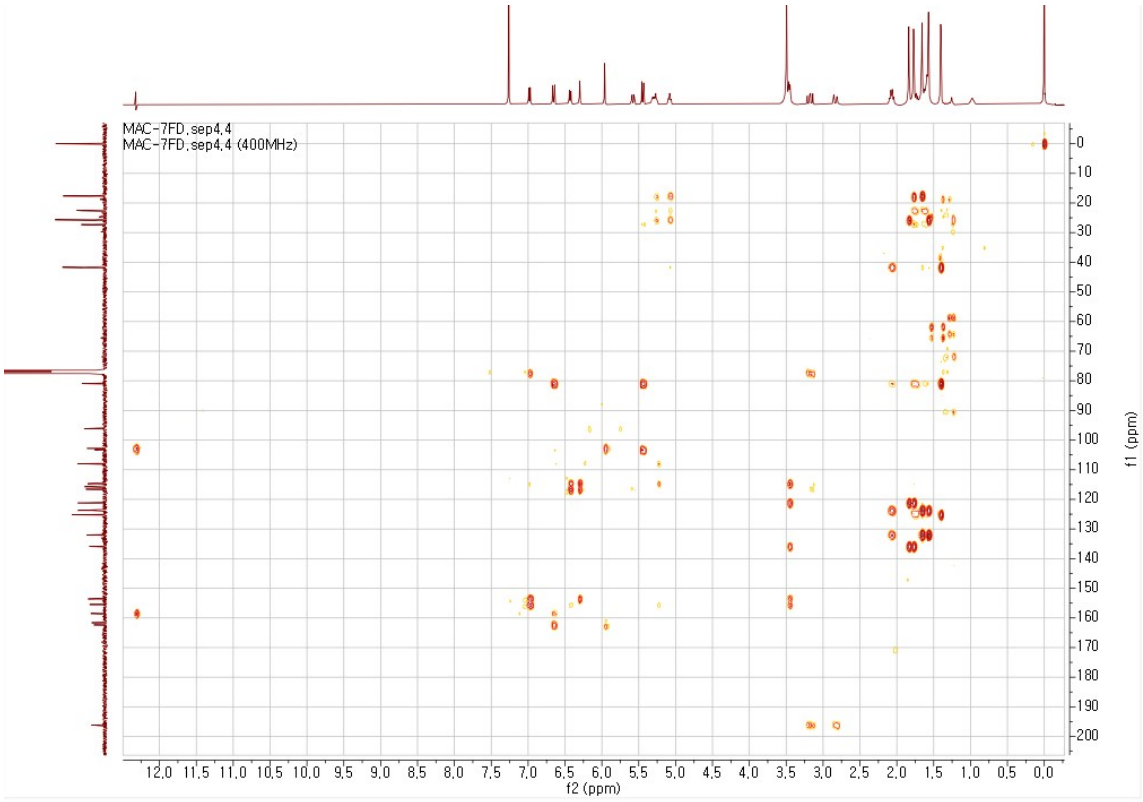

Figure S39. HRESIMS spectrum of morusalnol F (**4**)

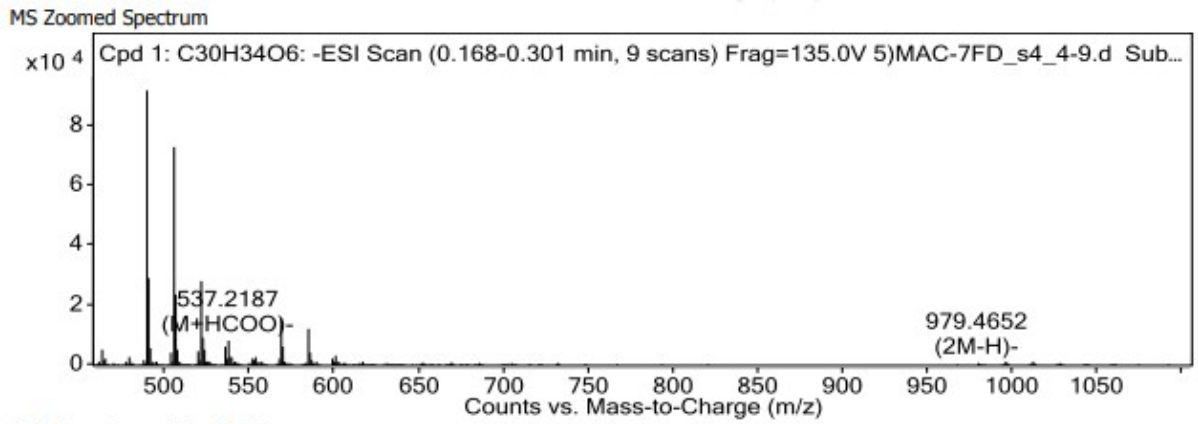

MS Spectrum Peak List

m/z	*Calc m/z*	Diff(ppm)	z	Abund	Formula	Ion
489.2304	489.2283	4.3		91714	C30 H33 O6	(M-H)-
507.2325	507.1944	75.11	-1	5411	C30 H32 Cl O5	(M+Cl)-[-H2O]
525.2109	525.2049	11.31	-1	1322	C30 H34 Cl O6	(M+Cl)-
535.2316	535.2337	-3.99	-1	6420	C31 H35 O8	(M+HCOO)-
585.2212	585.2106	18.11	-1	4503	C32 H32 F3 O7	(M+CF3COO)-[-H2O]
603.2168	603.2211	-7.15	-1	709	C32 H34 F3 O8	(M+CF3COO)-
979.4652	979.4638	1.43	-1	1055	C60 H67 O12	(2M-H)-
997.4671	997.4299	37.33	-1	512	C60 H66 Cl O11	(2M+Cl)-[-H2O]
1041.4312	1041.3794	49.71	-1	428	C60 H66 Br O11	(2M+Br)-[-H2O]
1059.4386	1059.39	45.88	-1	381	C60 H68 Br O12	(2M+Br)-

Figure S40. ECD spectrum of morusalnol F (**4**)

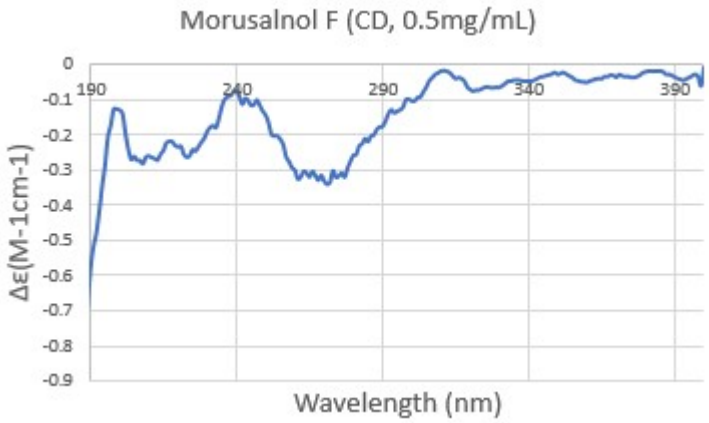

Figure S41. IR spectrum of morusalnol F (**4**)

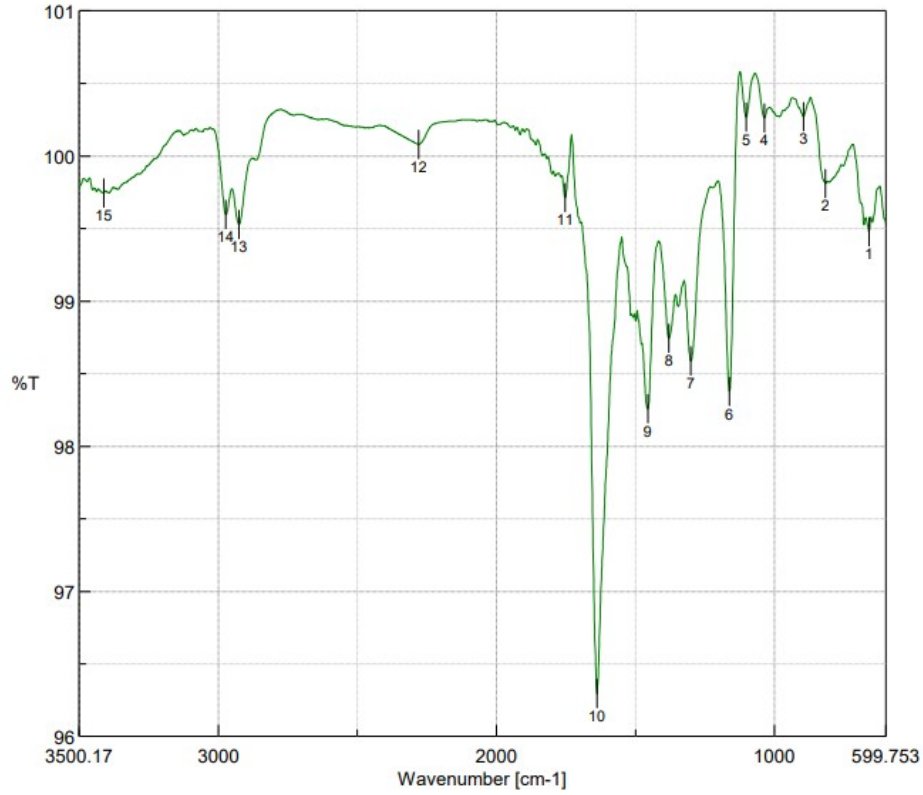

Result of Peak Picking

No.	Position	Intensity	No.	Position	Intensity
1	660.5	99.478	2	816.706	99.81
3	895.773	100.27	4	1036.55	100.261
5	1102.12	100.268	6	1161.9	98.3777
7	1300.75	98.5856	8	1379.82	98.7423
9	1455.99	98.2559	10	1638.23	96.2941
11	1752.98	99.7106	12	2279.45	100.079
13	2925.48	99.5268	14	2972.73	99.5956
15	3411.46	99.7426			

Figure S42–S48. 1D and 2D NMR, MS, and IR spectra of neovanone A (**5**)

Figure S42. ^{1}H NMR spectrum of neovanone A (**5**) in methanol-d_4

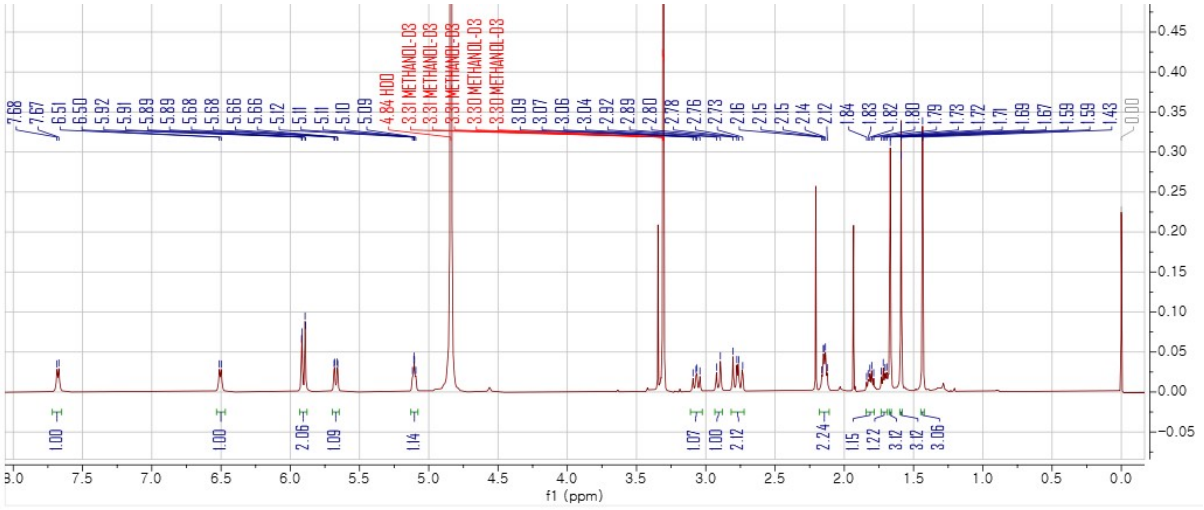

Figure S43. ^{13}C NMR spectrum of neovanone A (**5**) in methanol-d_4

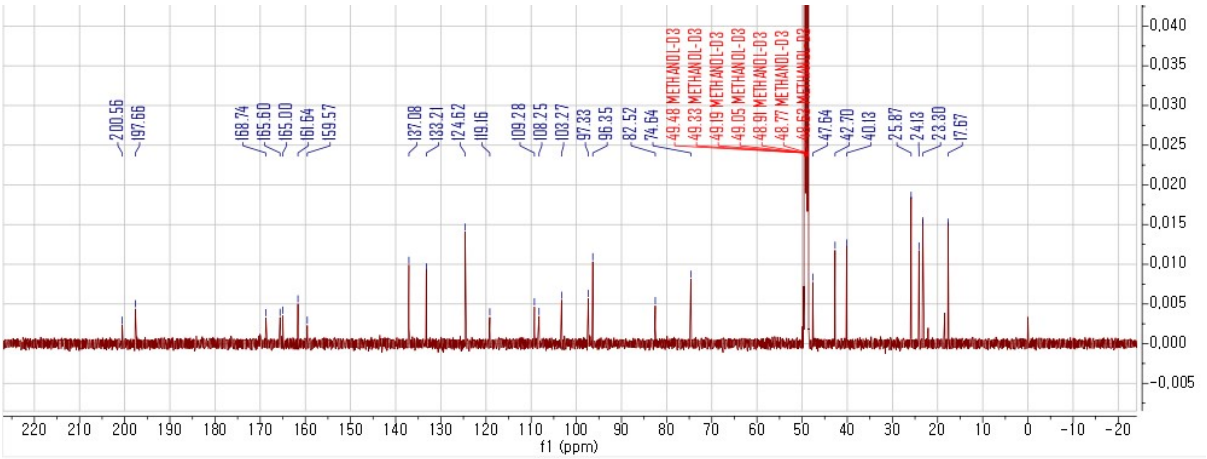

Figure S44. HSQC spectrum of neovanone A (**5**) in methanol-d_4

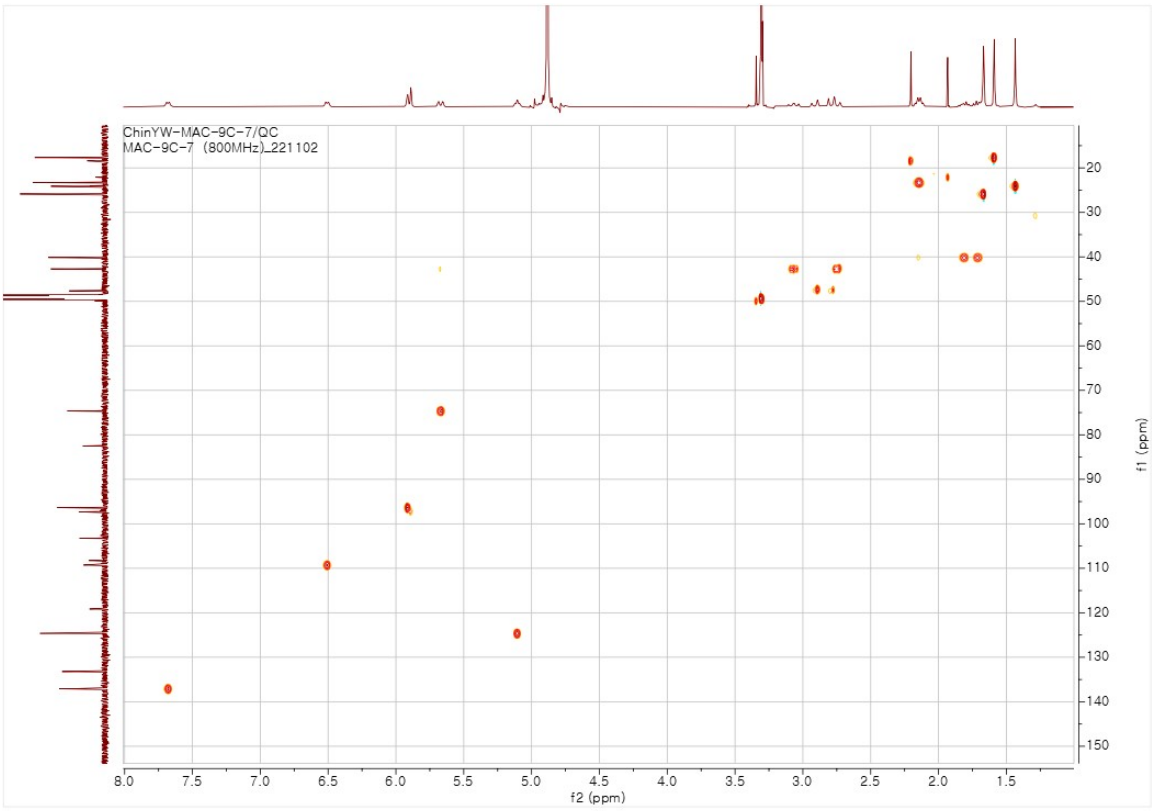

Figure S45. COSY spectrum of neovanone A (**5**) in methanol-d_4

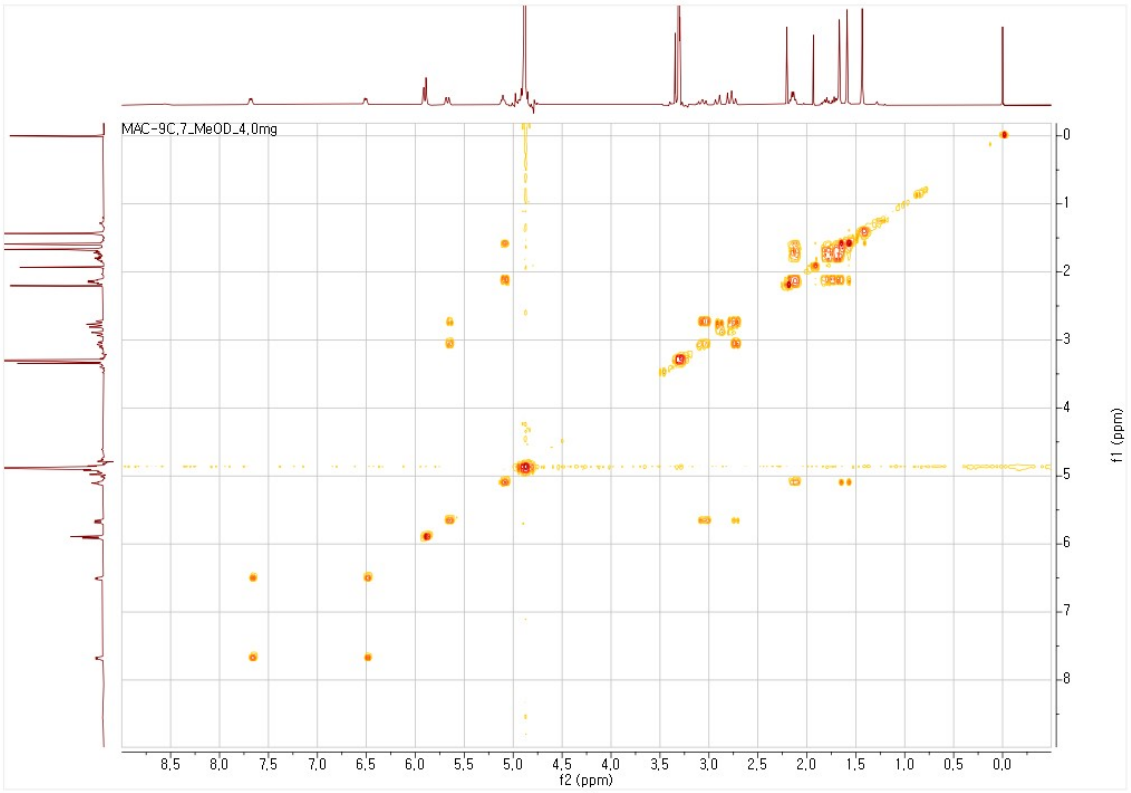

Figure S46. HMBC spectrum of neovanone A (**5**) in methanol-d_4

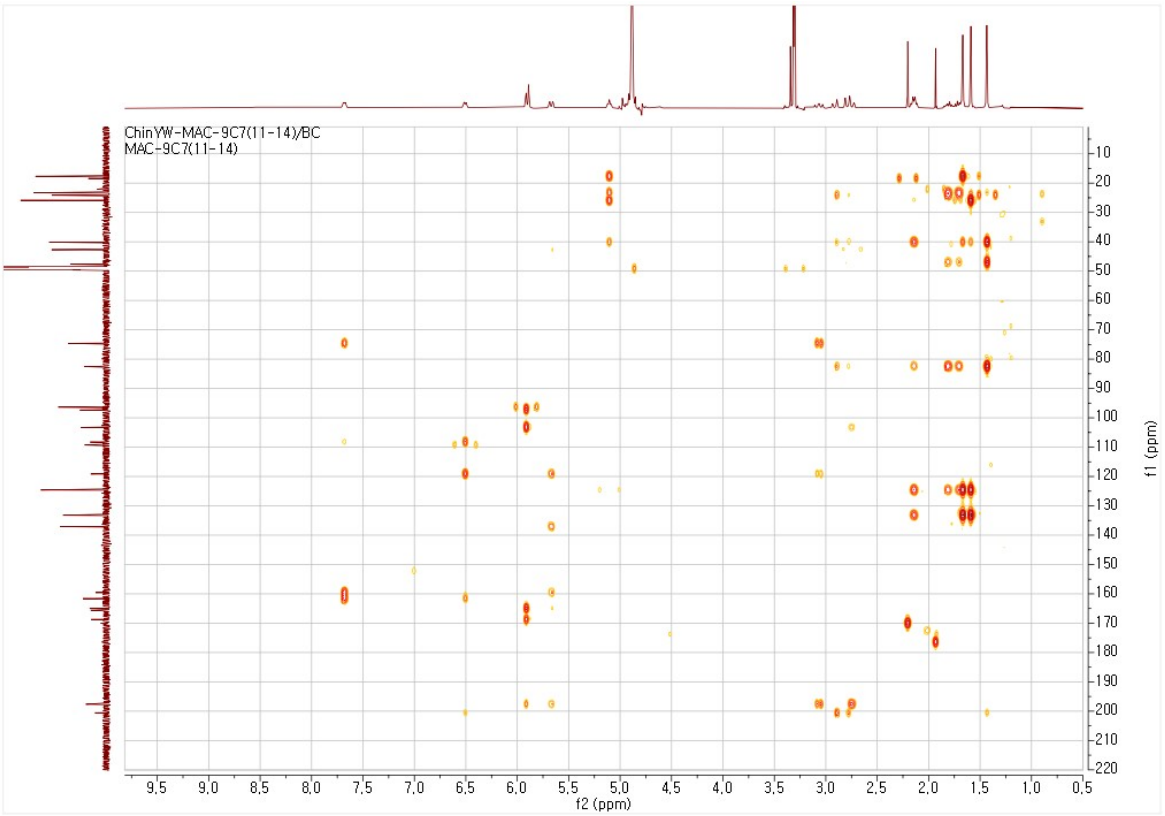

Figure S47. HRESIMS spectrum of neovanone A (**5**)

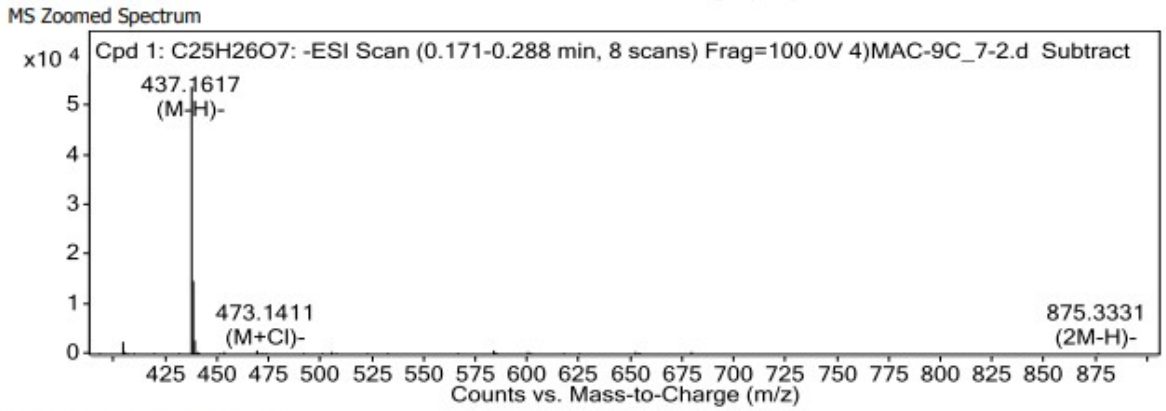

MS Spectrum Peak List

m/z	*Calc m/z*	Diff(ppm)	z	Abund	Formula	Ion
239.9037				4003		
241.8987				67032		
243.8994				48973		
245.895				18149		
419.147	419.15	-7.22	-1	247	C25 H23 O6	(M-H)-[-H2O]
437.1617	437.1606	2.46	-1	53752	C25 H25 O7	(M-H)-
438.1653	438.164	2.96	-1	14734	C25 H25 O7	(M-H)-
473.1411	473.1373	8.11	-1	181	C25 H26 Cl O7	(M+Cl)-
533.1405	533.1429	-4.47	-1	133	C27 H24 F3 O8	(M+CF3COO)-[-H2O]
875.3331	875.3284	5.31	-1	190	C50 H51 O14	(2M-H)-

Figure S48. IR spectrum of neovanone A (**5**)

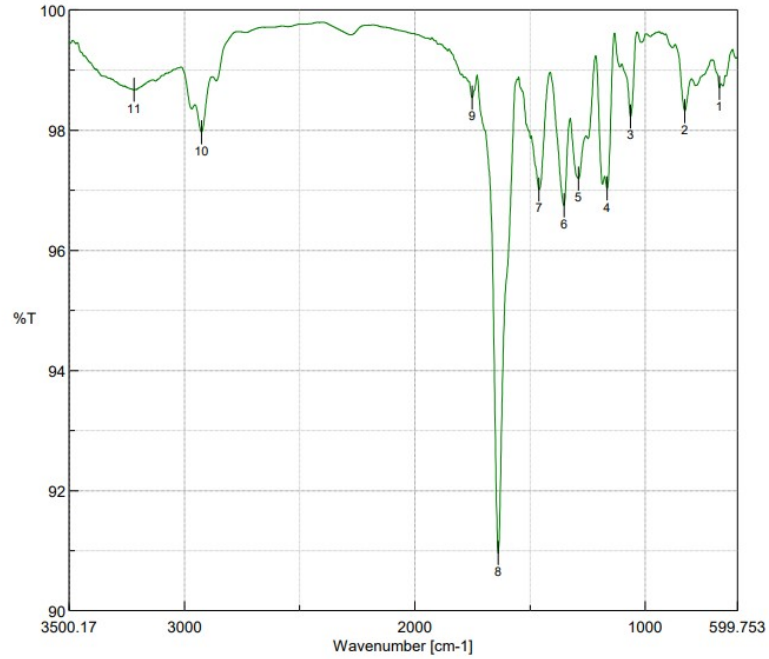

Result of Peak Picking

No.	Position	Intensity	No.	Position	Intensity
1	678.82	98.6999	2	828.277	98.3154
3	1063.55	98.226	4	1165.76	97.0259
5	1290.14	97.1922	6	1352.82	96.7439
7	1461.78	97.012	8	1638.23	90.9563
9	1751.05	98.5397	10	2925.48	97.9638
11	3218.61	98.6702			

Figure S49–S57. 1D and 2D NMR, MS, and IR spectra of neovanone B (**6**)

Figure S49. ^{1}H NMR spectrum of neovanone B (**6**) in methanol-d_4

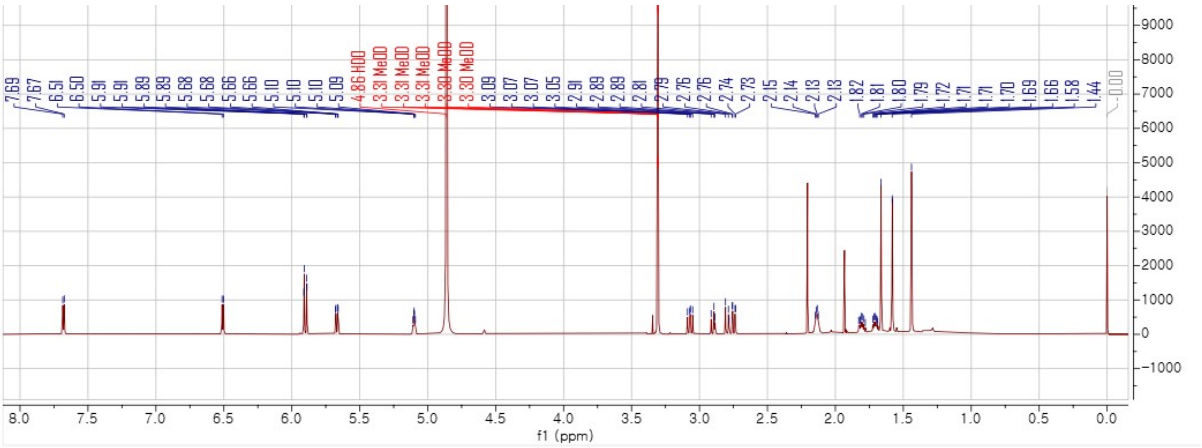

Figure S50. ^{13}C NMR spectrum of neovanone B (**6**) in methanol-d_4

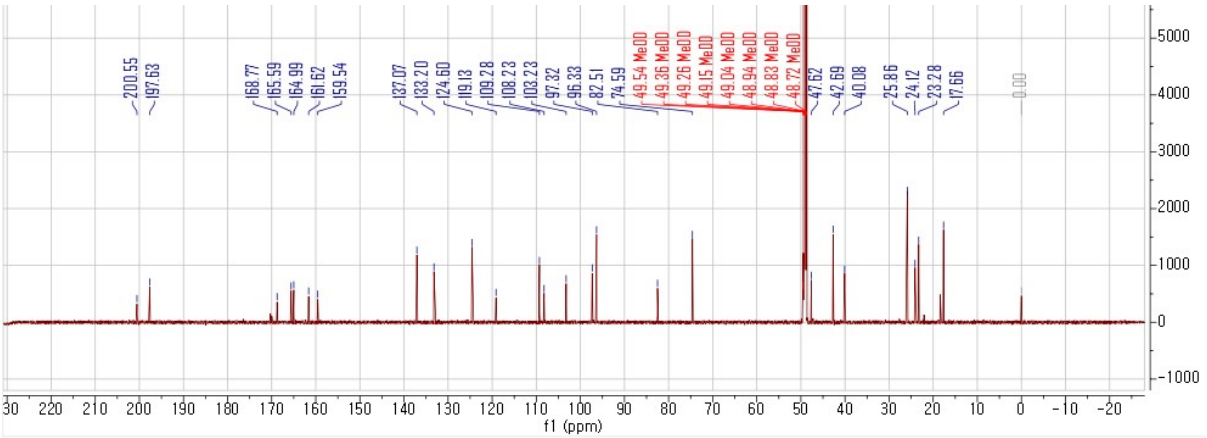

Figure S51. HSQC spectrum of neovanone B (**6**) in methanol-d_4

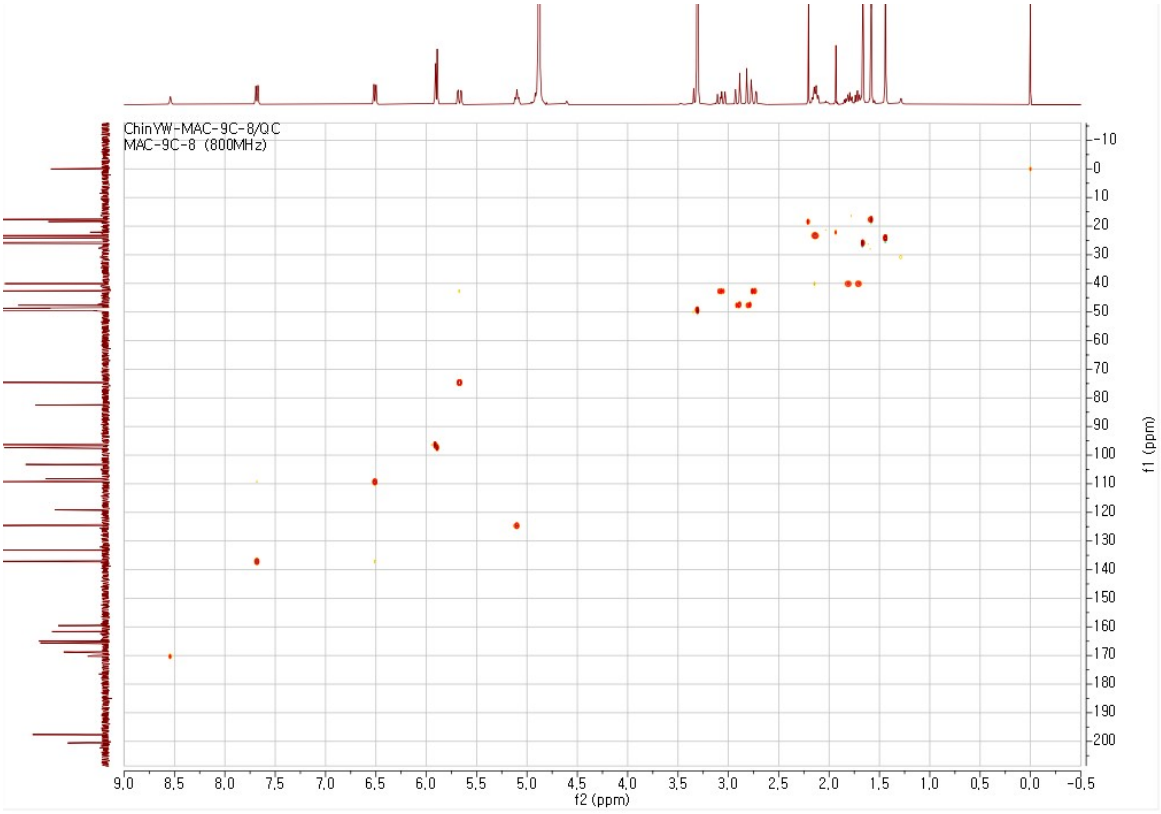

Figure S52. COSY spectrum of neovanone B (**6**) in methanol-d_4

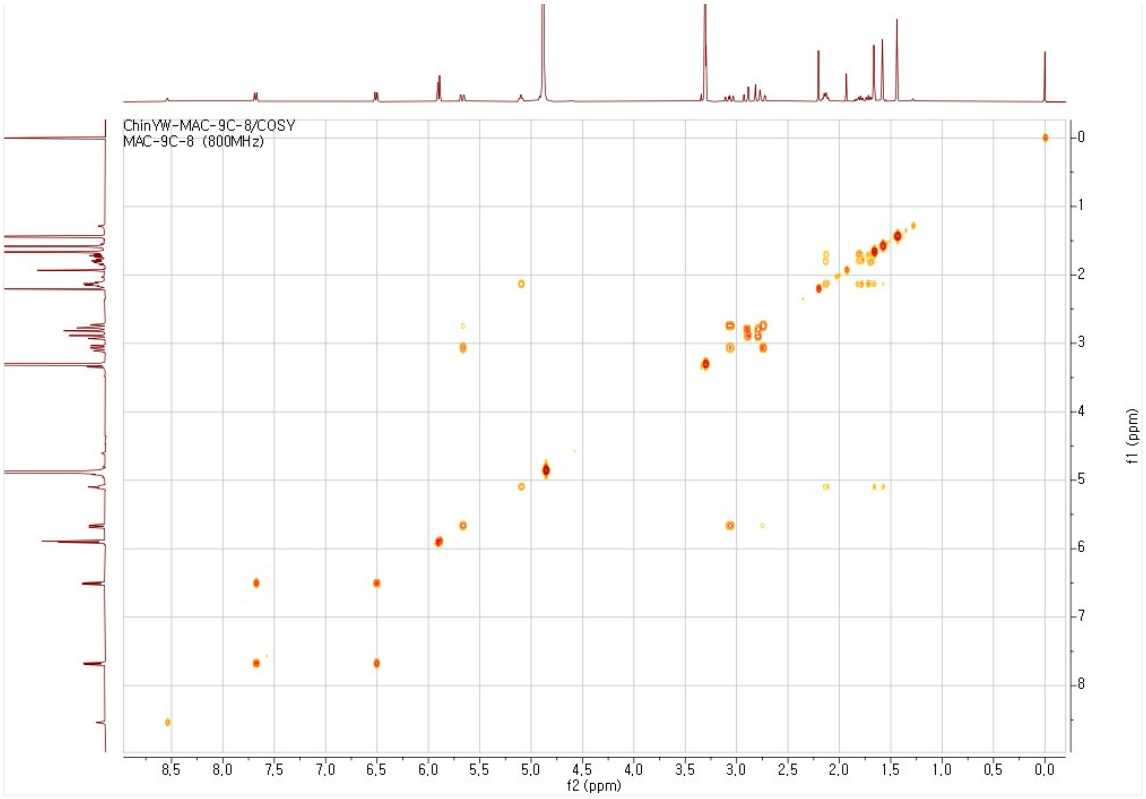

Figure S53. HMBC spectrum of neovanone B (**6**) in methanol-d_4

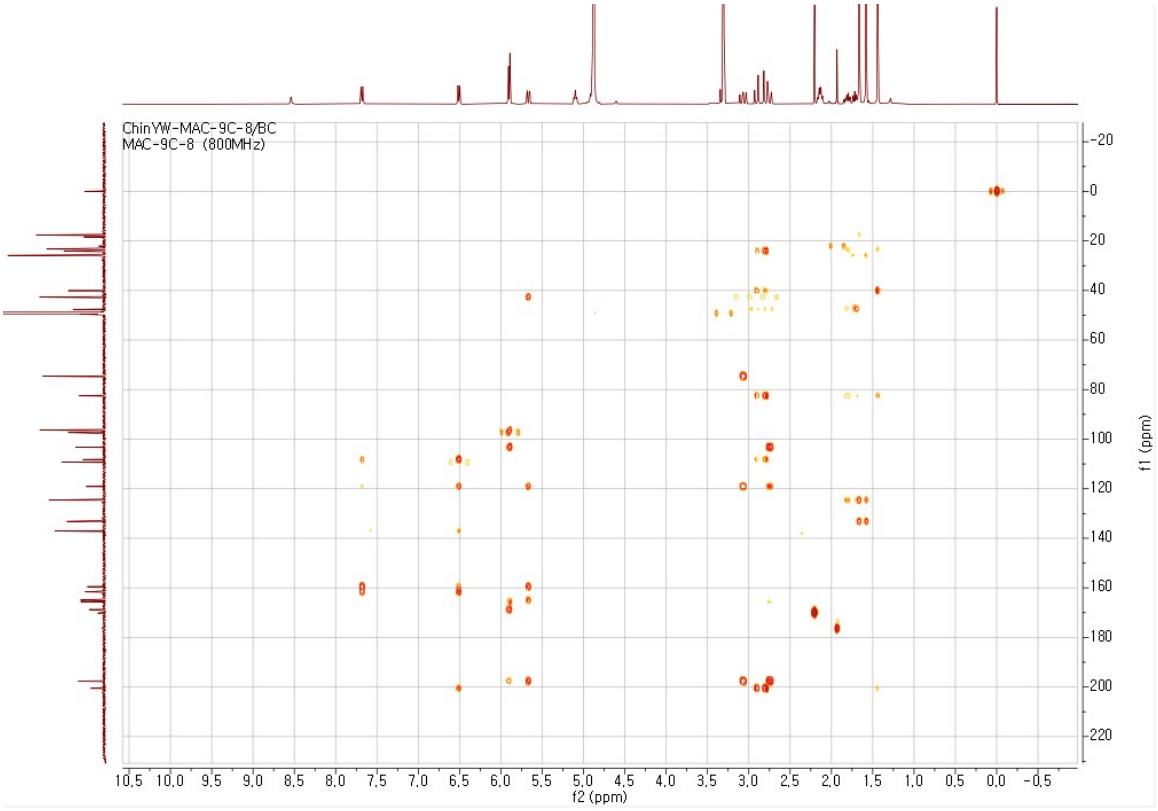

Figure S54. HRESIMS spectrum of neovanone B (**6**)

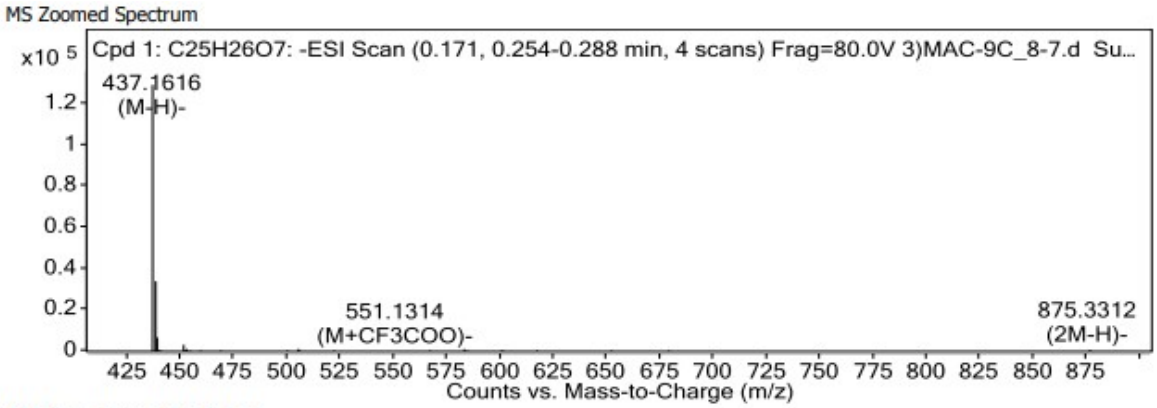

MS Spectrum Peak List

m/z	*Calc m/z*	Diff(ppm)	z	Abund	Formula	Ion
437.1616	437.1606	2.33		128914	C25 H25 O7	(M-H)-
438.1658	438.164	4.07		33889	C25 H25 O7	(M-H)-
438.2808				1459		
438.3486				1116		
439.1685	439.1666	4.2		6702	C25 H25 O7	(M-H)-
455.1527	455.1267	57.11	-1	169	C25 H24 Cl O6	(M+Cl)-[-H2O]
473.1255	473.1373	-24.83	-1	127	C25 H26 Cl O7	(M+Cl)-
497.1507	497.1817	-62.33	-1	55	C27 H29 O9	(M+CH3COO)-
551.1314	551.1534	-39.93	-1	107	C27 H26 F3 O9	(M+CF3COO)-
875.3312	875.3284	3.21	-1	656	C50 H51 O14	(2M-H)-

Figure S55. IR spectrum of neovanone B (**6**)

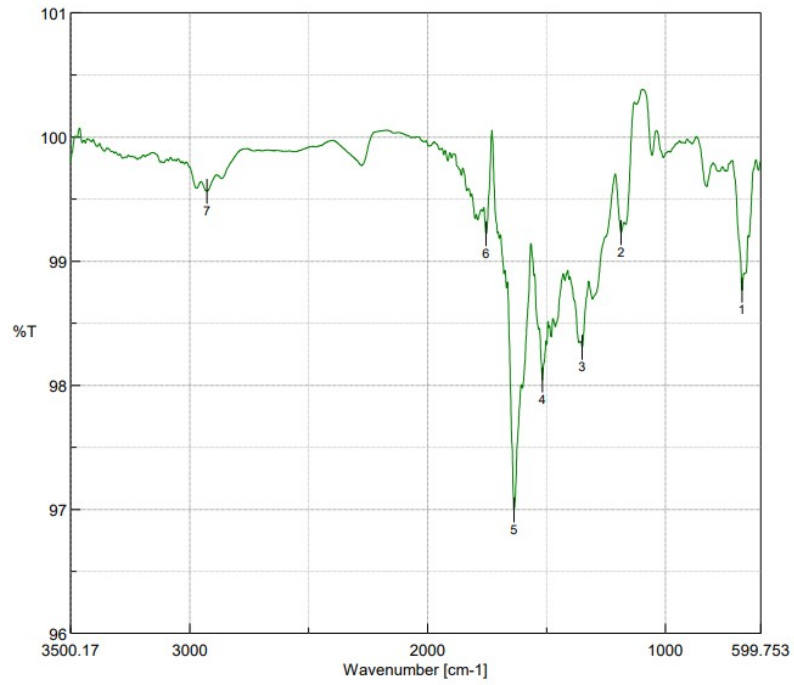

Result of Peak Picking

No.	Position	Intensity	No.	Position	Intensity
1	678.82	98.7635	2	1186.97	99.228
3	1349.93	98.3047	4	1517.7	98.0416
5	1637.27	96.9937	6	1753.94	99.2185
7	2927.41	99.5625			

Figure S56. HPLC chromatogram for MAC-9C

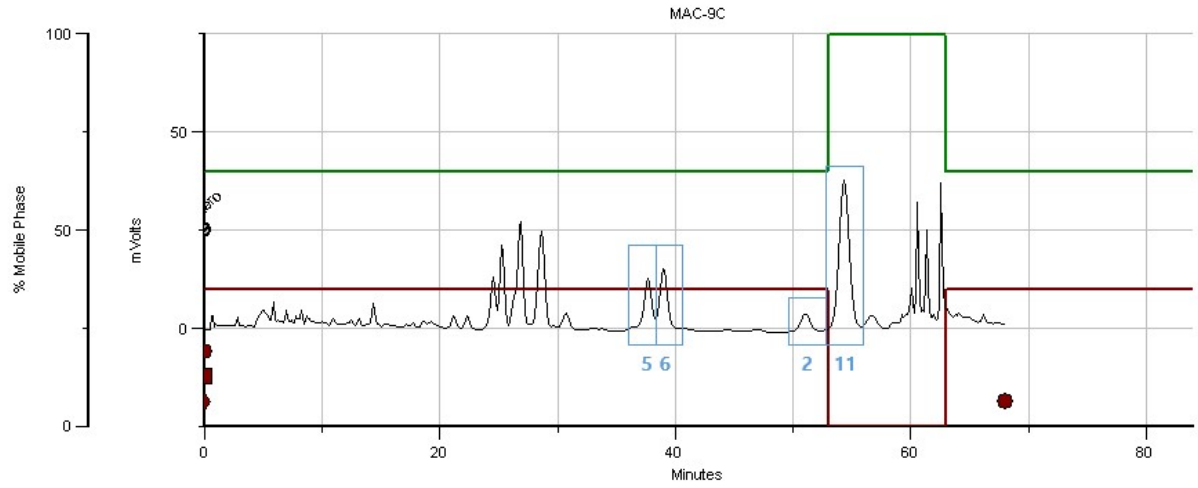

HPLC chromatogram of injected MAC-9C sample (Luna 5 µm C18(2), 250 x 10 mm, CH_3CN (0.1% FA) 65% isocratic, 3 mL/min, 280 nm) to obtain **5** (t_R = 37 min), **6** (t_R = 39 min), **2** (t_R = 50 min), and 11 (t_R = 53 min)

Figure S57. Experimental CD spectra of neovanone A (**5**) and B (**6**)

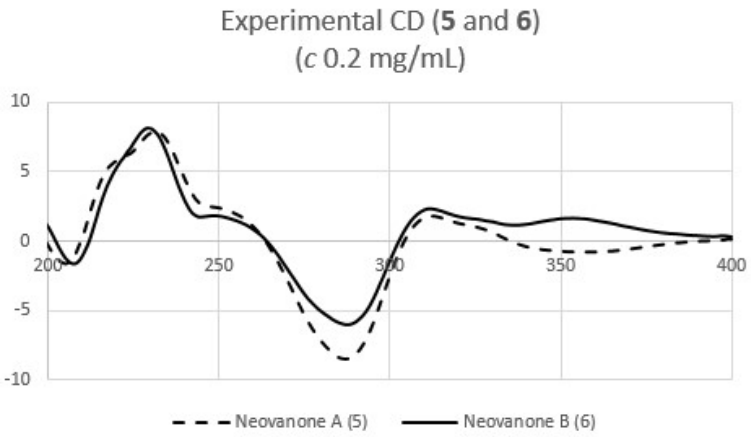

Figure S58–S85. ^{1}H and ^{13}C NMR spectra of known compounds (**7–20**)

Figure S58. ^{1}H NMR spectrum of abyssinoflavanone V (**7**) in $CDCl_3$

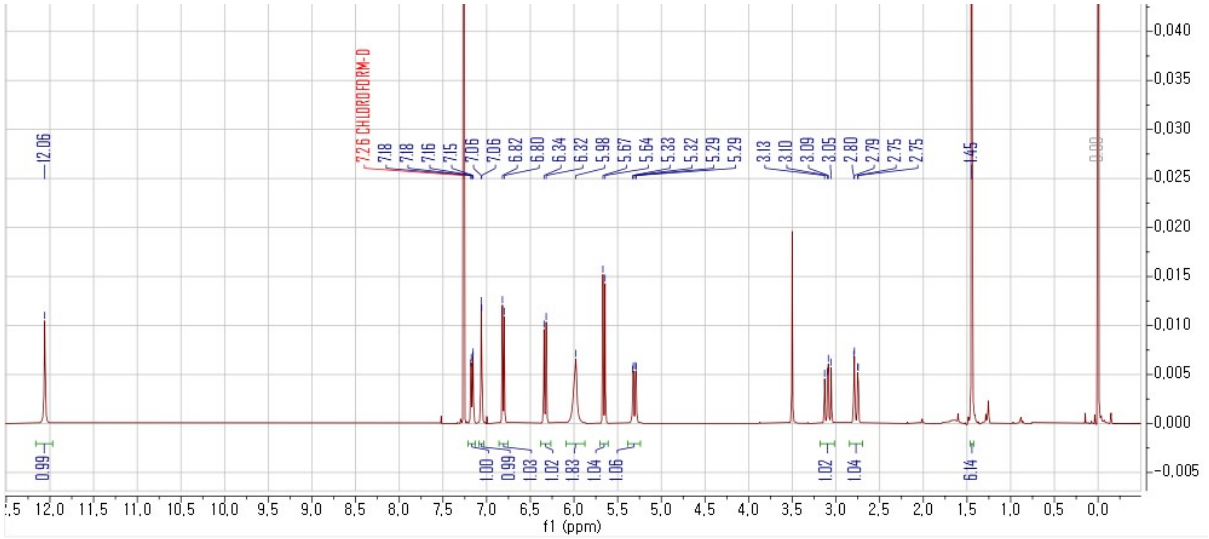

Figure S59. ^{13}C NMR spectrum of abyssinoflavanone V (**7**) in $CDCl_3$

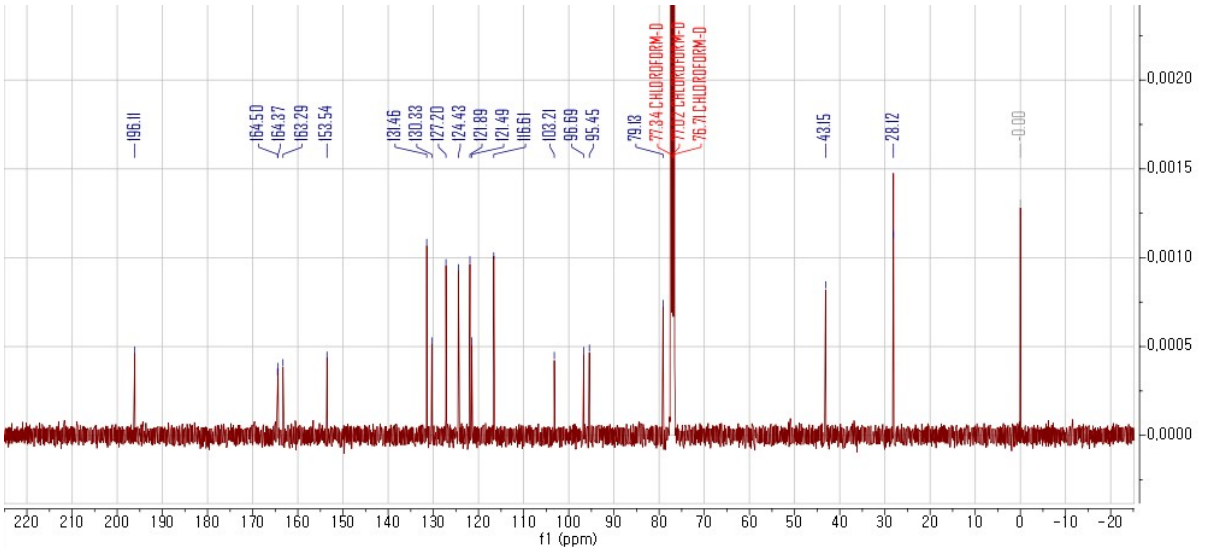

Figure S60. ^{1}H NMR spectrum of sanggenol O (**8**) in $CDCl_3$

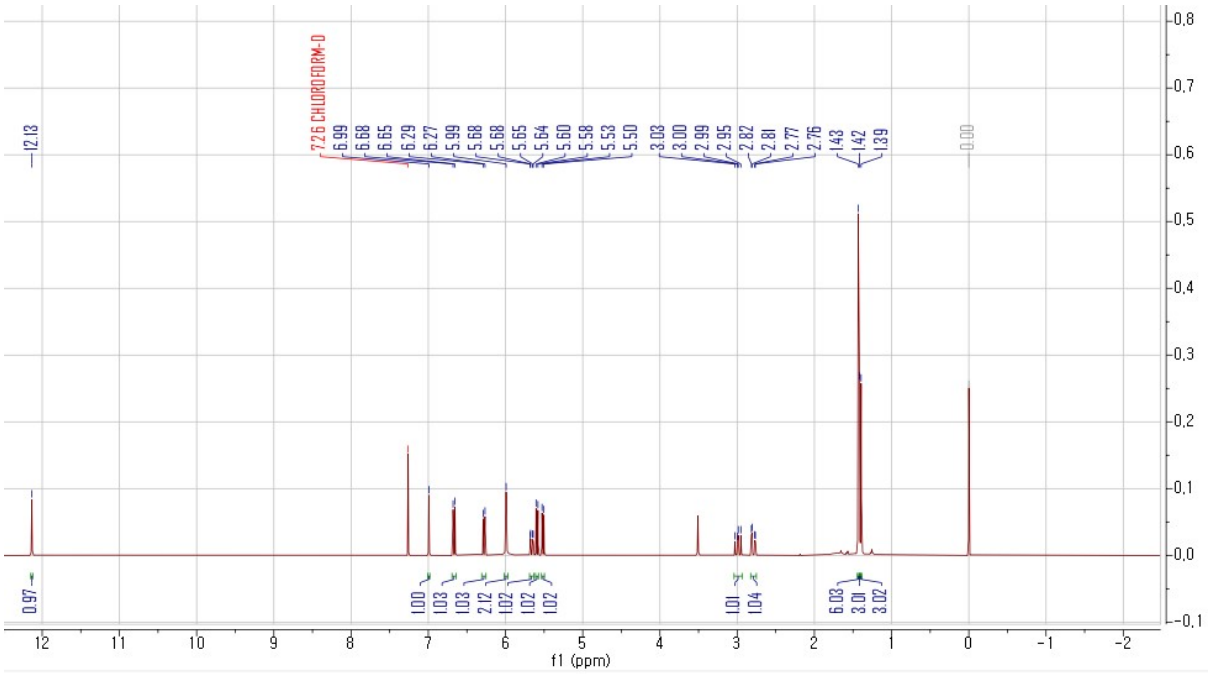

Figure S61. ^{13}C NMR spectrum of sanggenol O (**8**) in $CDCl_3$

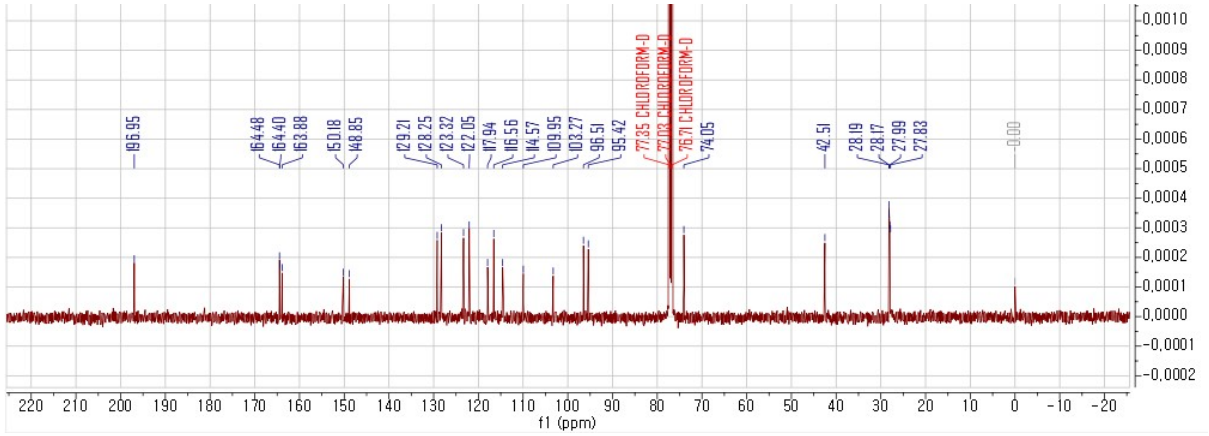

Figure S62. ^{1}H NMR spectrum of cyclomorusin (**9**) in methanol-d_4

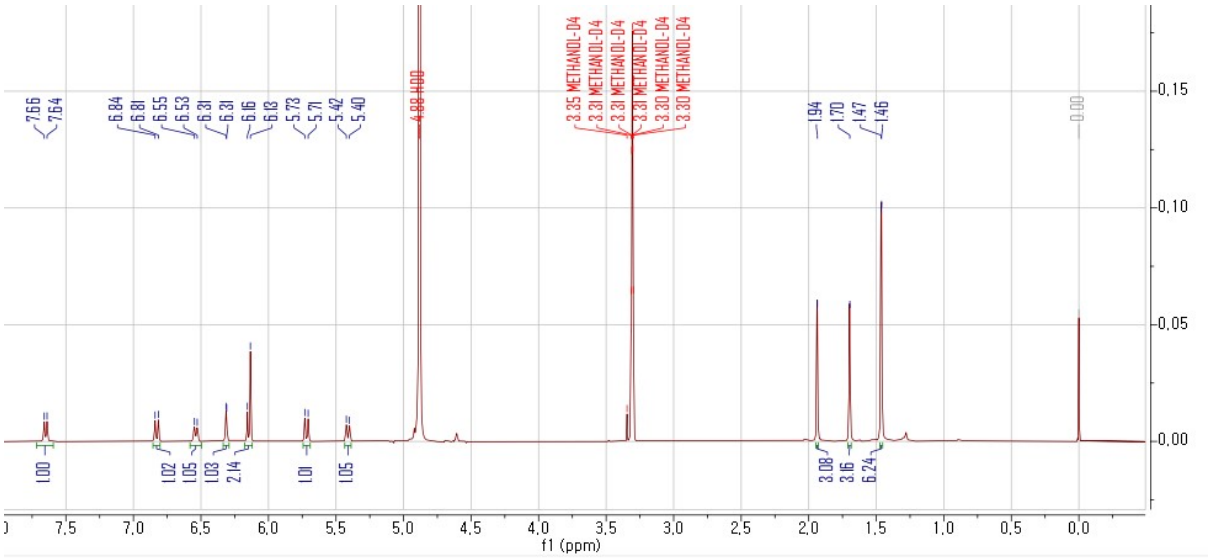

Figure S63. ^{13}C NMR spectrum of cyclomorusin (**9**) in methanol-d_4

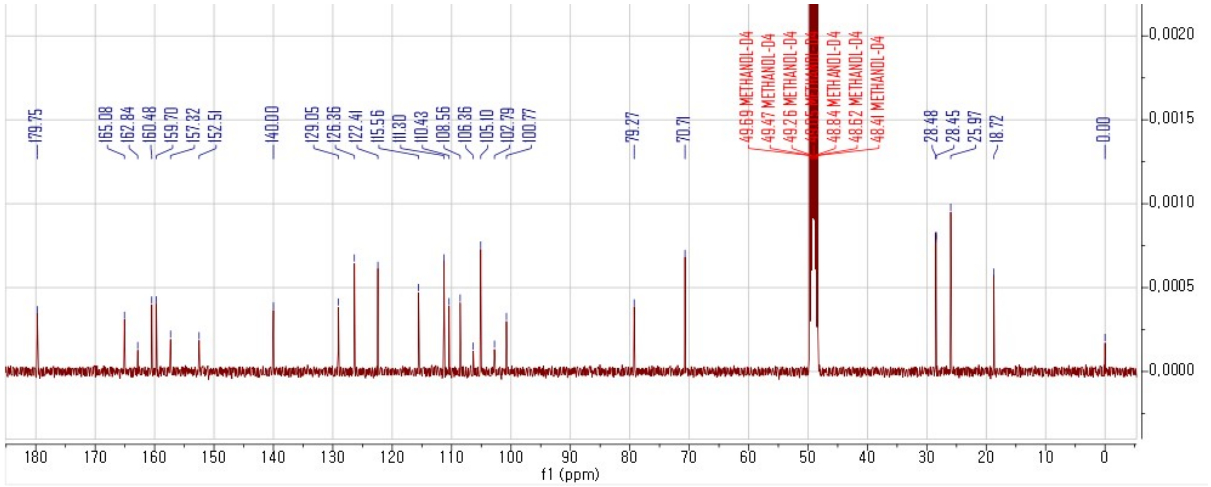

Figure S64. ^{1}H NMR spectrum of cycloaltilisin 7 (**10**) in $CDCl_3$

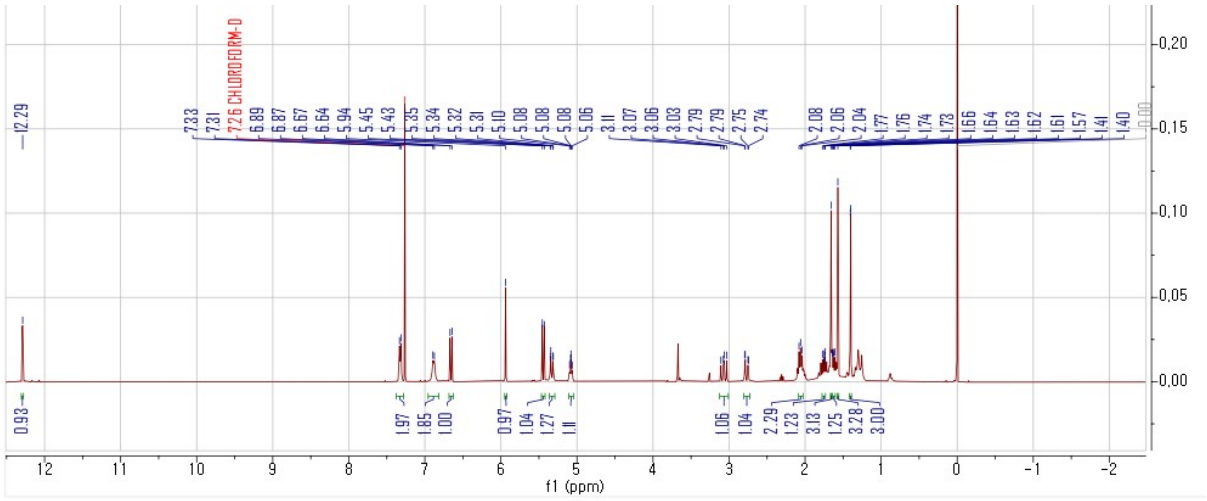

Figure S65. ^{13}C NMR spectrum of cycloaltilisin 7 (**10**) in $CDCl_3$

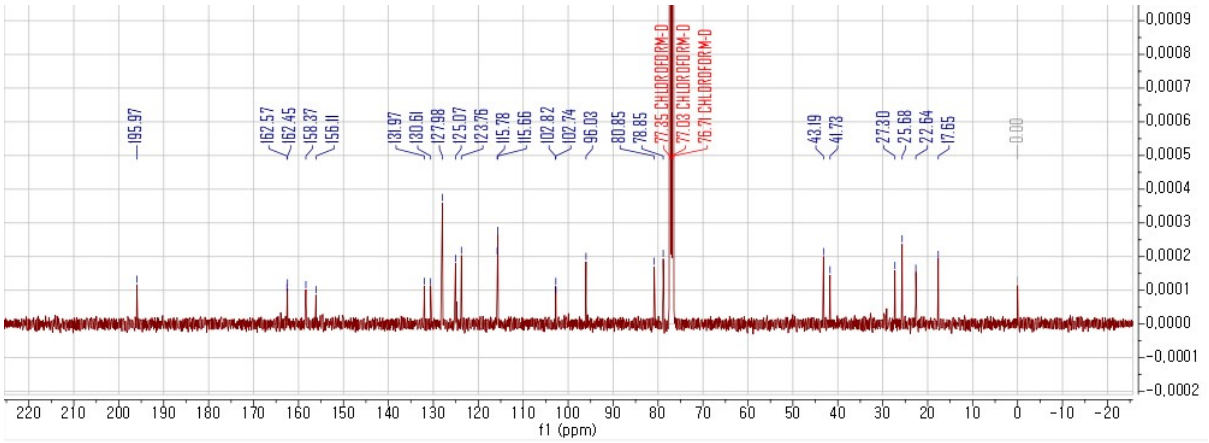

Figure S66. ^{1}H NMR spectrum of sanggenol P (**11**) in methanol-d_4

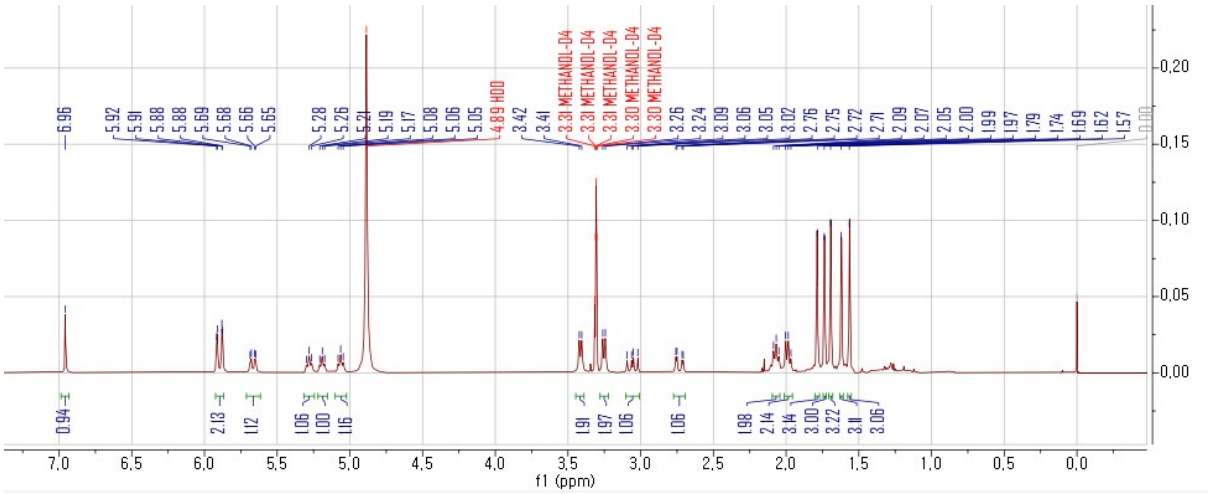

Figure S67. ^{13}C NMR spectrum of sanggenol P (**11**) in methanol-d_4

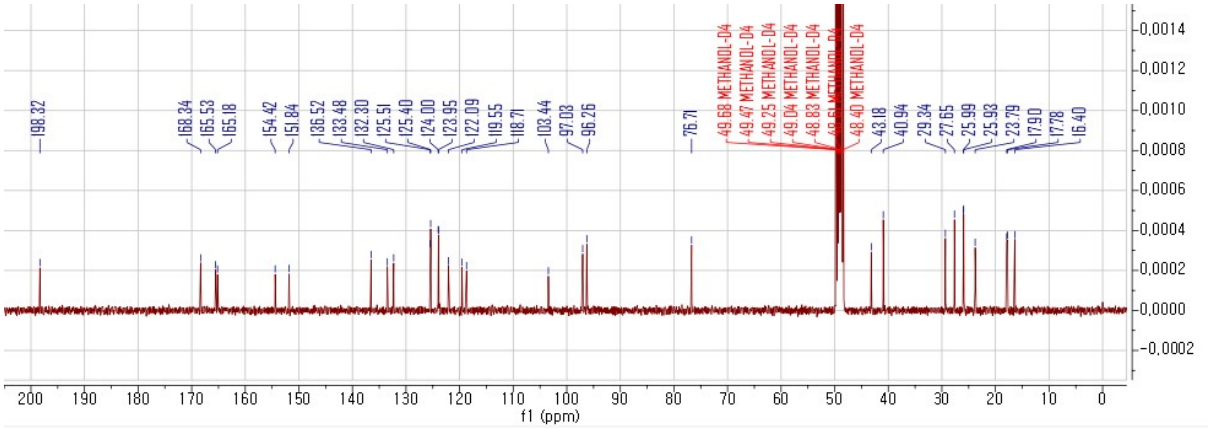

Figure S68. ^{1}H NMR spectrum of morachalcone A (**12**) in methanol-d_4

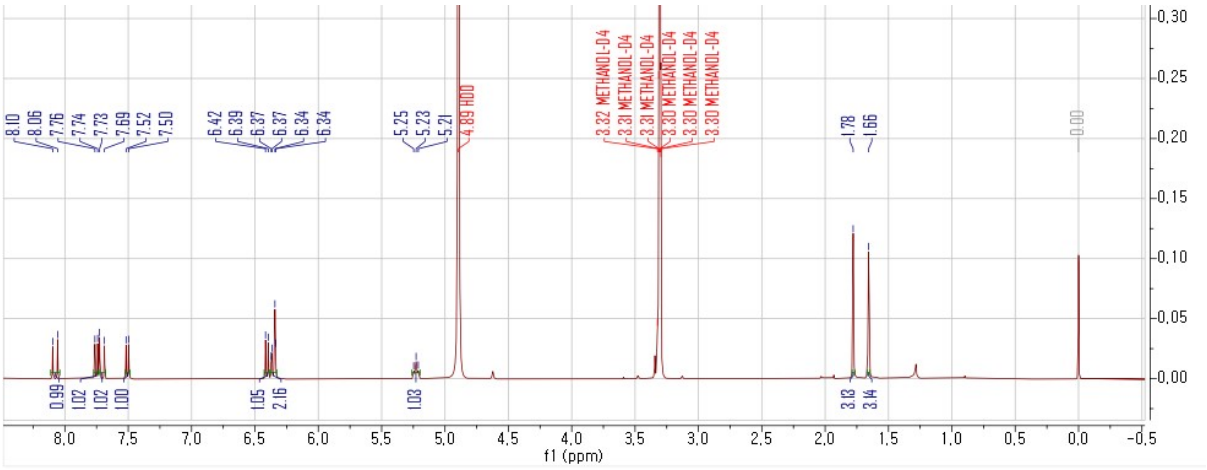

Figure S69. ^{13}C NMR spectrum of morachalcone A (**12**) in methanol-d_4

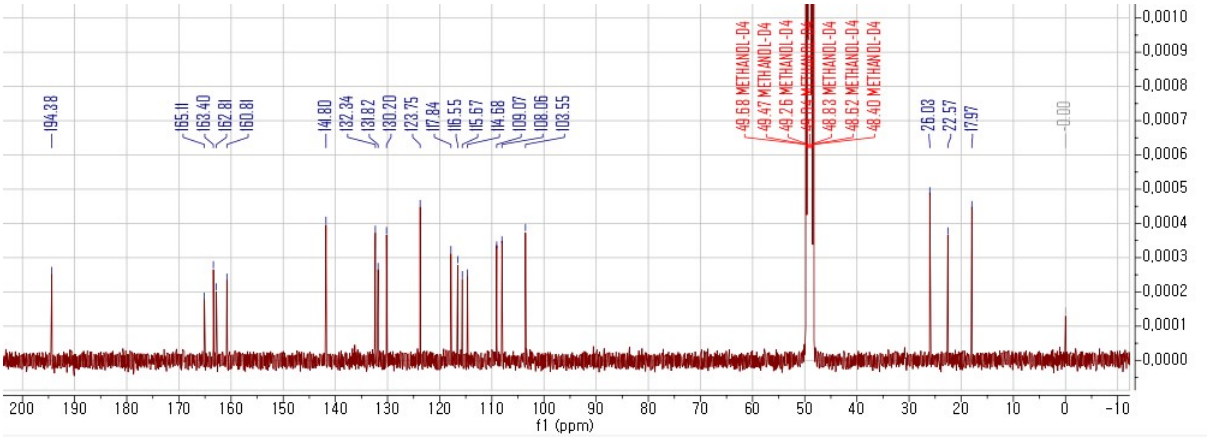

Figure S70. ^{1}H NMR spectrum of betulinic acid (**13**) in $CDCl_3$

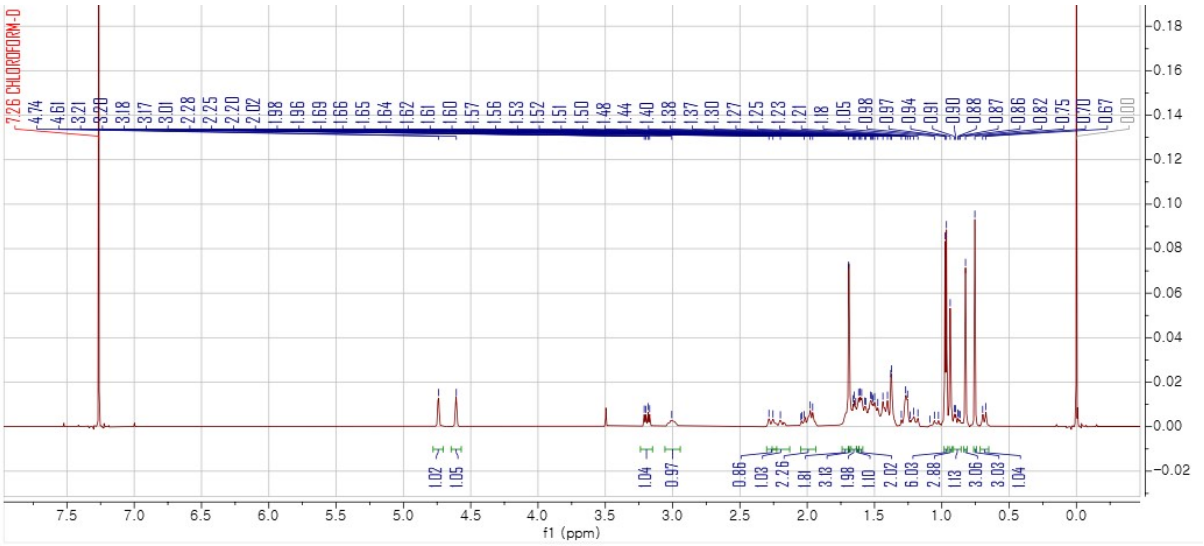

Figure S71. ^{13}C NMR spectrum of betulinic acid (**13**) in $CDCl_3$

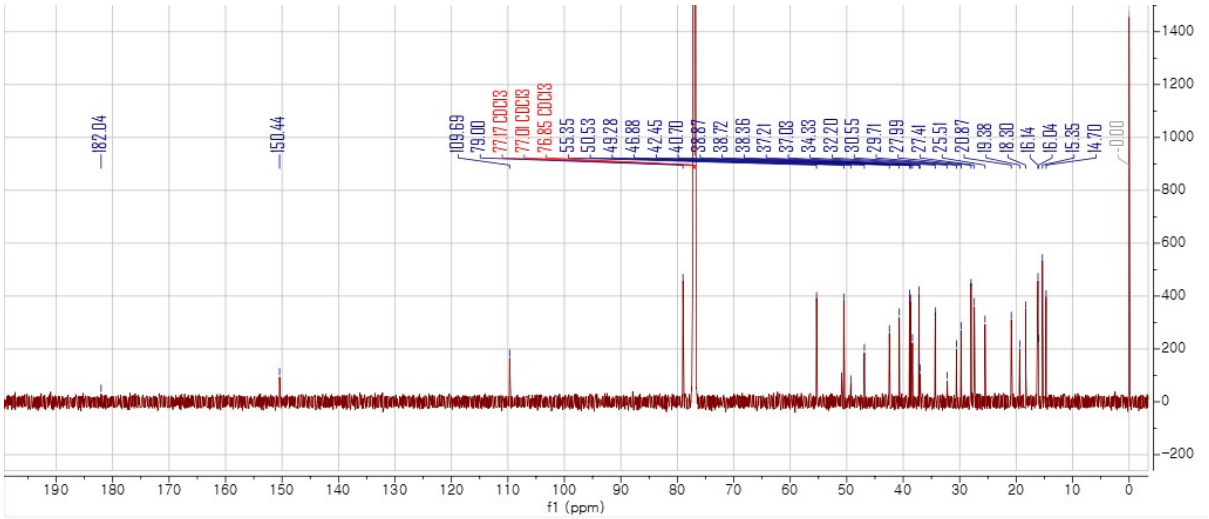

Figure S72. ^{1}H NMR spectrum of scopoletin (**14**) in methanol-d_4

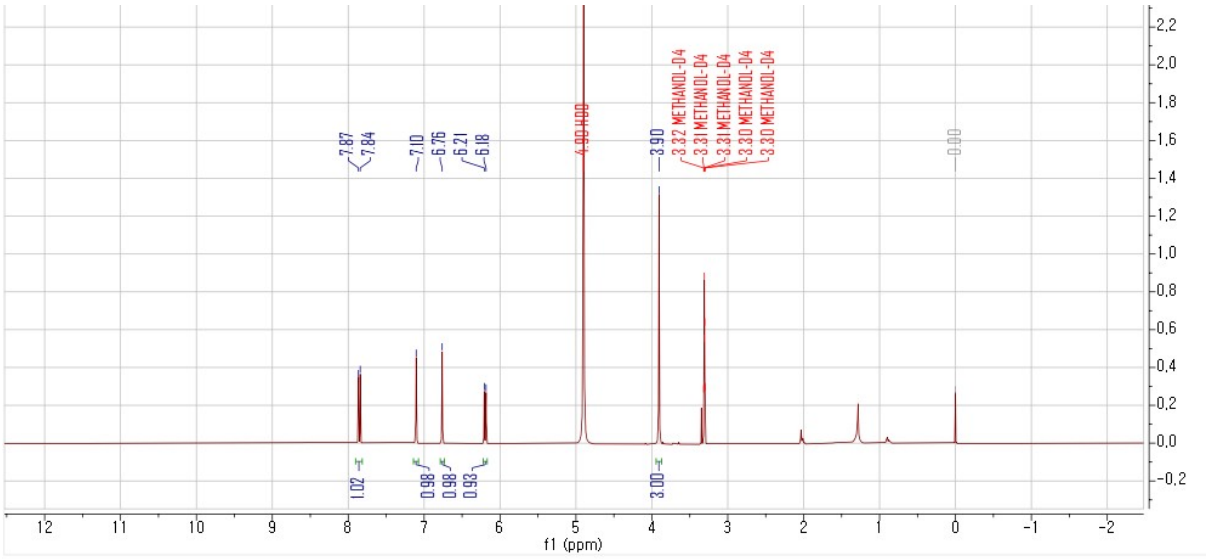

Figure S73. ^{13}C NMR spectrum of scopoletin (**14**) in methanol-d_4

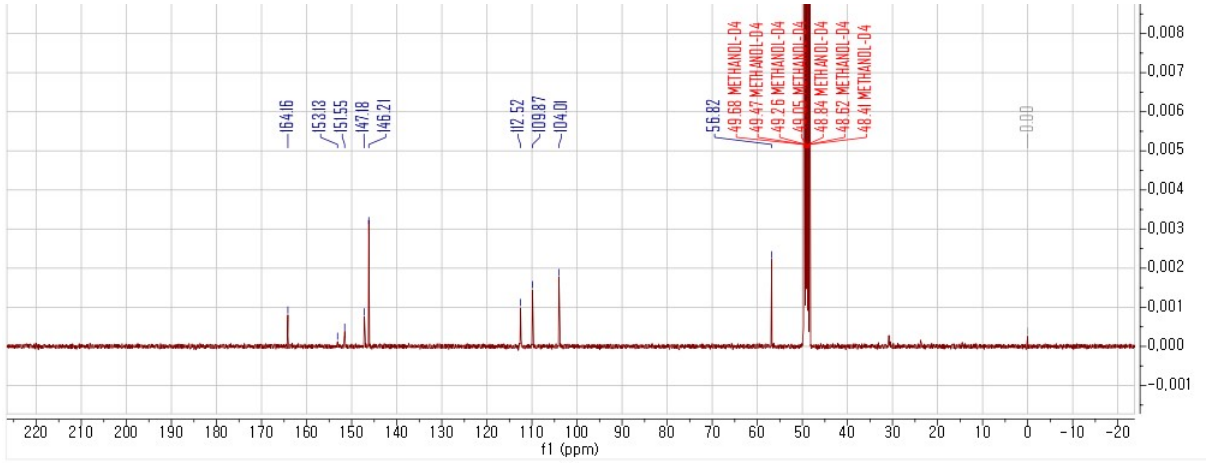

Figure S74. ^{1}H NMR spectrum of umbelliferone (**15**) in methanol-d_4

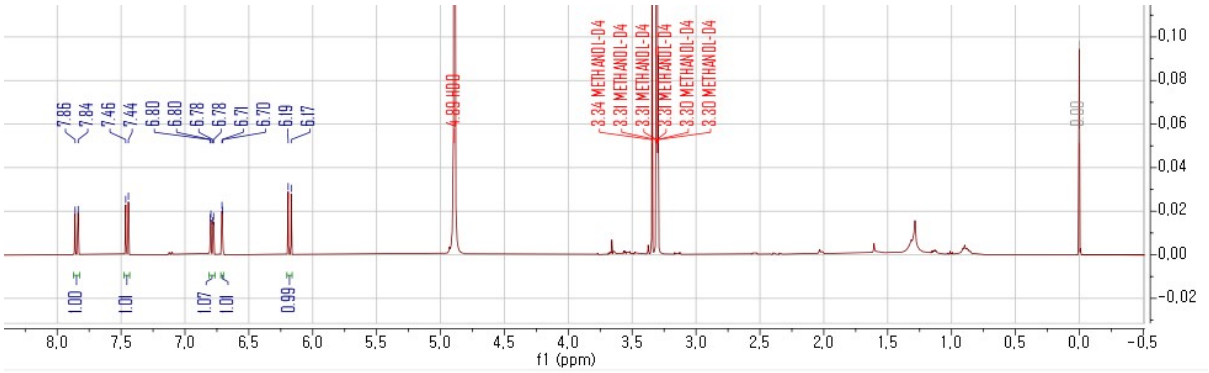

Figure S75. ^{13}C NMR spectrum of umbelliferone (**15**) in methanol-d_4

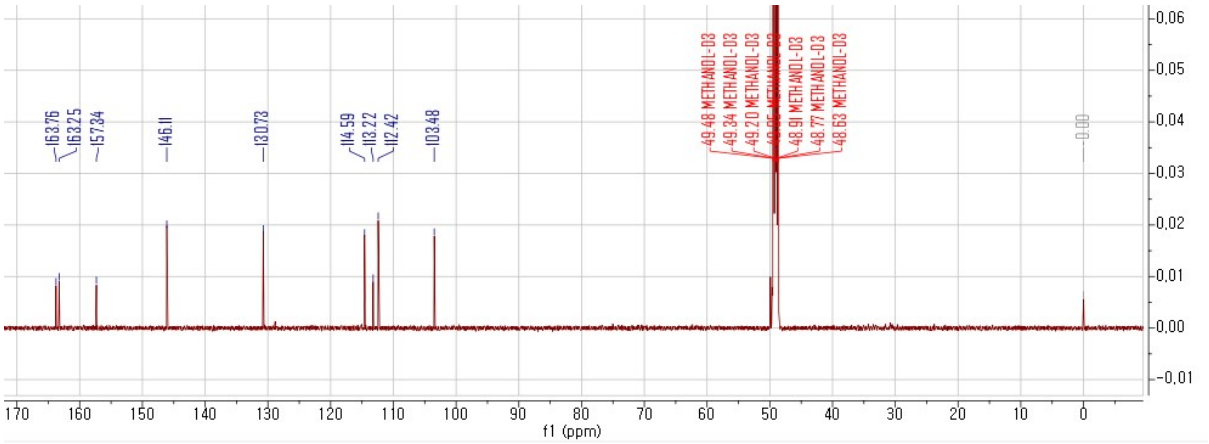

Figure S76. ^{1}H NMR spectrum of morusalfuran E (**16**) in $CDCl_3$

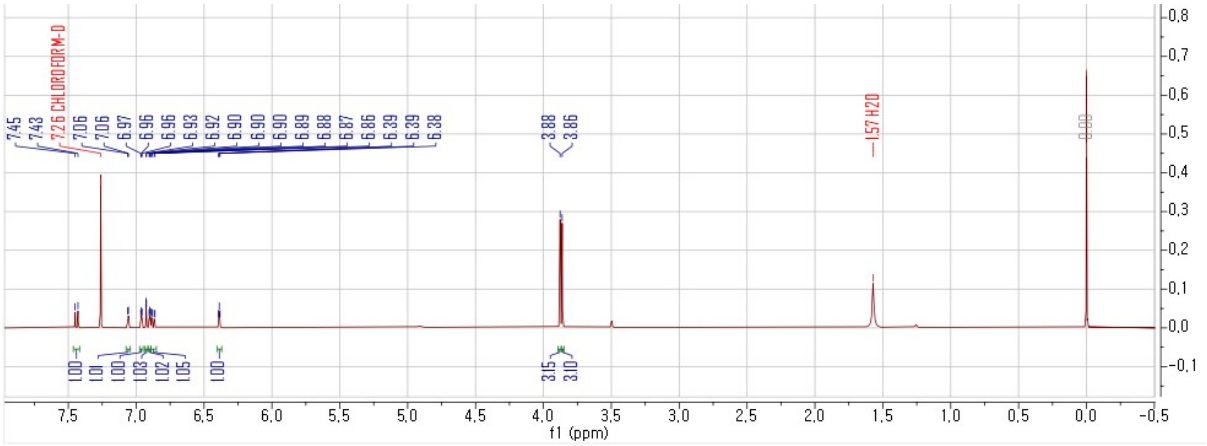

Figure S77. ^{13}C NMR spectrum of morusalfuran E (**16**) in $CDCl_3$

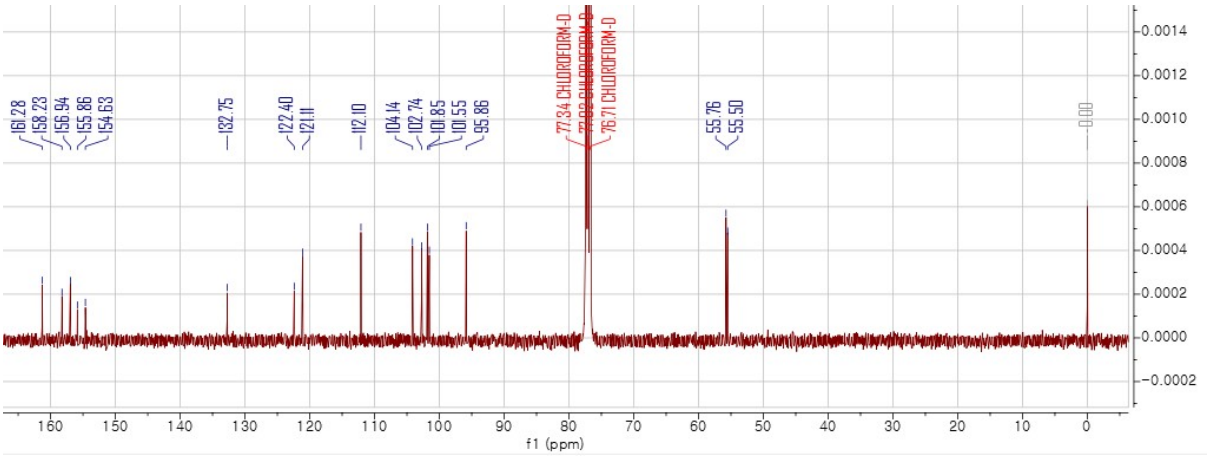

Figure S78. ^{1}H NMR spectrum of sanggenofuran B (**17**) in $CDCl_3$

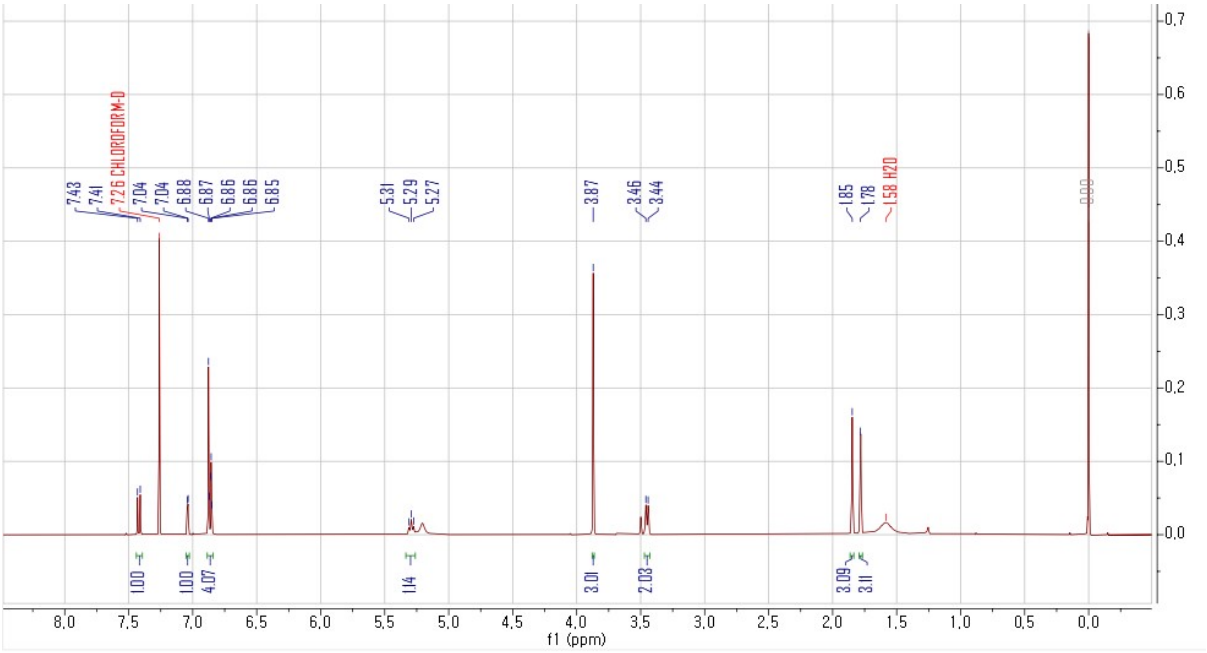

Figure S79. ^{13}C NMR spectrum of sanggenofuran B (**17**) in $CDCl_3$

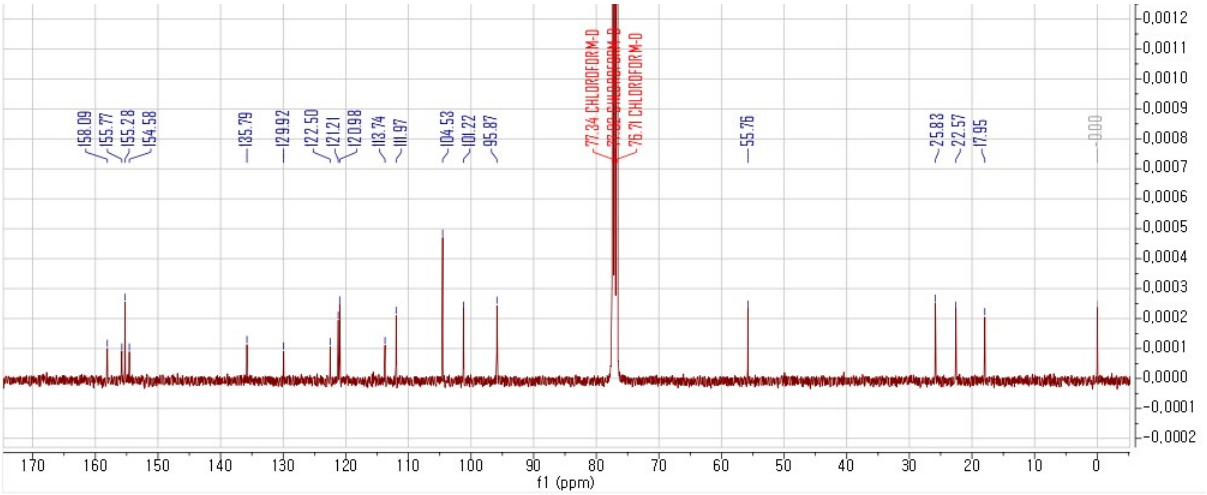

Figure S80. ^{1}H NMR spectrum of moracin M (**18**) in methanol-d_4

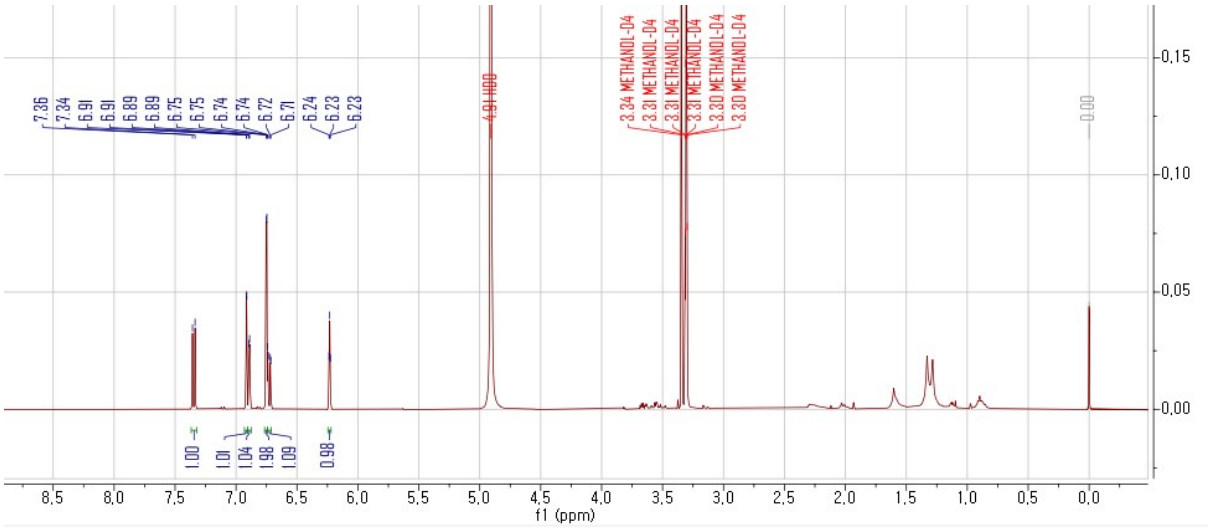

Figure S81. ^{13}C NMR spectrum of moracin M (**18**) in methanol-d_4

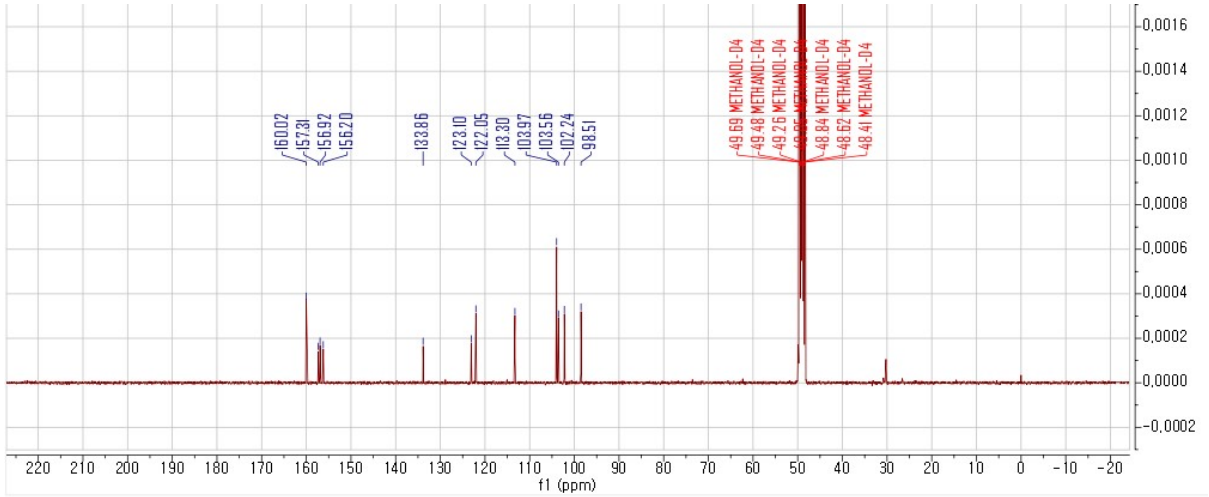

Figure S82. ^{1}H NMR spectrum of moracin B (**19**) in methanol-d_4

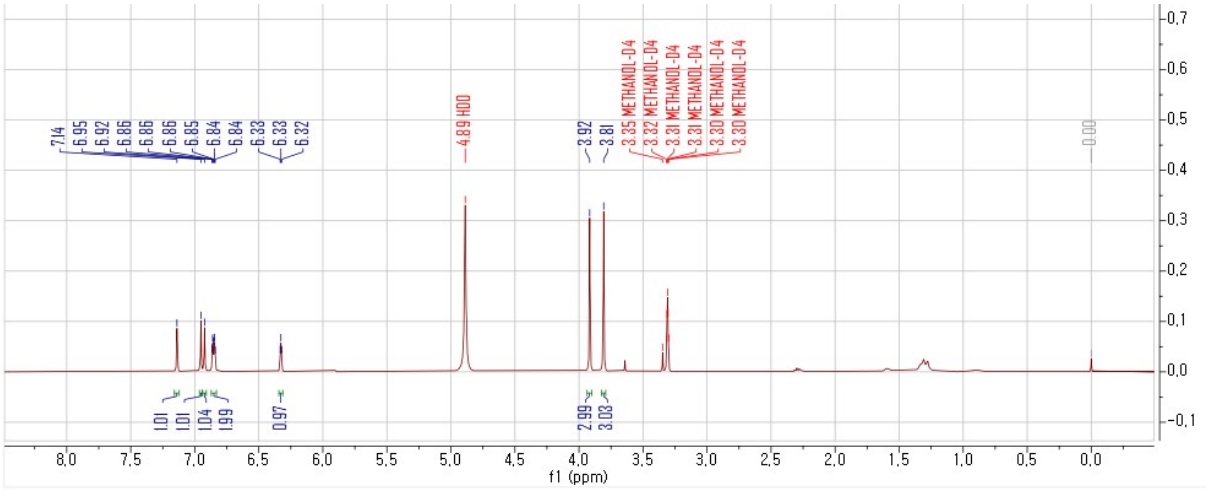

Figure S83. ^{13}C NMR spectrum of moracin B (**19**) in methanol-d_4

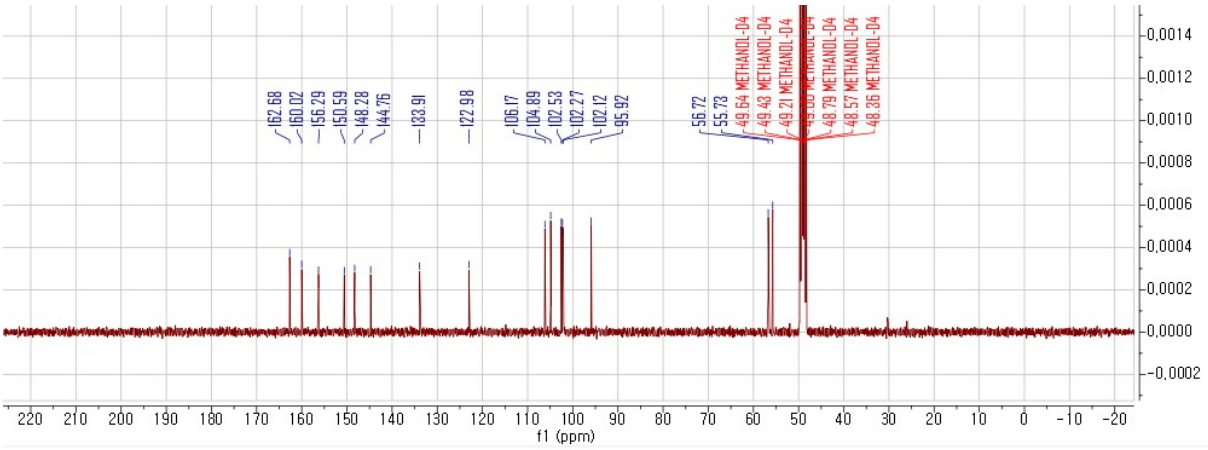

Figure S84. ^{1}H NMR spectrum of moracin S (**20**) in methanol-d_4

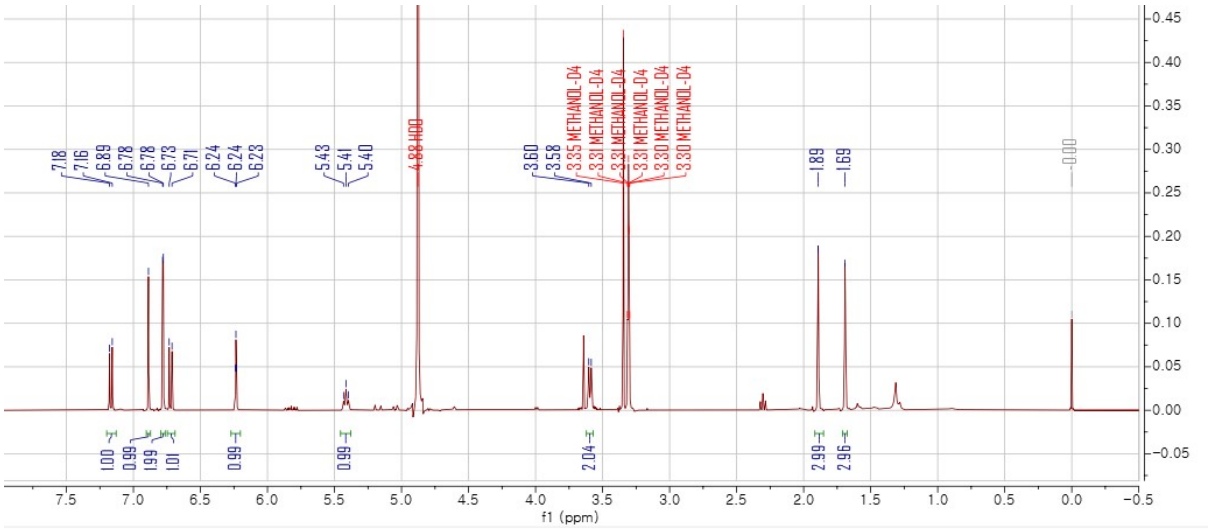

Figure S85. ^{13}C NMR spectrum of moracin S (**20**) in methanol-d_4